13 Methods in Neuronal Modeling
From Synapses to Networks
edited by Christof Koch and Idan Segev
The MIT Press 1988

CHAPTER 7

Associative Network Models for Central Pattern Generators

DAVID KLEINFELD and HAIM SOMPOLINSKY

7.1 Introduction

The collective properties of highly interconnected networks of model neurons have been the focus of much theoretical analysis. Recent work on this topic involves networks whose dynamics are governed by a cooperative relaxation process (e.g., Hopfield 1982, 1984; Peretto 1984; Amit, Gutfreund, and Sompolinsky 1985a, 1985b; Gardner 1988). Starting from an initial state, these networks will relax to one of a select number of stable states. The stable states are local minima of a suitable "energy" function. Network models of this form have been used for associative memory (Hopfield 1982) and for solving certain optimization problems (Hopfield and Tank 1986). The final, stable states represent the retrieved information or the optimized configuration.

Despite some very suggestive analogies between the network models and biological computational processes, their application in biology is unclear. The difficulty in relating the models to experimental observations reflects, in part, the difficulty in identifying a cooperative relaxational process in large, complex nervous systems. Similarities between associative memory networks and central nervous functions, such as place learning in the hippocampus (e.g., O'Keefe 1983), olfaction (Gelperin, Hopfield, and Tank 1985; Haberly 1985; Baird 1986) and visual processing (Koch, Marroquin, and Yuille 1986; Wang, Mathur, and Koch 1989) have been proposed. Yet the models remain untested at the level of neurophysiology.

In this chapter we study an associative network model whose collective outputs consist of temporally coherent patterns of linear or cyclic sequences of states (Sompolinsky and Kanter 1986; Kleinfeld 1986; Kleinfeld and Sompolinsky 1988). This model and its extensions may have a variety of implications for the learning and recall of temporally ordered information. Our objective in the present work is to draw a connection between the properties of the model and biological nervous

systems that produce fixed patterns of neural outputs. In particular, we focus on a class of biological systems known as central pattern generators.

Central pattern generators (CPGs) control the muscles involved in executing well-defined rhythmic behaviors, such as breathing, chewing, walking, swimming, and scratching. Some networks forming CPGs are anatomically well localized and may contain small numbers of neurons. Their output consists of coherent, oscillatory patterns. These features make CPGs strong candidates for studying the relation between the collective output properties of a biological network and its underlying circuitry.

A number of basic principles about CPGs have emerged from studies on a wide variety of rhythmic behaviors (for review, see Delcomyn 1980; Kristan 1980; Roberts and Roberts 1983; Cohen, Rossignol, and Grillner 1986; Selverston and Moulins 1986):

1. A rhythmic neural output can occur in the absence of sensory feedback from the muscles and structures controlled by the CPG, and in the absence of control by higher neural centers. These features are clearly demonstrated with "spinal" preparations (e.g., Grillner 1975), i.e., isolated segments of spinal cord. The output activity of the motor neurons in these preparations is similar to the rhythmic firing pattern observed in the intact animal.

2. Some CPGs function without a pacemaker cell, i.e., a single neuron whose firing rate determines the output period of the network. This implies that the rhythmic output is a collective property of the network. Examples include the CPG that controls swimming in the mollusc *Tritonia diomedea* (Getting 1981, and chapter 6) and possibly the CPGs that control flight in the locust (Wilson 1961; Robertson and Pearson 1985) and swimming in the leech (Stent, Kristan, Friesen, Ort, Poon, and Calabrese 1978; Weeks 1981).

3. The same set of motor neurons can be involved in a variety of rhythmic behaviors in an animal. This suggests that a CPG may be capable of producing multiple patterns of rhythmic outputs. Further, animals can rapidly switch between rhythmic behaviors and may blend different rhythms together (e.g., Stein, Camp, Robertson, and Mortin 1986).

4. The output of the CPG can be modulated by external inputs, such as feedback from proprioceptors and from higher neural centers.

For example, modulation is used both to turn on and off the CPG and to control the period of its rhythm.

The dynamic properties of several CPGs have been analyzed by performing detailed simulations of specific circuits. Simulation techniques have been used in the study of the lobster pyloric and gastric mill rhythms (Perkel 1965; Hartline 1979) and the swim rhythm in *Tritonia* (Getting 1983a, and chapter 6). This approach often involves simulating the equations that describe the dynamics of the neurons in the CPG, e.g., Hodgkin and Huxley-like equations (Hodgkin and Huxley 1952), using the known biophysical parameters for each neuron and the synaptic connections between neurons. Detailed simulations have been useful for determining the completeness of a set of measurements of a CPG (e.g., Getting 1983a, 1983b). A complementary approach for understanding the biological mechanisms responsible for pattern formation is to compare the properties of CPGs with those of simple network models (for a discussion of this approach, see Selverston 1980).

The smallest circuit that can produce a rhythmic output consists of two neurons coupled by reciprocal inhibitory synaptic connections (Harmon 1964; Reiss 1964). If both neurons are tonically excited and contain a mechanism for synaptic fatigue, they will alternately produce a bursting output. The period of the output oscillation is proportional to the time scale of the fatigue. The two-neuron oscillator and networks of coupled two-neuron oscillators provided an early basis for understanding some aspects of the motor system controlling flight in the locust (Wilson and Waldron 1968).

A generalization of the two-neuron oscillator was made by Kling and Szekély (1968). They studied networks containing closed loops of neurons connected by inhibitory synapses. This topology results in recurrent, cyclic inhibitory pathways that allow the networks to produce a rich set of oscillatory patterns. These networks have been used, although with limited success, as a basis for understanding the CPG controlling the swim rhythm in the leech (Friesen and Stent 1977).

The mechanism of recurrent cyclic inhibition can be extended to arbitrarily large networks. However, certain features of these networks make them inappropriate as general models of CPGs. All of the synaptic connections in a loop are inhibitory; this precludes the use of loops for modeling CPGs that also contain excitatory synapses. The loops rely on a specific cyclic topology of their connections in order to function. Finally, simulations have indicated that each loop is capable of producing only a *single* stable output pattern (Kling and Szekély 1968).

Several other network models have been studied as candidates for CPGs (Harth, Lewis, and Csermely 1975; Glass and Young 1979; Thompson 1982; Kopell 1986). A mechanism for the generation of multiple, coherent patterns by highly interconnected networks is, however, lacking in these models.

In this chapter we present a general model for producing rhythmic patterns in associative neural network models. The network consists of highly interconnected model neurons whose essential feature is a nonlinear relation between their inputs and their firing rate. The form of the output patterns is encoded in the strength of the synaptic connections between pairs of neurons. Rhythmic output emerges as a collective property of the network.

Many of the structural and dynamic properties of our model are similar to those observed in CPGs. The network can produce rhythmic output in the absence of external feedback. It can naturally produce multiple stable patterns of rhythmic outputs. Well-defined mechanisms exist for modulating the output period of the patterns and for switching between individual patterns. Both excitatory and inhibitory synapses are typically present. Thus the model may serve as a formal framework for understanding some biological systems that produce rhythmic output.

We compare the predictions of our model with Getting's detailed measurements on the CPG controlling the swim rhythm in *Tritonia* (Getting 1981, 1983a, 1983b; chapter 6). This CPG contains a small number of neurons and produces a single rhythmic output pattern. Yet the comparison will serve to highlight many features of the model and to assess its applicability to biological systems.

7.2 The Model

The present model is an extension of Hopfield's model of associative memory (Hopfield 1982, 1984). We consider a network that contains N interconnected model neurons. The output of each neuron, $V_i(t)$, varies between zero (quiescent) and unity (maximum firing rate). The state of the network is specified by the output activity of all of its neurons. It is represented by $V(t) = \{V_i(t)\}_{i=1}^{N}$.

A pattern is defined as a temporal sequence of a subset of all possible output states. The states, $V^{\mu} = \{V_i^{\mu}\}_{i=1}^{N}$, comprising this subset are referred to as the *embedded* states. For example, a pattern of length r consists of the sequence

$$V^1 \rightarrow V^2 \rightarrow V^3 \rightarrow \cdots \rightarrow V^{r-1} \rightarrow V^r$$

where each state V^μ is an embedded state. For the case of a cyclic sequence, of relevance for modeling CPGs, $V^r = V^1$. The networks can produce multiple patterns; we define $V^{\mu,\nu}$ as the μth embedded state in the νth pattern.

We consider patterns in which the output activity of the model neurons alternates between a relatively low firing rate and a relatively high rate. The precise form of this activity depends upon the detailed characteristics of the neurons. We therefore assume for simplicity that the output of each neuron, while the network is in an embedded state, alternates between quiescence and its maximum firing rate. Each component $V_i^{\mu,\nu}$ of the embedded states is thus given by either 0 or +1. This assumption allows us to focus on properties of the networks that result specifically from the form of the connections between neurons.

In the remainder of this chapter we first define the rules for encoding the output patterns in the synaptic connections. Next we describe the dynamics of the network, followed by a description of its general properties. Some of these properties are illustrated by numerical examples.

7.2.1 Synaptic Connections and Their Response Time

The desired output patterns are encoded in the form of the synaptic connections between the model neurons. We define the synaptic connection between the jth presynaptic neuron and the ith postsynaptic neuron as T_{ij}. A central feature of the present model is that each connection T_{ij} is *functionally* separated into two components, denoted T_{ij}^S and T_{ij}^L. The two components are hypothesized to have different characteristic response times. The synaptic connections T_{ij}^S act on the shorter of the two time scales. This time scale, τ_S, determines the time required for the network to settle in each of the embedded states. The synaptic connections denoted T_{ij}^L act on the longer of the two times. This time scale, $\tau_L (\tau_L \gg \tau_S)$, sets the time for the onset of the transitions between consecutive states in the pattern. Thus the duration of an individual state in a pattern will be $\sim \tau_L$, while the transitions between states occur on the faster time scale of τ_S.

The role of the connection strengths T_{ij}^S is to stabilize the network in an embedded state, until a transition to the next state occurs. This is achieved by defining the T_{ij} in terms of a formal version of the Hebb (1949) learning rule (see also Hopfield 1982), i.e.,

$$T_{ij}^S = \frac{J_0}{N} \sum_{\nu=1}^{q} \sum_{\mu=1}^{r} (2V_i^{\mu,\nu} - 1)(2V_j^{\mu,\nu} - 1), \qquad i \neq j, \quad J_0 > 0 \tag{7.1}$$

where q is the total number of patterns, $r = r(\nu)$ is the length of the νth pattern, and $T_{ii}^S = 0$. The prefactor J_0/N ensures that the magnitude of the total synaptic input is of order J_0. The variable $(2V_i^{\mu,\nu} - 1)$ has a value of either -1 (quiescent) or $+1$ (maximally firing) so that inhibitory as well as excitatory synapses are formed.

The role of the connection strengths T_{ij}^L is to induce transitions from the μth embedded state to the $\mu+1$th state. Thus we define

$$T_{ij}^L = \lambda \frac{J_0}{N} \sum_{\nu=1}^{q} \sum_{\mu=1}^{r-1} (2V_i^{\mu+1,\nu} - 1)(2V_j^{\mu,\nu} - 1), \qquad i \neq j, \quad \lambda > 0 \tag{7.2}$$

where λ is a scaling parameter for the transition strength and $T_{ii}^L = 0$. We will discuss the constraints on λ in a later section. For the case of cyclic patterns, $V^{r,\nu} = V^{1,\nu}$. Note that the T_{ij}^L synapses, which depend on the consecutive output activity of the neurons, are asymmetric ($T_{ij}^L \neq T_{ji}^L$), while the T_{ij}^S synapses, which depend only on the activity within the individual states, are symmetric.

The rule for forming the T_{ij}^L synapses (eq. 7.2) encodes transitions between pairs of embedded states. This allows the network to generate patterns that involve unambiguous transitions between states. The permissible patterns correspond either to linear sequences (fig. 7.1A), cyclic sequences (fig. 7.1B) or sequences *down* a tree structure (fig. 7.1C). Several different patterns, as well as isolated, stable states, can be embedded in the same network. Patterns that involve ambiguous transitions, such as when two patterns share the same embedded state, cannot be reliably produced by the present network. This includes patterns that involve transitions *up* a tree. We will return to this issue in section 7.4.

The rules defined by eqs. 7.1 and 7.2 for forming the synaptic components are applicable only when the overlaps between the embedded states are small, i.e.,

$$\frac{1}{N} \sum_{j=1}^{N} (2V_j^{\mu,\nu} - 1)(2V_j^{\mu',\nu'} - 1) \simeq 0 \quad \text{for} \quad (\mu,\nu) \neq (\mu',\nu') \tag{7.3}$$

and when, on average, half of the neurons are active in each of the embedded states, i.e.,

$$\frac{1}{N} \sum_{j=1}^{N} (2V_j^{\mu,\nu} - 1) \simeq 0 \tag{7.4}$$

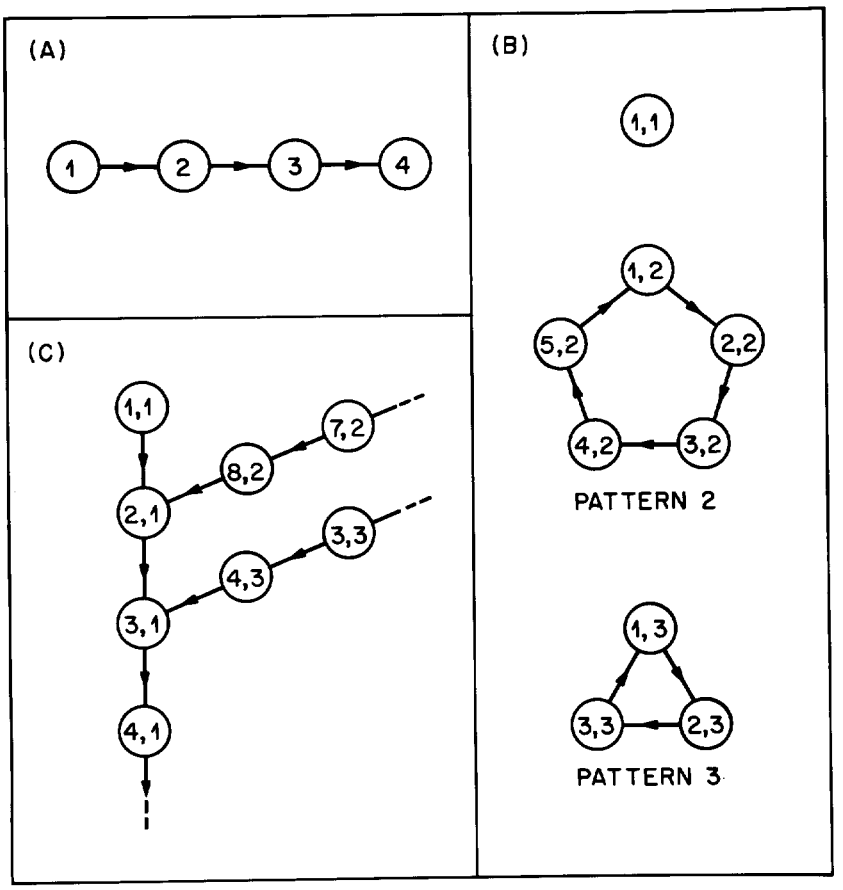

Figure 7.1
State diagrams of the different topologies of patterns that can be produced by the model network. Circles correspond to stable outputs, i.e., embedded states, and arrows correspond to the transitions between these states. (A) A linear sequence of embedded states. The network will remain in the final state, V^4, after completing the sequence. (B) Cyclic sequences of embedded states. Two cyclic patterns, along with an isolated stable state, $V^{1,1}$, are shown. This arrangement of patterns was used in the simulation shown in fig. 7.6. (C) A tree structure, in which two or more sequences ultimately share the same set of embedded states.

These relations will be satisfied if the embedded states are approximately orthogonal to each other. For a large network, eqs. 7.3 and 7.4 are satisfied if the embedded states are chosen from a random sample; the average overlap in this case is $\sim \sqrt{1/N}$. Alternative rules, appropriate for embedding states that have a high degree of overlap, are described in Appendix 7.A.

Synaptic Inputs The integrated synaptic input to each model neuron is assumed to be a *linear* summation of the outputs of the presynaptic neurons. The total synaptic input to the ith neuron via the fast components of the synapses , $h_i^S(t)$, is

$$h_i^S(t) = \sum_{j=1}^{N} T_{ij}^S \, V_j(t) \tag{7.5}$$

The total synaptic input via the slow components, $h_i^L(t)$, is

$$h_i^L(t) = \sum_{j=1}^{N} T_{ij}^L \, \overline{V_j(t)} \tag{7.6}$$

where $\overline{V_j(t)}$ is the time-averaged output of the neuron, i.e.,

$$\overline{V_i(t)} = \int_0^\infty V_i(t - t') \, w(t') \, dt' \tag{7.7}$$

The synaptic response function $w(t)$ for the slow, T_{ij}^L, components is a non-negative function that is normalized to unity, i.e.,

$$\int_0^\infty w(t) \, dt = 1 \tag{7.8}$$

and characterized by a mean time constant τ_L, i.e.,

$$\int_0^\infty t \, w(t) \, dt = \tau_L. \tag{7.9}$$

The inputs $h_i^L(t)$ correspond to a weighted average over the histories of the neural activities, with a characteristic averaging time of τ_L. An example of the time course of a postsynaptic response to a short presynaptic stimulus is illustrated in fig. 7.2.

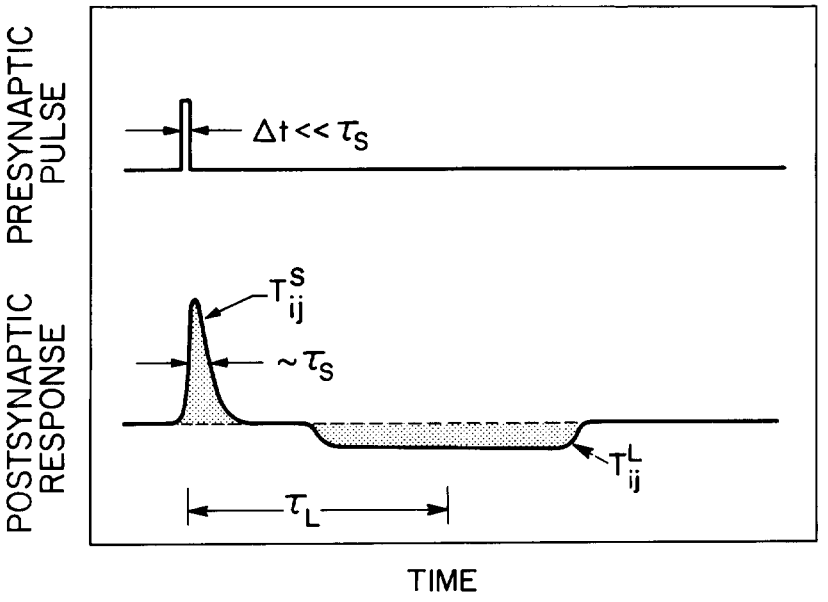

Figure 7.2
Illustration of a two-component synaptic connection from the jth to the ith neuron. The components are resolved following a short pulse ($\Delta t \ll \tau_S$) of activity in the presynaptic neuron. The area (shaded region) under the fast synaptic response is equal to T_{ij}^S (eq. 7.1); in this example T_{ij}^S is taken to be excitatory. The area (shaded region) under the slow synaptic response is equal to T_{ij}^L; in this example T_{ij}^L is taken to be inhibitory. The ratio of these areas, averaged over all pairs of synapses, equals the transition strength λ (eqs. 7.2 and 7.10). The time course of the slow synaptic response corresponds to the response function $w(t)$ (eq. 7.6); it has a time constant of τ_L.

7.2.2 Network Dynamics

Before we define the detailed dynamics of the network, we present a qualitative description in terms of the time dependence of the neural inputs. For simplicity of notation we consider a network that produces a single pattern. Immediately after a transition from the μ–1th embedded state to the μth state, the output of the network is $V(t) = V^{\mu}$, and the time-averaged output is $\overline{V(t)} \simeq V^{\mu-1}$. The inputs via the fast synaptic components are (eq. 7.5)

$$\begin{aligned} h_i^S(t) &= \sum_{j=1}^{N} T_{ij}^S V_j^{\mu} \\ &= \frac{J_0}{2} \sum_{\eta=1}^{r} (2V_i^{\eta} - 1) \left(\frac{1}{N} \sum_{j=1}^{N} (2V_j^{\eta} - 1)(2V_j^{\mu} - 1) \right. \\ &\qquad \left. + \frac{1}{N} \sum_{j=1}^{N} (2V_j^{\eta} - 1) \right) \\ &\simeq \frac{J_0}{2} (2V_i^{\mu} - 1) \end{aligned}$$

where we used eqs. 7.1–7.4. The synaptic input $h_i^S(t)$ is negative, i.e., inhibitory, if $V_i^{\nu} = 0$ (quiescent) and is positive, i.e., excitatory, if $V_i^{\nu} = 1$ (maximally firing). The inputs via the slow synaptic components are (eqs. 7.6 and 7.7)

$$h_i^L(t) = \sum_{j=1}^{N} T_{ij}^L V_j^{\mu-1} \simeq \lambda \frac{J_0}{2} (2V_i^{\mu} - 1)$$

Thus both $h^S(t)$ and $h^L(t)$ tend to stabilize the network in its current state. With increasing time, $\overline{V(t)}$ gradually shifts away from $V^{\mu-1}$ and toward the current state V^{μ}. This shift generates an increasingly large component of $h^L(t)$ that is conjugate to $V^{\mu+1}$. After the network has remained in the state V^{μ} for an interval $\sim \tau_L$, the inputs become

$$h_i^S(t) = \sum_{j=1}^{N} T_{ij}^S V_j^{\mu} \simeq \frac{J_0}{2} (2V_i^{\mu} - 1)$$

and

$$h_i^L(t) = \sum_{j=1}^{N} T_{ij}^L V_j^\mu \quad \simeq \lambda \frac{J_0}{2}(2V_i^{\mu+1} - 1)$$

The new values of $h_i^L(t)$ tend to drive the network toward the state $V^{\mu+1}$. For sufficiently large values of λ ($\lambda \gtrsim 1$) the network makes a rapid transition to the μ+1th embedded state.

A persistent sequential output pattern does not emerge if the T_{ij}^S and T_{ij}^L synaptic components act on the same time scale (i.e., $\tau_S \simeq \tau_L$). The transitions occur too frequently to allow the network to settle in an embedded state, resulting in an irregular output pattern that quickly dephases.

Detailed Dynamics The dynamic evolution of the network is described by the equations

$$\begin{aligned} \tau_S \frac{du_i(t)}{dt} + u_i(t) &= h_i^S(t) + h_i^L(t) + I_{stim_i} \\ &= \sum_{j=1}^{N} \left(T_{ij}^S V_j(t) + T_{ij}^L \overline{V_j(t)} \right) + I_{stim_i} \end{aligned} \tag{7.10}$$

where $u_i(t)$ is the net input to the ith neuron and I_{stim_i} represents an external input to the ith neuron. The equivalent electrical circuit described by these equations is shown schematically in fig. 7.3.

The output of a model neuron, $V_i(t)$, is related to its net input, $u_i(t)$, by a nonlinear gain function

$$V_i(t) = g[u_i(t) - \theta_i] \tag{7.11}$$

where θ_i is defined as the mean operating level of the neuron.[1] The dynamic features of the network do not depend on the details of the gain function;[2] fig. 7.4 illustrates an appropriate form (e.g., Fuortes and Mantegazzini 1962). Note that the output of a neuron is most sensitive to changes in its input when $u_i(t) \simeq \theta_i$.

[1] This definition is more precise than the usual description in the literature on associative neural network models, in which θ_i is equated with the threshold level of a neuron. The later designation, however, is in discord with the neurobiological definition of the threshold level as the minimum input required to elicit a non-zero firing rate. The two definitions are equal only for neurons operating in the high-gain limit (see eq. 7.14).

[2] More generally, we require only that the postsynaptic response of a neuron is nonlinear. This can occur even if the firing frequency of the presynaptic neuron is a linear function of its input current.

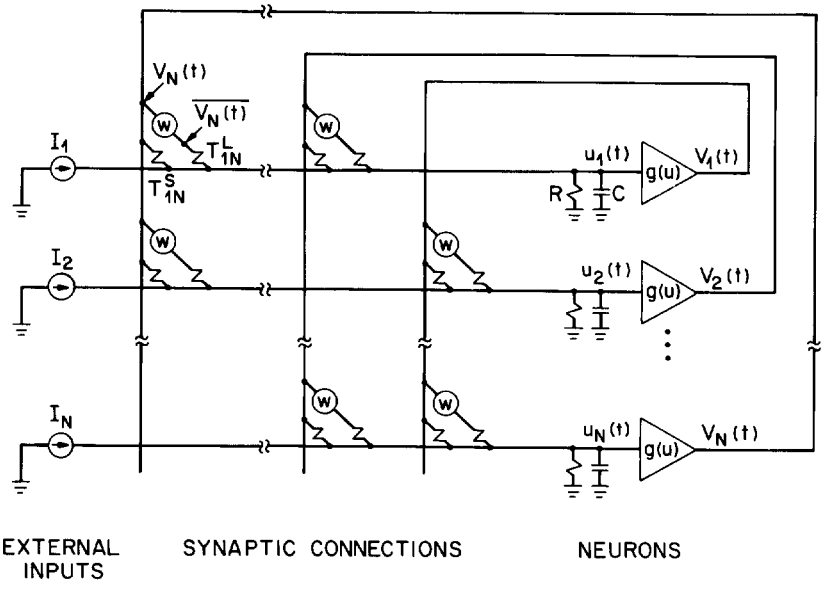

Figure 7.3
Schematic representation of the circuit diagram for the model network. Neurons are represented by saturating amplifiers (triangles; eq. 7.11) with a charging time of $\tau^N = RC$, where R represents the *net* input resistance of the neuron. Synaptic connections between each pair of neurons are represented by conductances (—∿—) proportional to T^S_{ij} (fast synaptic components; eq. 7.1) or T^L_{ij} (slow synaptic components; eq. 7.2). The response function of the slow synapses, $w(t)$ (circles; eqs. 7.7 to 7.9) has a characteristic time constant of τ_L. The fast response time of the network, τ_S, corresponds to the larger of τ^N or the time constant of the fast synapses. The detailed dynamics of the network are described by eq. 7.10.

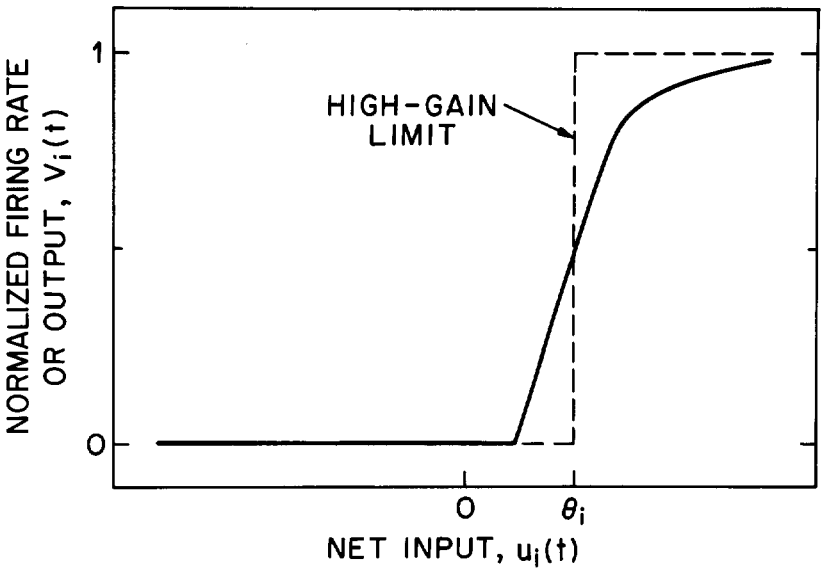

Figure 7.4
Schematic representation of a saturating gain function for a neuron. This function relates the output, or firing frequency of a neuron, $V_i(t)$, to the value of the net input, $u_i(t)$, and the mean operating level, θ_i (eq. 7.11). The output of a neuron is most sensitive to changes in its inputs when $u_i(t) \simeq \theta_i$ (eqs. 7.12 and 7.13).

The temporal relation between the fast and slow synaptic inputs, $h_i^S(t)$ and $h_i^L(t)$, respectively, the total input to the neuron, $u_i(t)$, and the output of the neuron, $V_i(t)$, are illustrated later in fig. 7.6B. The calculations leading to this figure are described later.

The biological interpretation of the short time constant (τ_S) in eq. 7.10 depends on the relative values of the response time, τ^S, of the *fast* synapses compared with the charging time, τ^N, of the neurons. In general, τ_S should be identified with the longest of the two time constants τ^N and τ^S. The emergence of patterns in our networks relies only on the time separation of τ_S and τ_L, i.e., $\tau_S \ll \tau_L$. In practice, a separation of time scales by a factor of approximately four or more is sufficient.

Output Period In the present model the time spent by the network in each embedded state is constant. This time is $t_0 \sim \tau_L$, while the time spent making the transition between two states is $\sim \tau_S$. Thus the period of a cyclic pattern comprised of r states will be $\simeq r \cdot t_0$. The time t_0 is a monotonically decreasing function of the transition strength λ. The precise value of t_0 depends on the value of λ, on the detailed form of the synaptic response function, $w(t)$, and on the length of the pattern. Expressions for t_0, valid for the special case of a very long sequence and for the case of biphasic oscillations, are given in Appendixes 7.B and 7.C.

Neuron Operating Levels In order that the patterns embedded in the T_{ij}^S and the T_{ij}^L synapses emerge as stable outputs of the network, the mean operating value of each neuron must be adjusted so that its output is maximally sensitive to changes in its input. This implies that the difference between the mean operating level of a neuron and the net input to that neuron, averaged over all its possible values, is small. This difference is denoted by $\Delta\theta_i$, where

$$\begin{aligned}\Delta\theta_i &= \theta_i - \frac{1}{2}\left[h_i^S(V_j(t)_{max}) + h_i^S(V_j(t)_{min})\right. \\ &\qquad \left. + h_i^L(V_j(t)_{max}) + h_i^L(V_j(t)_{min})\right] - I_{stim_i}(t) \qquad (7.12)\\ &= \theta_i - \frac{1}{2}\sum_{j=1}^{N}\left(T_{ij}^S + T_{ij}^L\right) - I_{stim_i}(t)\end{aligned}$$

We require that

$$\Delta\theta_i \simeq 0 \qquad (7.13)$$

More precisely, $\Delta\theta_i$ must be small compared to the typical value of the synaptic inputs present while the network is producing a pattern, i.e.,

$\Delta\theta_i \ll J_0$. A similar constraint holds for other associative networks (Little 1974; Hopfield 1982; Bruce, Gardner, and Wallace 1986).

High-Gain Limit The analysis of the dynamic properties of the network is simplified in the limiting case of a network containing two-state model neurons (McCulloch and Pitts 1943). These neurons are either quiescent or fully active, i.e., $V_i(t) = 0, +1$ (fig. 7.4). In this limit the analog circuit equations (eqs. 7.10 and 7.11) are replaced by the difference equations, or update rules,

$$\begin{aligned} V_i(t+\delta t) &= stp\left[h_i^S(t) + h_i^L(t) - \theta_i\right] \\ &= stp\left[\frac{1}{2}\sum_{j=1}^{N}\left(T_{ij}^S\left(2V_j(t)-1\right) + T_{ij}^L\left(2\overline{V_j(t)}-1\right)\right)\right] \end{aligned} \tag{7.14}$$

where the step function, $stp(x)$, is defined by

$$stp(x) = \begin{cases} +1; & x > 0 \\ 0; & x \leq 0 \end{cases}$$

In eq. 7.14 we assumed $\Delta\theta_i = 0$ with $I_{stim_i} = 0$ (eq. 7.13).

The update rules (eq. 7.14) can be implemented either synchronously or asynchronously. In synchronous updating the output of every neuron is changed simultaneously; in this case $\delta t = \tau_S$. In asynchronous updating a neuron is selected at random and its output is updated. In this case τ_S should be identified with the mean update time of the entire network and $\delta t = \tau_S/N$. Asynchronous updating more closely resembles the dynamic behavior of the analog network (eqs. 7.10 and 7.11) and may also provide a more realistic representation of biological systems.

The effect of stochastic noise can be incorporated into the model by replacing the deterministic update rules (eq. 7.14) with probabilistic update rules. A useful example of such rules is given by

$$P[V_i(t+\tau_S) = 1] = \frac{1}{1 + exp[-2\beta(h_i^L(t) + h_i^S(t) - \theta_i)]} \tag{7.15}$$

where $P(V_i = 1)$ is the probability that the ith neuron is firing (Little 1974). The parameter $1/\beta$ plays the role of temperature. It is a measure of the level of stochastic noise in the network; e.g., noise caused by rapid fluctuations in the strength of the synapses (e.g., Dionne 1984). In the limit $\beta \rightarrow \infty$ we recover eq. 7.14.

7.2.3 Adiabatically Varying Energy Function

It has been useful to describe the properties of some associative neural networks in terms of an energy function (Hopfield 1982, 1984; Cohen and Grossberg 1983; Amit et al. 1985a). Strictly speaking, such a function does not exist in our network. The stable outputs do *not* correspond to states that are local minima of an energy function. Nevertheless, we can describe the dynamics of our model in terms of a relaxational process to a local minimum of an adiabatically varying energy function. The parameters of this function depend on the history of the network. The relaxation process occurs on the fast time scale of τ_S, while the underlying energy landscape changes on the slower time scale of τ_L. An appropriate energy function for our network is:

$$\begin{aligned} E &= -\frac{1}{2}\sum_{i=1}^{N}\sum_{j=1}^{N}(2V_i-1)\,T_{ij}^{S}\,(2V_j-1) \\ &\quad -\sum_{i=1}^{N}(2V_i-1)\left(2h_i^L(t)-\sum_{j=1}^{N}T_{ij}^{L}\right) \end{aligned} \tag{7.16}$$

In writing eq. 7.16 we assumed for simplicity that the outputs of the neurons are close to saturation; this corresponds to the high-gain limit (eq. 7.14). The first term in eq. 7.16 is identical to the energy function of the Hopfield's associative network (Hopfield 1982). The embedded states, $V^{\mu,\nu}$, are robust minima of this term. The second term in the energy (eq. 7.16) is a field term that varies with the slow time dependence of $h^L(t)$ (eqs. 7.6–7.9).

The time dependence of the energy landscape is illustrated by the surfaces shown in fig. 7.5. Each cross-point on a surface corresponds to a state of the network. The minima in the surface correspond to the embedded states V^{μ} and $V^{\mu+1}$. The "distance" between two cross-points is equal to the number of neurons whose output is different between the two corresponding states. The path between the states V^{μ} and $V^{\mu+1}$ passes through a set of unstable, intermediate states that are present only during a transition.

After the network has settled into the μth embedded state the field term, $h^L(t)$, initially acts to stabilize the network in this state (fig. 7.5A). As the value of $h^L(t)$ evolves, the energy minimum at the current state in the pattern weakens while that at the next state, $V^{\mu+1}$, grows deeper (fig. 7.5B). Eventually the minimum at V^{μ} disappears and the network makes a rapid transition to the state $V^{\mu+1}$ (fig. 7.5C).

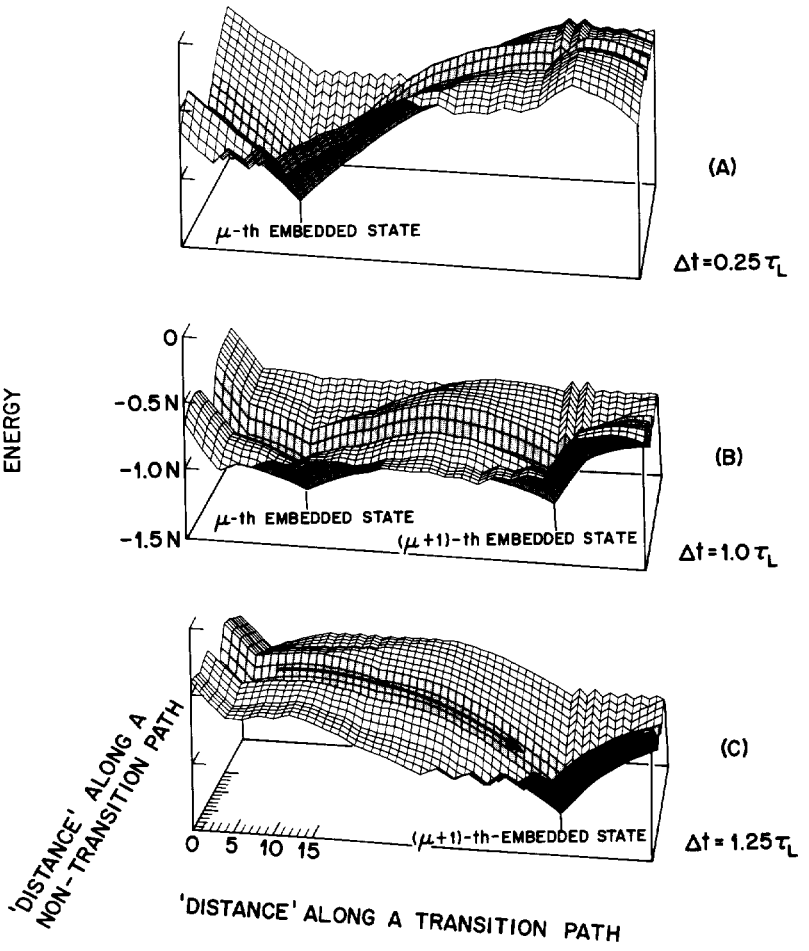

Figure 7.5
The time dependence of the adiabatic energy function for a network operating in the high-gain limit (eq. 7.16). A network containing 64 neurons was constructed to produce a cyclic pattern among seven (orthogonal) embedded states (eqs. 7.1, 7.2, 7.7, 7.12 with $\Delta\theta_i = 0$, and 7.14). The slow synaptic response was $w(t) = 1/\tau_L$ for $\tau_L/2 < t < 3\tau_L/2$ and $w(t) = 0$, otherwise with $\tau_L = 20\tau_S$ and $\lambda = 2$. To form the energy surface we defined a plane in the output space of the network in terms of a path that runs along the output sequence, i.e., $\cdots \rightarrow V^{\mu-1} \rightarrow V^{\mu} \rightarrow V^{\mu+1} \rightarrow \cdots$, and a path that runs approximately orthogonal to this sequence. Each of the cross-points on this plane corresponds to a possible output state of the network. (A) The energy values after the network has made a transition to the μth state. The delayed output corresponds to $\overline{V(t)} \simeq V^{\mu-1}$. The field term in the energy (eq. 7.16) has deepened the minimum at the μth embedded state at the expense of the minimum at the $\mu-1$th state (not shown) and the $\mu+1$th state. (B) The energy values after the delayed output has changed to $\overline{V(t)} \simeq 0.5V^{\mu-1} + 0.5V^{\mu}$. The field term contributes equally to the minima at the μth and the $\mu+1$th embedded states. (C) The energy values after the field term has completely removed the minimum at the μth embedded state, causing the network to make a transition to the $\mu+1$th state. The time spent in each state, $t_0 = 1.25\tau_L$, is in accord with theory.

The existence of an approximate energy function suggests that the output patterns are robust against moderate levels of static and dynamic noise in the network. In the case of stochastic noise (see eq. 7.16), the dynamics of the network are governed by an adiabatically varying free-energy function with a "temperature," $1/\beta$, determined by the amplitude of the noise.

7.2.4 Numerical Simulations and Additional Properties of the Model

A number of general features of the model were examined by numerical simulations and analytical techniques. Simulations were performed using eqs. 7.7 and 7.10 and the gain function

$$V_i(t) = \frac{1}{1 + exp[-2G\,(u_i(t) - \theta_i)]} \tag{7.17}$$

where G is the gain constant. The form of the gain function was chosen because of its similarity to the form of the stochastic update rules (cf. eqs. 7.15 and 7.17). Note, however, that the gain function is part of an analog system of equations (eq. 7.10) that describes *deterministic* dynamics.

Example: A Network with Multiple Patterns To illustrate some of the properties of the model we simulated a network consisting of 100 neurons with nine randomly selected embedded states. These states were arranged as a single isolated state, a cyclic pattern among five states, and a cyclic pattern among three states (fig. 7.1B). We chose a delayed, uniform-averaging function for the slow synaptic response, i.e.,

$$w(t) = \begin{cases} \frac{1}{\tau_L} & \frac{1}{2}\tau_L < t < \frac{3}{2}\tau_L \\ 0 & \text{otherwise} \end{cases}$$

with $\tau_L = 20\tau_S$ and took $\lambda = 2$ (eq. 7.2) and $G^{-1} = J_0/4$ (eq. 7.17). The connection strengths were formed according to eqs. 7.1 and 7.2, and the analog network equations (eqs. 7.7, 7.10, and 7.17, and eq. 7.12 with $\Delta\theta = 0$) were approximated using finite difference methods (Appendix 7.D). We interpreted the values for the neuronal outputs, $V_i(t)$, as the probability that the ith neuron fired in the interval τ_S. These probabilities were used to construct the firing patterns for each neuron.

Figure 7.6A shows the firing pattern obtained from the output of 8 of the 100 neurons; the remainder of the neurons exhibited a similar firing pattern. The network was initially in the isolated, stable state $V^{1,1}$. At time t_1 an external input $I_{stim}(t_1)$, with duration $\Delta t = \tau_L$, was applied

to drive the network into state $V^{1,2}$ of the (ν=2)th pattern. At the later time t_2 a second external input $I_{stim}(t_2)$ was applied to drive the network into a state in the (ν=3)th pattern. The appearance of stable patterns after each input illustrates how the same network can produce multiple output patterns.

Figure 7.6B illustrates the temporal relation between the synaptic inputs to the (i=8)th neuron, $h_8^S(t)$ and $h_8^L(t)$, the net input $u_8(t)$, and the output $V_8(t)$; these values coincide with the output marked by the box in fig. 7.6A. The peak values of $h_8^L(t)$ are approximately twice the amplitude of the peak values of $h_8^S(t)$ because of the choice $\lambda = 2$.

In the above simulation the output of each neuron is either quiescent or firing near its maximum rate. This feature of the output behavior results from the saturation characteristics of the gain function (eq. 7.17) chosen for this example. Other choices for a gain function can lead to stable output patterns in which the firing rate of the neurons does not saturate in each of the embedded states.

Maximum Number of Embedded States A network can contain several patterns. The total number of embedded states in these patterns, p, is

$$p = \sum_{\nu=1}^{q} r(\nu) \tag{7.18}$$

(eqs. 7.1 and 7.2). The value of p is limited to

$$p < \alpha_c N \tag{7.19}$$

where the coefficient α_c depends on the length and topology of the embedded patterns, the transition strength λ, and the form of the slow synaptic response function $w(t)$. When $w(t)$ is given by a simple time delay, i.e., $w(t) = \delta(t - \tau_L)$, the value of the coefficient is $\alpha_c \simeq 0.3$ ($\lambda = 1$ to 2). This value is larger than the value $\alpha_c = 0.14$ for Hopfield's associative memory (Amit et al. 1985b; Crisanti, Amit, and Gutfreund 1986; see also Gutfreund and Mézard 1988). When $w(t)$ is represented by a smoothly varying function of time, the value of the coefficient is reduced to $\alpha_c \lesssim 0.1$.

The input to each neuron will contain a static noise term of order $\sqrt{p/N}$ when the number of embedded states is close to its maximum value. This noise may enhance the transitions between the embedded states. This enhancement, in turn, will reduce the minimum value of the transition strength necessary to generate patterns to a value $\lambda \lesssim 1$.

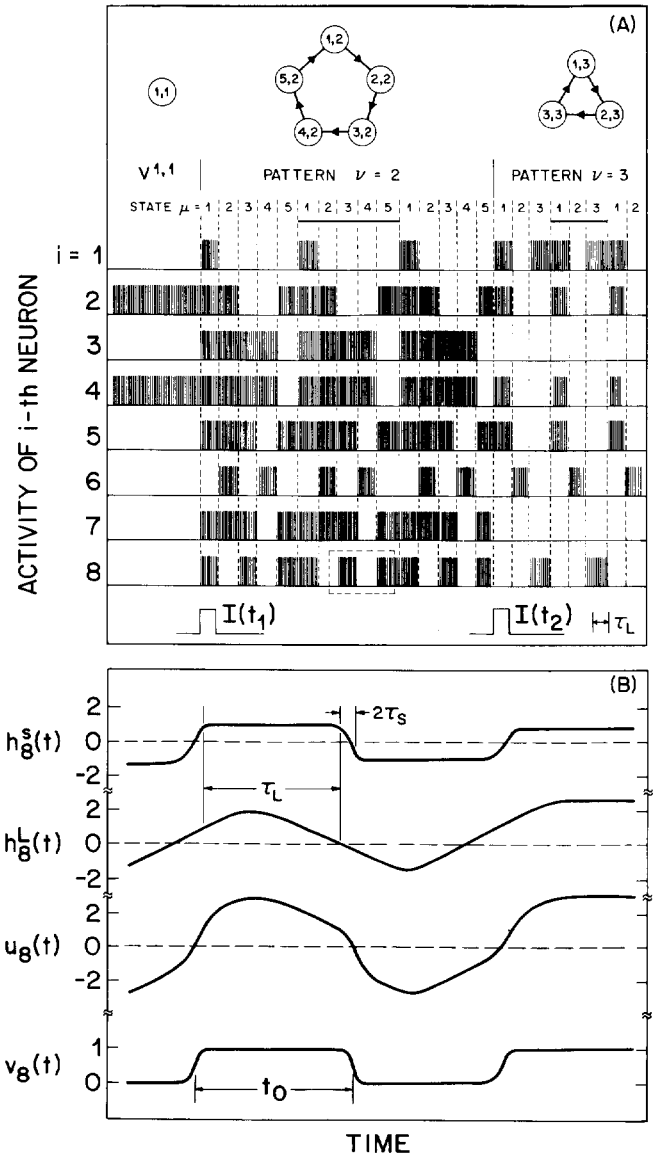

Figure 7.6
Simulation of a network containing 100 neurons with nine embedded states; see text for details. The heavy lines at the top of the figure correspond to the output period of each pattern. (A) The firing pattern calculated from the outputs $V_i(t)$ of 8 of the 100 neurons. The network was initialized in state $V^{1,2}$. At time t_1 an external input $I_{stim}(t_1)$ was applied for a time τ_L. This input drove the network into state $V^{2,1}$ and thus initiated the (ν=2)th pattern. Similarly, the external input $I_{stim}(t_2)$ was applied at time t_2 to drive the network into state $V^{1,3}$ and initiate the (ν=3)th pattern. (B) Details of the dynamic behavior of the (i=8)th neuron for the period of time delineated by the box in (A). Shown are the inputs from the fast synaptic components, $h_8^S(t)$, the inputs from the slow synaptic components, $h_8^L(t)$, the net synaptic input, $u_8(t)$, and the output of the neuron, $V_8(t)$.

Eliminating Synaptic Connections The model we described assumes the existence of synaptic connections between all pairs of neurons. Biological networks may contain a much smaller set of connections either intrinsically or as a result of damage or disease. Will our network function with a reduced set of connections?

The performance of the network model is only marginally affected when up to 50% of the fast components of the synaptic connections (T_{ij}^S) are eliminated at random. The main effect of eliminating a fraction, c^S, of these components is to proportionately decrease the maximum number of states that can be embedded in the network (see eq. 7.18). Eliminating the slow components of the synaptic connections (T_{ij}^L) has a relatively small effect on this number (except for the case of $w(t) \simeq \delta(t-\tau_L)$). However, random elimination of a fraction, c^L, of the T_{ij}^L synapses will decrease the ability of the network to make a transition between the embedded states. This decrease can be offset by a compensating increase in the value of λ. The effective transition strength, λ^{eff}, in this case is

$$\lambda^{eff} \simeq \lambda \frac{1-c^L}{1-c^S} \tag{7.20}$$

The value of λ^{eff} must be greater than 1, implying that

$$\lambda \gtrsim \frac{1-c^S}{1-c^L}$$

Analog Versus Two-State Neurons The analog character of the model neurons does not play a major role in our network, as it does not in Hopfield's network (Hopfield 1984). Patterns are reliably generated when the gain of the neuron, G in eq. 7.17, is chosen to be larger than a critical value, G_c. The value of G_c^{-1} is approximately equal to the value of the typical net input to the neuron, i.e., $G_c^{-1} \simeq J_0$. Its precise value depends on both the number of embedded states and on the topology of the patterns. At moderate values of gain, $G \gtrsim G_c$, the transitions between the embedded states are enhanced. This reduces the minimum value of the transition strength to $\lambda < 1$, similar to the effect found using two-state neurons with the stochastic update rules (eq. 7.15).

7.2.5 Biphasic Oscillations

A particularly simple pattern is one that oscillates between an embedded state $V^\mu = \{V_i^\mu\}_{i=1}^N$ and its antiphase, $(1-V^\mu)$, in which the quiescent neurons are now firing and vice versa. Multiple patterns of this form

can be embedded in our network. The resulting synaptic strengths are (eqs. 7.1 and 7.2)

$$T_{ij}^S = \frac{J_0}{N} \sum_{\mu=1}^{q} (2V_i^\mu - 1)(2V_j^\mu - 1), \qquad i \neq j, \quad J_0 > 0 \tag{7.21}$$

and

$$T_{ij}^L = \lambda \frac{J_0}{N} \sum_{\mu=1}^{q} [2(1 - V_i^\nu) - 1](2V_j^\mu - 1) = -\lambda T_{ij}^S, \quad i \neq j, \ \lambda \geq 1 \tag{7.22}$$

where k is the number of patterns and $T_{ii}^S = T_{ii}^L = 0$.

Although the synaptic components T_{ij}^L are, in general, asymmetric (i.e., $T_{ji}^L \neq T_{ij}^L$) they are symmetric for the special case of biphasic oscillations (cf. eqs. 7.2 and 7.21). The relation $T_{ij}^L = -\lambda T_{ij}^S$ implies that the connections between each pair of neurons correspond either to short-term reciprocal inhibition followed by delayed excitation, or to short-term reciprocal excitation followed by delayed inhibition. Note that even in this case, the symmetry in both the T_{ij}^S and the T_{ij}^L components may be broken, e.g., by eliminating synaptic connections, without strongly affecting the output behavior of the network.

In Appendix 7.C we derive an analytical expression (eq. 7.40) that relates the duration of each state, t_0, to the slow synaptic response time, τ_L, the transition strength, λ, and the form of the synaptic response function, $w(t)$. We use this expression to calculate the dependence of t_0 on λ for a number of response functions (Table 7.3).

7.3 Central Pattern Generator in Tritonia

In this section we draw a connection between our model and detailed measurements on the central pattern generator controlling the swim rhythm in the mollusc *Tritonia diomedea*. A description of the swim rhythm can be found in the previous chapter.

The CPG in *Tritonia* consists of four neural groups, denoted by VSI-A, VSI-B, C2, and DSI. [3] The VSI neurons are the ventral swim in-

[3] There are three DSI neurons connected to each other by strong, fast-acting excitatory connections. Following Getting (1981), we group all three as a single neuron. The role of the DSI neurons as single neurons pertains to the turning on and off of the cyclic response (Getting and Dekin 1985), a topic we do not consider in detail. The fast, excitatory interaction among the DSI neurons may be incorporated by including a nonzero self-coupling term, i.e., T_{22}^S, into the model. An analysis shows that the inclusion of this term has a relatively minor effect on the output of the network (Kleinfeld and Sompolinsky 1988).

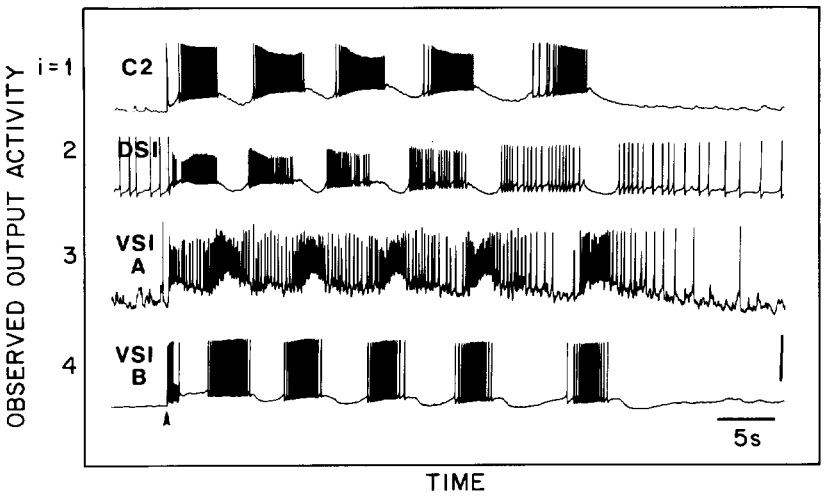

Figure 7.7
The output activity simultaneously measured from a C2, DSI, VSI-A, and VSI-B neuron in an isolated brain preparation from *Tritonia*. These neurons comprise the CPG that controls the escape swim sequence. Their output corresponds to $V_1(t)$, $V_2(t)$, $V_3(t)$, and $V_4(t)$, respectively, in the analysis presented in section 7.3. The arrow indicates the initiation of the sequence. Note that in the present work we are concerned only with the oscillatory behavior of the CPG, and not with the gradual dephasing that leads to its turning off. Vertical bar: 50 mV for C2, DSI, and VSI-B and 25 mV for VSI-A. Adapted from Getting (1983b).

terneurons, C2 is a cerebral neuron, and DSI represents the dorsal swim interneurons. The observed output pattern consists of bursting output from VSI-A and VSI-B neurons alternating with bursts from the C2 and DSI neurons (figs. 7.7, 6.1A). The time interval between consecutive action potentials within a bursting state is $\sim$ 0.01 *sec* to 0.1 *sec*, and the duration of each state is, on average, approximately 5 *sec*.

Of primary importance is Getting's observation that some of the synaptic connections have components that act on two different time scales. For example, the synaptic input to C2 from DSI shows a rapid excitatory response followed by a much slower inhibitory response (figs. 7.8, 6.5B). The observed form of the synaptic response in *Tritonia* suggests that there is an analogy between the mechanism for oscillations in our theory and the biological mechanism for oscillations in this CPG.

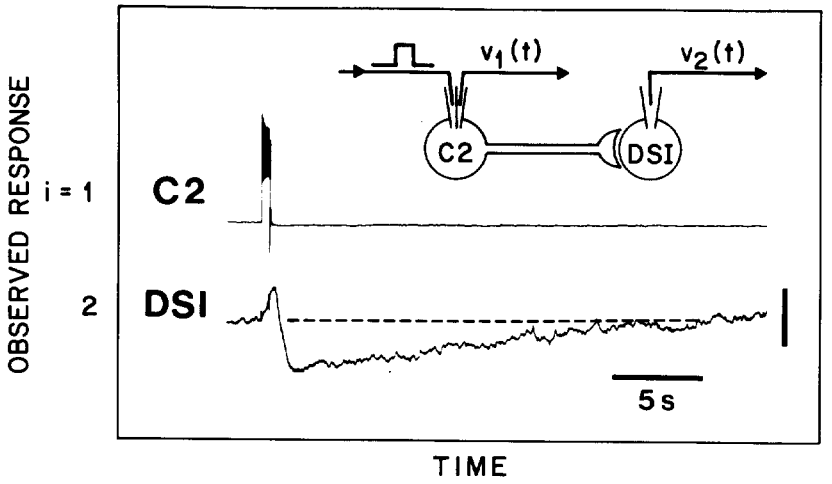

Figure 7.8
An example of the synaptic interaction between two neurons in the CPG in *Tritonia*. Shown is the presynaptic activity measured in the C2 neuron, $v_1(t)$, and the postsynaptic response measured in a DSI neuron, $v_2(t)$, as the result of a short pulse of current injected into C2. The measurement was performed under conditions that insured that only monosynaptic connections contributed to the observation. The observed response applies to two out of the three DSI neurons (DSI_B and DSI_C); the other DSI neuron (DSI_A) exhibits only a slow response. The area under the initial, positive-going response corresponds roughly to T_{21}^S; that under the slowly decaying response corresponds to T_{21}^L. The time dependence of the slow decay corresponds to the time dependence of the slow synaptic response function, $w(t)$. Vertical bar: 40 mV for C2 and 2 mV for DSI. Adapted from Getting (1981).

The focus of our analysis is to determine if the properties of the CPG in *Tritonia* support the mechanism we propose for generating patterns. Specifically, we ask:

1. Are the observed synaptic strengths consistent with those calculated from the form of the observed output states?
2. Are the simple update rules (eq. 7.14) sufficient to demonstrate the emergence of an oscillatory output that qualitatively resembles the observed pattern?
3. Is the period of the observed output pattern accounted for in terms of the magnitude and form of the observed slow synaptic response?
4. Are the observed operating levels of the neurons consistent with the constraint that their output is maximally sensitive to changes in their net synaptic input (eq. 7.13)?

It is important to emphasize that we are not attempting to reproduce accurately all of the details of the output behavior of *Tritonia*. For this one would necessarily include the detailed biophysical properties of the neurons and their synaptic connections, as was discussed in chapter 6.

7.3.1 Synaptic Connections

The observed output sequences will be approximated by an oscillation between a state V^+ and its antiphase $V^- \equiv (1 - V^+)$, where

$$V^+ = \begin{pmatrix} \text{activity of} & C2 \\ & DSI \\ & VSI-A \\ & VSI-B \end{pmatrix} = \begin{pmatrix} +1 \\ +1 \\ 0 \\ 0 \end{pmatrix} \quad \text{and}$$

$$V^- = \begin{pmatrix} 0 \\ 0 \\ +1 \\ +1 \end{pmatrix} \tag{7.23}$$

These states are used as the stable embedded states in our model. The short-term connection strengths T_{ij}^S, and the long-term connection strengths T_{ij}^L, deduced from the outputs V^+ and V^- (eqs. 7.21 to 7.23), are shown in table 7.1. Note that these matrices contain *all* possible connections that can be present between pairs of neurons.

How do the predicted synaptic strengths compare with the observed values? The strength of a synaptic connection is proportional to the

Fast Synaptic Components, T_{ij}^{S}		Slow Synaptic Components, T_{ij}^{L}
Theory	$\frac{J_0}{4}\begin{bmatrix} 0 & \mathbf{+1} & -1 & \mathbf{-1} \\ \mathbf{+1} & 0 & \mathbf{-1} & \mathbf{-1} \\ \mathbf{-1} & \mathbf{-1} & 0 & \mathbf{+1} \\ -1 & -1 & +1 & 0 \end{bmatrix}$	$j = 1\ \ 2\ \ 3\ \ 4$ $\lambda\frac{J_0}{4}\begin{bmatrix} 0 & -1 & +1 & +1 \\ \mathbf{-1} & 0 & +1 & +1 \\ \mathbf{+1} & \mathbf{+1} & 0 & -1 \\ \mathbf{+1} & +1 & -1 & 0 \end{bmatrix}$ $i = 1, 2, 3, 4$
Observed[a]	$\frac{J_0}{4}\begin{bmatrix} 0 & +1 & \bullet & -1 \\ +1 & 0 & -1 & -1 \\ -1 & -1 & 0 & +1 \\ \bullet & -1 & \bullet & 0 \end{bmatrix}$	$C\ \ D\ \ VA\ \ VB$ (pre / post) $\lambda\frac{J_0}{4}\begin{bmatrix} 0 & \bullet & \bullet & \bullet \\ -1 & 0 & \bullet & \bullet \\ +1 & +1 & -0 & \bullet \\ +1 & \bullet & \bullet & -0 \end{bmatrix}$ C, D, VA, VB

(a) Abstracted from the data of Getting (1981, 1983b); see text for details. Dots (•) indicate synaptic connections that are not present in *Tritonia*; their value is taken to be zero for purposes of calculation [*e.g.*, Eqs. (3.3) to (3.5)].

Table 7.1
Synaptic connection strengths for *Tritonia*.

time integral of the conductance changes induced in the postsynaptic neuron by a short ($t < \tau_S$) pulse of activity in the presynaptic neuron. These integrals can be *estimated* from measurements of the potentials induced in the postsynaptic neuron by a short ($t < \tau_S$) burst of action potentials in the presynaptic neuron. The action potentials in the postsynaptic neurons must be suppressed so that only direct interactions, i.e., monosynaptic pathways, contribute to the observed response.

The strength of the observed synaptic components T_{ij}^S and T_{ij}^L were estimated from the pairwise measurements reported by Getting (1981, 1983b, Appendix 6.B) (e.g., fig. 7.8). We grouped the data according to the time scale of the observed synaptic response. Synaptic components that decayed on a time scale less than 1 *sec* were designated as fast, whereas synaptic components that decayed on a time scale substantially greater than 1 *sec* were designated as slow. For this simple system we need only consider the *sign* of the measured response, and thus detailed variations between the values of the individual T_{ij}^S connection strengths and between the T_{ij}^L connection strengths were neglected. We did not include synaptic components whose strengths were considerably weak in comparison with the other components. For example, the observed synaptic connection from C2 to DSI (fig. 7.8) was parameterized by the values $T_{21}^S = T_0/4$ and $T_{21}^L = -\lambda T_0/4$.

The complete set of connection strengths T_{ij}^S and T_{ij}^L that we abstracted from Getting's data are summarized in table 7.1; note that theoretically possible connections that are not present in *Tritonia* are taken as zeros. This set was also used to construct the equivalent circuit shown in fig. 7.9. Ambiguities in our assignment of the connection strengths will be discussed at the end of this section.

The observed transition strength, λ (eq. 7.2), was determined by calculating the average magnitude of the fast synaptic components relative to that of the slow components. This determination contains a large uncertainty, in part because of the difficulty in separating the fast and slow contributions to the measured synaptic response. We roughly estimate

$$\lambda = 5 \text{ to } 10 \tag{7.24}$$

The signs of the experimentally observed synaptic strengths match those of the theoretically predicted strengths (table 7.1). Three of the possible twelve synaptic connections show both a short-term and a long-term response. Connections $(i,j) = (3,1)$ and $(i,j) = (3,2)$ both show short-term inhibition followed by a long-term excitation, while connection $(i,j) = (2,1)$ shows short-term excitation followed by long-term

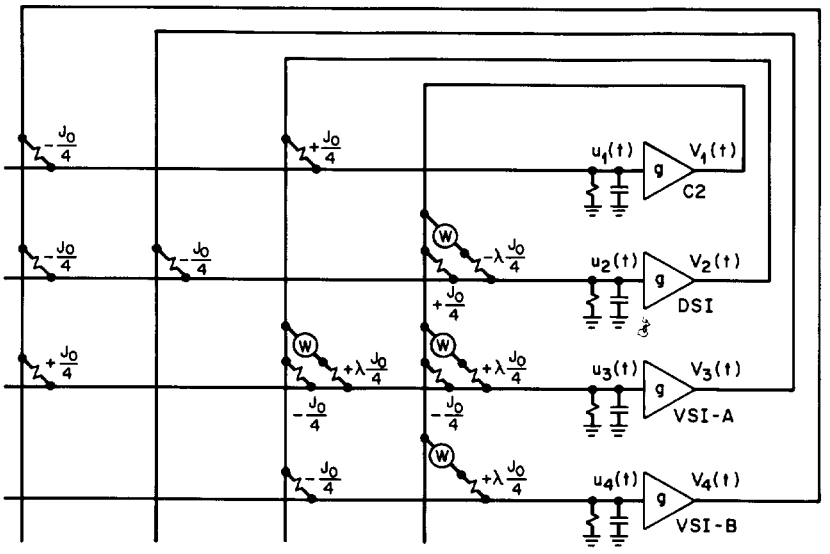

Figure 7.9
Schematic representation of the equivalent circuit for the analog network model describing the CPG in *Tritonia*; symbols as in fig. 7.3. The synaptic strengths contained in this circuit correspond to the observed connections T_{ij}^S and T_{ij}^L (table 7.1).

inhibition. The form of these three connections illustrates how the sign of the net synaptic input to a neuron can change over time.

7.3.2 Network Dynamics

We now examine whether the observed network parameters in *Tritonia* indeed give rise to rhythmic output in the network model. We begin our analysis with a simplified model that accents the role of the observed synaptic connections in generating stable oscillations. For this simplified analysis we use two-state neurons with synchronous update rules (eq. 7.14 with $\delta t = \tau_s$) and a delta function delay for the slow synaptic response function, i.e., $w(t) = \delta(t - \tau_L)$. A more detailed analysis, using analog model neurons and a smooth synaptic response function, is presented later.

Immediately after the network has stabilized in the embedded state V^+, the output of the ith neuron is $V_i(t) = V_i^+$, but the delayed output is $\overline{V_i(t)} = V_i(t - \tau_L) = V_i^-$. The output of the ith neuron after the next update is

$$
\begin{aligned}
V_i(t+\tau_S) &= stp\left[\frac{1}{2}\sum_{j=1}^{4} T_{ij}^S\,(2V_j^+ - 1) + T_{ij}^L\,(2V_j^- - 1)\right] \qquad (7.25)\\
&= stp\left[\frac{J_0}{8}\begin{pmatrix} 0 & +1 & 0 & -1 \\ +1 & 0 & -1 & -1 \\ -1 & -1 & 0 & +1 \\ 0 & -1 & 0 & 0 \end{pmatrix}\begin{pmatrix} +1 \\ +1 \\ -1 \\ -1 \end{pmatrix}\right.\\
&\qquad \left. +\lambda\frac{J_0}{8}\begin{pmatrix} 0 & 0 & 0 & 0 \\ -1 & 0 & 0 & 0 \\ +1 & +1 & 0 & 0 \\ +1 & 0 & 0 & 0 \end{pmatrix}\begin{pmatrix} -1 \\ -1 \\ +1 \\ +1 \end{pmatrix}\right]\\
&= stp\left[\frac{J_0}{8}\begin{pmatrix} 2 \\ 3+\lambda \\ -3-2\lambda \\ -1-\lambda \end{pmatrix}\right] = \begin{pmatrix} +1 \\ +1 \\ 0 \\ 0 \end{pmatrix} \quad \text{for} \quad \lambda > 0\\
&= V_i^+
\end{aligned}
$$

Thus the output of the network is stable on the time scale of τ_S. After the network has remained in the state V^+ for a time τ_L, the delayed output changes to $\overline{V(t+\tau_L)} = V(t) = V^+$. The output of the ith neuron after the next update is

$$V_i(t+\tau_L+\tau_S) = stp\left[\frac{1}{2}\sum_{j=1}^{4} T_{ij}^S\,(2V_j^+ - 1) + T_{ij}^L\,(2V_j^+ - 1)\right] \quad (7.26)$$

$$= stp\left[\frac{J_0}{8}\begin{pmatrix} 2 \\ 3-\lambda \\ -3+2\lambda \\ -1+\lambda \end{pmatrix}\right] = \begin{pmatrix} +1 \\ 0 \\ +1 \\ +1 \end{pmatrix} \quad \text{for } \lambda > 3$$

The network is now in a mixed, unstable state. Using this new value for the current state in the update procedure gives

$$V_i(t+\tau_L+2\tau_S) = stp\left[\frac{1}{2}\sum_{j=1}^{4} T_{ij}^S\,(2V_j(t+\tau_L+\tau_S)-1) + T_{ij}^L\,(2V_j^+ - 1)\right] \quad (7.27)$$

$$= stp\left[\frac{J_0}{8}\begin{pmatrix} -2 \\ -1-\lambda \\ 1+2\lambda \\ 1+\lambda \end{pmatrix}\right] = \begin{pmatrix} 0 \\ 0 \\ +1 \\ +1 \end{pmatrix}$$

$$= V_i^-$$

The network has now completed a transition from the state V^+ to the state V^-. It will remain in this state for a time $t_0 \simeq \tau_L$, after which the cycle will repeat itself. The output of the network will oscillate only if the transition strength is $\lambda > 3$ (eq. 7.26). This value is consistent with the observed value (eq. 7.24) of $\lambda = 5$ to 10.

The simplified analysis presented above suggests that the observed connection strengths can give rise to rhythmic output in the model network. We now examine the steady-state behavior of the network model for *Tritonia* (fig. 7.9) using analog dynamics and a synaptic response function that is a smooth function of time. The observed form of the response function, $w(t)$, is approximated by an exponential, i.e.,

$$w(t) = \begin{cases} \frac{1}{\tau_L} e^{-t/\tau_L} & 0 \le t < \infty \\ 0 & \text{otherwise} \end{cases}$$

The analog equations (eqs. 7.7, 7.10, and 7.17, and eq. 7.12 with $\Delta\theta_i = 0$) were simulated (Appendix 7.D) using the observed connection strengths

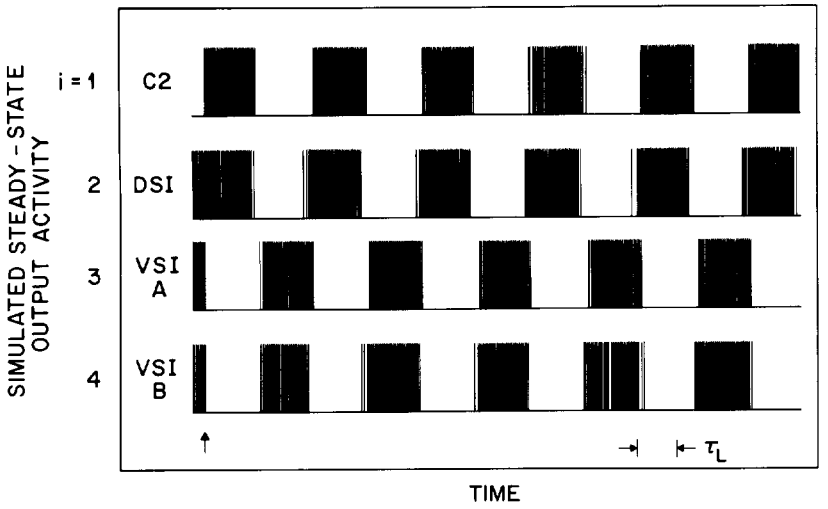

Figure 7.10
Simulated output activity from the analog network model describing the CPG in *Tritonia* (fig. 7.9). The arrows indicate the start of the simulated output from the initial states $V(t < 0) = \overline{V(t < 0)} = (\ 0\ 1\ 1\ 1\ )^T$. The network equations were simultated using the observed values of T_{ij}^S and T_{ij}^L; see text for details.

T_{ij}^S and T_{ij}^L (table 7.1), the above form for $w(t)$, $\tau_L = 10\tau_S$, and $G^{-1} = J_0/10$ for the gain parameter (eq. 7.17). Stable oscillations of the form described by the previous simplified analysis (eqs. 7.25 to 7.27) were observed. The output activity for the transition strength $\lambda = 10$ is shown in fig. 7.10.

The period observed for the output of the CPG in *Tritonia* is $2t_0 =$ 6 *sec* to 10 *sec* (fig. 7.7), while the time constant for the slow synaptic response (eq. 7.9) lies in the range $\tau_L = 2$ *sec* to 5 *sec* (Appendix 6.B). Is this value for the period accounted for by the model? As discussed in the previous section, the predicted value for t_0 depends on the values of τ_L and λ and on the form of the response function $w(t)$. In Table 7.3 we give an analytic expression for t_0 appropriate for the above weighting function, from which we find $2t_0 = 1$ *sec* to 4 *sec* for values of τ_L in the range 2 *sec* to 5 *sec* and λ in the range 5 to 10. However, this estimate of $2t_0$ may be inaccurate; the effective value of the λ should be significantly smaller than the observed value because of the relatively

large number of T_{ij}^L connections that are absent. We checked this point by simulating the analog equations for the network (see above) with different values for λ; the dependence of $2t_0$ on λ is shown in fig. 7.11. As expected, the theoretical range of values for the duration was longer, i.e., we calculated $2t_0 = 5$ *sec* to 20 *sec*. The estimate compares favorably with the experimentally observed range $2t_0 = 6$ *sec* to 10 *sec* ($2t_0 = 2.5\tau_L \simeq 5$ *sec* to 12 *sec* for $\lambda = 10$; fig. 7.10).

7.3.3 Neuron Operating Levels

We now consider the issue of the mean operating level of each neuron, θ_i. As discussed in section 7.2, the mean operating levels should obey the relation given by eq. 7.13 in order that the firing rate of each neuron is most sensitive to changes in the value of its input. For *Tritonia*, this relation becomes

$$\theta_i \simeq I_{stim_i} + \frac{1}{2}\sum_{j=1}^{4}(T_{ij}^S + T_{ij}^L) = I_{stim_i} + \frac{J_0}{8}\begin{pmatrix} 0 \\ -1-\lambda \\ -1+2\lambda \\ -1+\lambda \end{pmatrix} \qquad (7.28)$$

with $\lambda = 5$ to 10. We first consider the DSI neuron ($i = 2$): eq. 7.28 implies either that this neuron should be in a tonically excited state when it is functionally isolated from its synaptic inputs ($\theta_2 < 0$), or that this neuron requires an external excitatory input for the CPG to be active ($I_{stim_i} > 0$). A combination of both of these features is observed *in vivo* (Getting 1983a; Getting and Dekin 1985). The DSI neurons fire tonically, although at a reduced rate, in isolation (Getting 1983a). Activation of the CPG in *Tritonia* requires an effective excitatory input to the DSI neurons (Getting and Dekin 1985). After this input is removed the output from the CPG gradually dephases and the CPG becomes inactive. We next consider the VSI neurons. In the absence of synaptic inputs and external inputs, the output of VSI-B is expected to be quiescent ($\theta_4 > 0$). This result is in agreement with observation (Getting 1983b).

The problematic neuron is VSI-A, which is not known to receive an external input while the CPG is producing oscillatory output. Thus, according to eq. 7.28, VSI-A should have a positive operating level. In practice, VSI-A exhibits a weak tonic output when it is functionally isolated (Getting 1983a). Violation of eq. 7.28 suggests, by the arguments of section 7.2, that the oscillations in the output of VSI-A will be less robust than those of the other neurons. This conclusion is consistent with the observed outputs, i.e., the relative change in the firing rate of

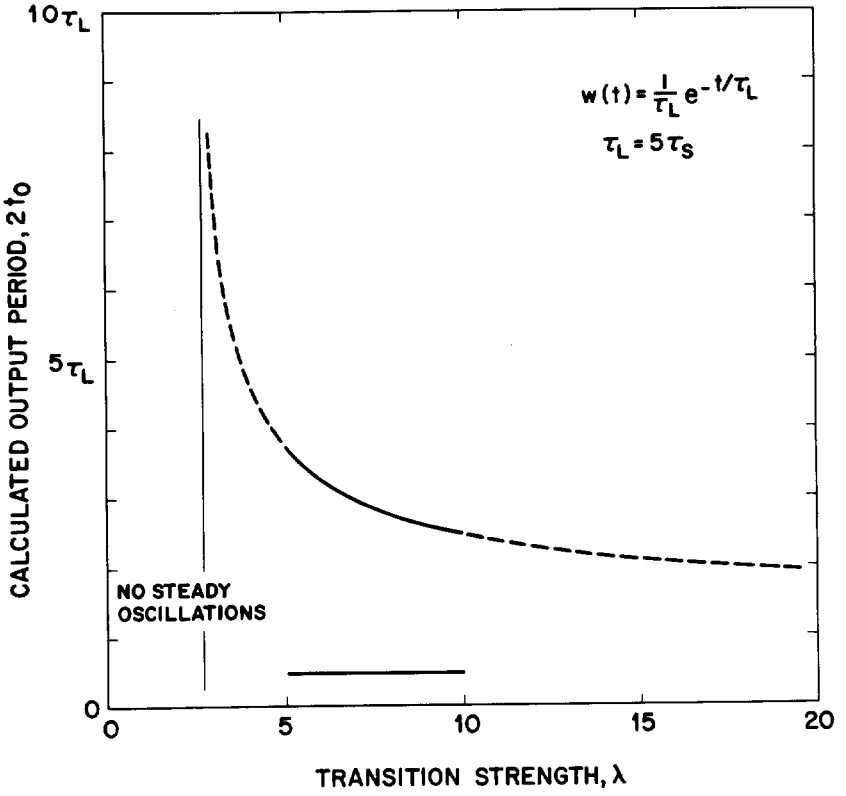

Figure 7.11
The output period, $2t_0$, of the analog network model for *Tritonia* (fig. 7.9) as a function of the average transition strength λ. A period of $2t_0 \simeq 6$ *sec* to 10 *sec*, roughly equivalent to $2\tau_L \lesssim 2t_0 \lesssim 5\tau_L$, corresponds to the period observed in *Tritonia* (fig. 7.7). The solid line delimits the range of values for λ estimated from the measured connection strengths (e.g., fig. 7.8). For a value of λ near 10, the period deduced from the model is in accord with the observed period. The spectrum $2t_0(\lambda)$ was determined by simulating the network equations using the observed values of T_{ij}^S and T_{ij}^L; see text for details.

VSI-A during the oscillations is smaller than that of the other neurons in the CPG (fig. 7.7). Note also that this neuron is weakly coupled to other neurons in the network (table 7.1). Hence VSI-A is expected to play a relatively minor role in the CPG, as noted previously (Getting and Dekin 1985).

7.3.4 Reexamination of the Connection Strengths

We consider in detail several assumptions that were made in assigning the T_{ij}^S and T_{ij}^L synaptic strengths. The connection from DSI to C2 exhibits short-term excitation followed by a much weaker long-term excitation. We ignored the weak long-term effect; thus $T_{12}^S = +J_0/4$ and $T_{12}^L = 0$. A similar choice was made for the inhibitory connection from VSI-B to the DSI, i.e., $T_{24}^S = -J_0/4$ and $T_{24}^L = 0$. Both of these relatively weak long-term components are believed to contribute primarily to the turning off of the CPG (Getting, unpublished), an effect we do not consider at present.

The synaptic connection from the DSI to VSI-A exhibits two short-term responses as well as a long-term response. Short-term inhibition is preceded by a relatively shorter period of excitation, with the pair followed by long-term excitation. We ignored the initial excitation and assigned $T_{32}^S = -J_0/4$ and $T_{32}^L = +\lambda J_0/4$. A different choice for the sign of T_{32}^S does *not* significantly affect the output pattern of the network.

The synaptic coupling between VSI-A and VSI-B could not be measured under conditions that suppressed possible indirect interactions, i.e., polysynaptic pathways, between these neurons (Getting 1983b). Externally exciting VSI-B caused VSI-A to fire weakly; we assigned $T_{34}^S = +J_0/4$ and $T_{34}^L = 0$. Externally exciting VSI-A caused a slow depolarization in VSI-B, but did not cause it to fire. We chose $T_{43}^S = T_{43}^L = 0$, but one cannot rule out the possibility $T_{21}^S = 0$ and $T_{21}^L > 0$. An analysis of the network dynamics, similar to that performed above (eqs. 7.25 to 7.27), shows that stable oscillations persist as long as T_{43}^L is weaker (by approximately 25% or more) than the other slow synaptic components.

7.4 Discussion

7.4.1 Properties of the Model

We have presented an associative neural network model that is capable of generating patterns of linear sequences or cyclic sequences of states. The patterns are stored in synaptic connections that have two components. One component, with a fast response time, stabilizes the individ-

ual states that comprise a pattern. The second component, with a slow response time, triggers the transitions between the consecutive states in a pattern.

The present model for generating output patterns has several attractive structural and functional features. It describes pattern generation in arbitrarily large, highly interconnected networks. The model does not necessarily rely on specific organization of the connections (e.g., a ring-like organization). The synaptic connections are not symmetric and the network can contain both excitatory and inhibitory synapses.

The distributed nature of the network and the inherent feedback between neurons endows the network with a high robustness. Removing at random as many as half of the synaptic connections does not affect the generation of patterns, except for reducing the number of states that can be embedded, i.e., used to form patterns, in the network. The patterns are stable to moderate levels of stochastic noise. An individual pattern can be accessed in an associative manner, such as by an input that only partially resembles one of the embedded states in the pattern. Finally, the model employs a simple relation between the output patterns and the synaptic connections.

The network can produce multiple patterns of different lengths and topologies. Neither the embedded states nor the patterns need to have any specific structure. In fact, the model works optimally with patterns of random, uncorrelated states. The number of states that can be embedded in the network scales linearly with the number of neurons in the network.

The present model does not use pacemaking cells or a system clock to generate patterns. Rather, the sequential output results from the interplay between fast synaptic components, which stabilize the embedded states, and slow synaptic components, which trigger the transitions. The detailed form of the slow synaptic response function is not critical. It can be either a sharp function of time, such as a delta function delay, or a smooth function, such as a low-pass filter. In particular, the form of the slow synaptic response may fluctuate from one synapse to another. The network will function properly so long as most of the slow components have roughly the same time constant.

Amari (1972), Fukushima (1973), and Kohonen (1980) have proposed models for generating temporal patterns in which *all* of the synaptic connections are formed according to rules similar to the rule we use to form the *slow* synaptic components (eq. 7.2). In contrast to the model we present, these models function as finite state machines in which the

existence of temporal patterns is dependent upon an internal synchronizing clock and on synaptic delays that are sharp functions of time.[4]

Initiation of a Pattern A particular output pattern can be selected by an external input, I_{stim_i} (eq. 7.10 and fig. 7.3). This input must place the network in an initial state that has a substantial overlap with one of the embedded states in the desired pattern. The network will rapidly relax to this embedded state and subsequently proceed to generate the full pattern. The external input need be present only for a brief time, $\Delta t \lesssim \tau_L$, if the mean operating levels of the neurons are properly matched to their average synaptic input (eq. 7.13). Otherwise, lasting inputs may be required to maintain the output pattern.

A variety of mechanisms exist for terminating a cyclic output sequence. A direct way is to use an external input to drive the network into a state that is not part of the pattern (fig. 7.1B). Similarly, raising the mean operating level, θ_i, of the majority of the neurons will halt the output. An indirect way of ending a pattern is to change the value of the transition strength, λ, to a value outside the range of stability (see Appendixes 7.B and 7.C). The output will gradually dephase until the pattern has effectively decayed. A similar decay will occur for an output pattern that is initiated in a network in which the number of embedded states is above its maximum value (α_c, see eq. 7.18).

Modulation of the Output Period The output period of a pattern is proportional to t_0, the time spent by the network in each state. This time scales linearly with the time constant, τ_L, of the slow synaptic response, but is a decreasing function of the transition strength, λ.[5] Thus a change in either τ_L or λ will induce a substantial change in the output period. The value of t_0, and thus the period, is fairly insensitive to changes in either the operating level, θ_i, or the gain, G, of the neurons. A change in either of these parameters will change t_0 by at most the value of $\sim \tau_S$.

Patterns of Correlated States We employed formalized Hebb (1949) learning rules to specify the strength at the synaptic connections in terms

[4] A model that relies on time-dependent synaptic strengths to produce rhythmic output has been suggested by Peretto and Niez (1986). Dehaene, Changeux, and Nadel (1987) considered a model for temporal sequences, in the context of bird song, that uses high-order synapses. A model in which a rhythmic output is driven by stochastic noise has been proposed by Buhmann and Schulten (1987).

[5] The period of the output is independent of λ when the response function of the slow synapses is given by a delta function time delay, i.e., $w(t) = \delta(t - \tau_L)$; see tables 7.2, 7.3.

of the embedded states. These rules are appropriate when the overlaps between the states in a pattern are small. However, when the states are correlated, i.e., when they have substantial overlaps, the number of states that can be embedded in the network is severely limited.

Correlations among output states are expected in biological systems. For example, some regions of the vertebrate nervous system exhibit low levels of activity, i.e., only a small fraction of the neurons fire simultaneously (Shepherd 1979). The large fraction of neurons with quiescent outputs suggests that the embedded states of these networks are substantially correlated. Correlations among the embedded states exist naturally in problems of pattern and speech recognition.

Rules that are suitable for embedding correlated states in our network are presented in Appendix 7.A. With these rules, the number of states that can be embedded scales linearly with the size of the network, independent of the correlations. The underlying mechanism for pattern generation with these new rules is the same as with the formalized Hebb (1949) rules.

Overlapping Patterns A limitation of the model we described is its inability to generate overlapping patterns. Consider a network in which two of the patterns share the same embedded state, e.g., fig. 7.12. When the output of the network reaches the state in common to both patterns ($(\mu,\nu) = (6,1)$ in fig. 7.12), there is an ambiguity as to which state occurs next in the pattern. The reason for this ambiguity is that only transitions between consecutive states are encoded in the synaptic connections. This problem can be rectified by encoding transitions that map more "distant" states along the pattern. The delay time of these additional synaptic connections will be proportional to the "distance" between the states. For instance, the ambiguity that occurs when patterns cross (fig. 7.12) can be resolved by adding synaptic components of the form (cf. eq. 7.2)

$$T_{ij}^{L(2)} = \lambda_2 \frac{J_0}{N} \sum_{\nu=1}^{q} \sum_{\mu=1}^{r-2} (2V_i^{\mu+2,\nu} - 1)(2V_j^{\mu,\nu} - 1), \quad i \neq j, \ \lambda_2 > 0 \quad (7.29)$$

The additional contribution to the input of each neuron via the above synapses is

$$h_i^{L(2)}(t) = \sum_{j=1}^{N} T_{ij}^{L(2)} \int_0^\infty V_j(t-t')\, w^{(2)}(t')\, dt' \quad (7.30)$$

The (normalized) synaptic response function $w^{(2)}(t)$ averages over the output histories of the neurons with an averaging time of $t \simeq 2\tau_L$. The contributions of the neural inputs $h_i^{L(2)}(t)$, together with $h_i^L(t)$, cause the transitions to depend on the previous *two* output states of the network. With reference to fig. 7.12, the network will make a transition to the state $(\mu, \nu) = (7, 1)$, and not the state $(\mu, \nu) = (7, 2)$, if the output history of the network is $(4, 1) \rightarrow (5, 1) \rightarrow (6, 1)$.

The synaptic strength and the corresponding neural inputs defined by eqs. 7.29 and 7.30 can be generalized to incorporate patterns that share several states in common (e.g., Keeler 1987). The dynamics of these generalized networks can be analyzed using the adiabatically varying energy defined in eq. 7.16, where $h^L(t)$ now represents the sum of all the time-delayed contributions. This scheme for embedding sequences in synapses with multiple time delays has been recently applied to speech recognition problems by Tank and Hopfield (1987). Their implementation used a layered neural architecture with a localized representation for both the embedded states and the patterns. The effect of adding synapses with multiple time delays on the storage capabilities of fully interconnected networks, especially those using a distributed representation, is yet to be studied.

Finally, we note that the problem of embedding correlated states as well as overlapping patterns can be circumvented by adding neurons that function as "hidden units," i.e., neurons that do not provide a direct output from the CPG. These neurons may enlarge the representation of the embedded states in a manner that reduces the overlaps between different states or patterns. This suggests that the number of motor-controlling outputs from a CPG can be much smaller than the total number of neurons in the network.

7.4.2 Biological Feasibility

Analysis of the CPG in Tritonia We used our associative network model to analyze the CPG controlling the swim rhythm in the mollusc *Tritonia*. This is a small network, yet it contains many of the basic features inherent in our model. The rhythmic output could be understood by a simplified analysis that employed threshold units as neurons and that replaced the response function of the slow synapses by a simple time delay. The simplified analysis served to emphasize the role of the connections between neurons in determining the collective output of this CPG. A more extensive analysis showed that our model accounts for the period of the observed output and for the mean operating characteristics of the individual neurons.

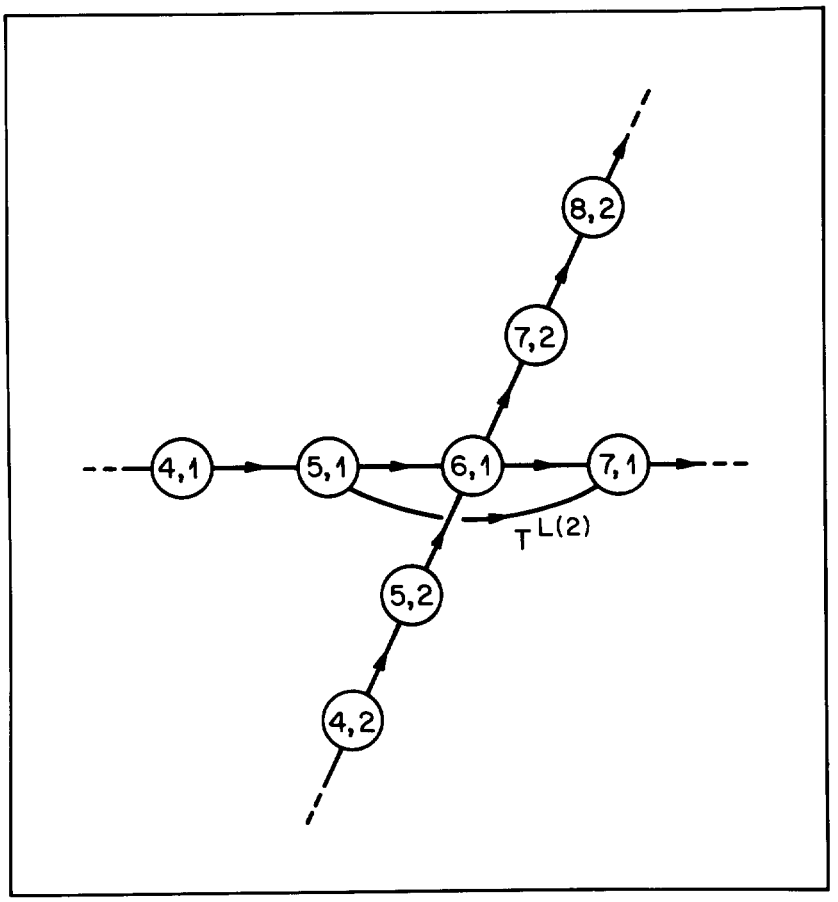

Figure 7.12
State diagram of two patterns that share a single state, i.e., $V^{6,1} = V^{6,2}$, in common. The transition labeled $\mathbf{T}^{L(2)}$ refers to a set of synaptic strengths $T_{ij}^{L(2)} \propto (2V_i^{7,1} - 1)(2V_j^{5,1} - 1)$. For a network producing the ν–1th pattern, but not for one producing the ν–2th pattern, these synaptic connections remove the ambiguity in choosing between $V^{7,1}$ and $V^{7,2}$ as the output state that should follow $V^{6,1}$.

The sign and time course of the observed synaptic strengths were in accord with the values predicted by the formalized Hebb (1949) learning rules (eqs. 7.1 and 7.2). This suggests the utility of such rules for predicting the strength of the underlying synaptic connections from the observed output states.

Our analysis demonstrates that, within the framework of our model, even a small network can function with the elimination of many of its theoretically possible connections. Many more fast synapses than slow synapses are present in *Tritonia*. The fast synaptic components stabilize the output states, and thus relatively few of these synapses can be eliminated (i.e., 25%; table 7.1). Partial elimination of the slow synaptic components can be offset by an increase in the transition strength, λ. This compensation is observed in *Tritonia*, where the relatively small fraction of slow components observed to be present (i.e., 75% of all possible connections are eliminated; table 7.1) is offset by a suitably large value for λ (i.e., $\lambda = 5$ to 10).

Our analysis also showed how the required balance between the mean operating level of each neuron and the value of its external inputs and the strength of its synaptic connections can be simply estimated. We argued (section 7.3) that the mean operating level of the VSI-A neuron in *Tritonia* is set too low. This result explained the relatively weak changes in the firing activity of VSI-A during periods of otherwise active output by the CPG (fig. 7.7). Our result further suggests that the activity of VSI-A will alternate more sharply between bursting and silence if its operating value is raised, e.g., by the injection of a small hyperpolarizing current.

Multiphasic Synapses and Synaptic Delays A variety of biophysical and biochemical mechanisms allow synaptic connections to act on more than a single time scale (for review, see Kehoe and Marty 1980). Chemically mediated synapses can show both fast and slow responses, as well as a combination of the two. For example, the synaptic connections in *Tritonia* act on time scales that differ by up to a factor of 30 (Getting 1981). Some of the chemically mediated synapses present in the network controlling the flight rhythm in the locust exhibit a delayed excitatory response (Robertson and Pearson 1985). Chemically mediated synapses in the stomatogastric ganglion of the lobster exhibit both prompt and delayed inhibitory responses (Hartline and Gassie 1979). Electrotonic connections provide a potential mechanism for the presence of both slow and fast synapses in a network. The high resistance of the electrotonic couplings between neurons in the CPG controlling

feeding in the snail *Helisoma* causes their response time to be an order of magnitude slower than other synapses in the network (Kaneko, Merickel, and Kater 1978). The converse situation occurs in the circuit controlling feeding in the mollusc *Navanax*, where the electrotonic couplings act rapidly compared with the chemically mediated synaptic connections (Spray, Spira, and Bennett 1980).

Synaptic delays can result from the delays inherent in active propagation along a relatively long process. For example, the transmission delays between ganglia of neurons in the leech are much longer than the response time of individual synapses (Stent et al. 1978). Synaptic delays may also occur when the synaptic connections T_{ij}^L between pairs of neurons are mediated by interneurons. For example, the postsynaptic response observed in pyramidal cells of the olfactory cortex contains a delayed inhibitory component. The delayed component probably results from a disynaptic pathway mediated by an interneuron (Haberly and Bower 1984). It may play a role in generating the rhythmic activity of the olfactory cortex (e.g., Freeman 1975).

Neurons may contain cellular as well as synaptic delays. Cellular delays can affect the response time of a neuron to many or all of its synaptic inputs. A general theory for associative network models that contain cellular delays does not yet exist. However, when the response time of the cellular delay is short compared to the slow synaptic response time, τ_L, the separation of the time scales between τ_S and τ_L is maintained and the output properties of the network model are unaffected. Some well-characterized cellular delays can be considered in terms of an effective synaptic delay. For example, the outward potassium current I_A (Connor and Stevens 1971) is responsible for the delayed response of the VSI-B neuron in *Tritonia* (Getting 1983b, and chapter 6). This current has the effect of allowing only *slow* excitatory inputs into VSI-B, but does not affect the time scale of the inhibitory connections (see table 7.1).

Lastly, our model is capable of producing rhythmic output in large networks that contain only monophasic connections. In this case, a synapse has either a fast time response or a slow time response, but not both. The strength of each synapse is chosen according to the appropriate Hebb rule (eqs. 7.1 and 7.2). The minimum value of the transition strength, λ, depends on the relative number of fast versus slow connections (eq. 7.20). This suggests that our model may be appropriate for analyzing CPGs that do not contain multiphasic synapses.

Modulation of the Output The output activity of many CPGs can be initiated and modulated by external inputs from command neurons

(Kennedy, Evoy, and Hanawaly 1966; Kupfermann and Weiss 1978). These neurons modulate a select fraction of neurons in the CPG. In addition, the output of CPG can be affected by the concentration of circulating neurohormones. These hormones affect the operating characteristics of neurons and possibly the strength of certain synaptic connections (e.g., Pinsker and Ayers 1983; Marder 1984; Harris-Warwick 1986).

By what mechanisms can these inputs or hormones function within the context of our model network? Large changes in the period of the output can occur if the external inputs or neurohormones affect either the time constant of the slow synaptic response, τ_L, or the transition strength, λ. For example, a neuromodulator that selectively augments the strength of the slow synaptic components, or diminishes that of the fast components, will shorten the period of the output. It will be interesting to see if neurophysiological correlates for these and related predictions are found.

It should be emphasized that we have considered so far only networks with parameters, e.g., synaptic strengths and neuron operating levels, that do not change in time. Biologically these parameters undergo slow changes, such as increases (facilitation) or decreases (fatigue) in the values of the synaptic strengths. These slow changes may modulate the overall behavior of the network. For example, a gradual *increase* in the mean operating levels will dephase the output pattern of a CPG. This will eventually terminate the oscillatory output, as observed for the CPG in *Tritonia* (fig. 7.7) (Lennard, Getting, and Hume 1980; Getting 1983b).

Networks with Only Inhibitory or Only Excitatory Connections The connection strengths T_{ij}^S and T_{ij}^L determined by the formalized Hebb rules (eqs. 7.1 and 7.2 with uncorrelated embedded states) contain both inhibitory and excitatory components. Biological systems may contain predominantly inhibitory or excitatory connections. We thus consider whether our model network can properly function when the synaptic connections are modified so that most or all of the connections have the same sign.

The stability of the model network depends on its ability to relax to one of the embedded states. This relaxation is governed by the fast synaptic components, T_{ij}^S. The mean value of these connections is approximately zero (eq. 7.1). For the simple case in which these synaptic strengths are uniformly shifted from the values determined by eq. 7.1, the modified strengths $T_{ij}^{S'}$ can be expressed as

$$T_{ij}^{S'} = T_{ij}^{S} + \frac{\overline{J}}{N} \tag{7.31}$$

The mean value of the synaptic strength is now $\overline{J}/N$; $\overline{J} < 0$ if the connections are primarily inhibitory and $\overline{J} > 0$ if the connections are primarily excitatory. The components T_{ij}^{S} contribute to the stabilizing term in the energy function for the network (first term in eq. 7.16). The mean value $\overline{J}/N$ contributes an additional term to the energy of the form

$$-\frac{1}{2}\sum_{i=1}^{N}\sum_{j=1}^{N}(2V_i - 1)\frac{\overline{J}}{N}(2V_j - 1) = -\frac{\overline{J}}{2N}\left(\sum_{i=1}^{N}(2V_i - 1)\right)^2 \tag{7.32}$$

When the components $T_{ij}^{S'}$ are predominantly inhibitory the additional term in the energy (eq. 7.32) is positive. This contribution is at a minimum for states in which the number of neurons that are firing roughly equals the number that are quiescent. The embedded states in the network correspond to stable states of this form. Thus the additional term in the energy does not change the function of the network. Consequently, our model can describe pattern generation in networks containing fast synaptic components that are only inhibitory.

When the fast synaptic components $T_{ij}^{S'}$ are predominantly excitatory, the additional term in the energy is negative. This term is at a minimum when all of the neurons are quiescent or when all of them are firing. When the mean excitation is sufficiently large, such that $\overline{J} > J_0$ (eq. 7.1), the network will tend to generate either an output state in which most of the neurons are firing or in a state in which most neurons are quiescent. Thus the embedded states are destabilized for large values of $\overline{J}$. The above arguments also hold for Hopfield's network (Denker 1986b).

The slow synaptic components T_{ij}^{L} do not substantially affect the stability of the states embedded in the network when the synaptic response function $w(t)$ is a smooth function of time. Our model network will function properly if the slow synaptic components are modified, as above, to be either predominantly inhibitory or predominantly excitatory. Note that adding an offset to either the T_{ij}^{S} or the T_{ij}^{L} components requires a concomitant change in the mean operating levels of the neurons (eqs. 7.12 and 7.13).

Application to Related Biological Phenomena We have focused our study on aspects of animal behavior that involve the generation of *rhythmic* motor outputs. However, many other behaviors can be described as a fixed *linear* sequence of motor outputs, such as bird song

and certain aspects of courtship (see, e.g., Lorenz 1970). The model we presented may be relevant for describing aspects of the neural circuitry that underlies this larger class of behaviors.

Another possible application of the model involves the relation between learning rules that depend on the history of a neuron's activity and the temporal associations inherent in classical conditioning (Barto and Sutton 1982; Tesauro 1986; Klopf 1987). Finally, the network models we described can be used for recognizing sequences of sensory input that correspond to a pattern of embedded states (Kleinfeld 1986; Amit 1988).

Learning and Plasticity One of the central features of the model is the simple relationship between the output patterns and the connections, i.e., the formalized Hebb (1949) learning rules (eqs. 7.1 and 7.2). These rules allow new patterns to be embedded in the network by modifying the synapses both incrementally in time and locally in space; the change to each synapse depends only on the activities of the postsynaptic and presynaptic neurons during the learning of the new pattern. Local updating of the synapses makes the present model particularly suitable for large, complex systems that are continuously updated as patterns are modified or added. Other learning rules may be used in biological systems, but they probably share many of these features (see also Appendix 7.A).

We introduced the relation between the "sequential" form of the T_{ij}^L synapses (eq. 7.2) and their slow dynamic response (eqs. 7.6 to 7.9) as an *ad hoc* assumption. These two features may, in fact, be closely related to each other. If one considers the evolution of the synaptic strengths in terms of a dynamic learning mechanism, the different final forms of the T_{ij}^S and the T_{ij}^L synaptic components may be the result of the different time scale of their dynamic response. For example, the T_{ij}^L components can relate two experiences that are separated by the characteristic response time of the slow components, while the T_{ij}^S components can only aid in recalling the presence of either experience. It would be interesting to implement this idea in a biologically plausible model for learning.

This work was supported in part by the National Science Foundation (Grant PHY82-17853). The address of David Kleinfeld is Room 1C-463, AT&T Bell Laboratories, Murray Hill, New Jersey 07974. Electronic mail should be addressed to dk@physics.att.com. The address of Haim Sompolinsky is Racah Institute of Physics, Hebrew University, Jerusalem, Israel 91904. Electronic mail should be addressed to sompoli@hbunos.bitnet.

Appendix 7.A: Rules for Forming Synapses with Correlated States

In this appendix we present rules for forming the T_{ij}^S and T_{ij}^L synaptic components that are suitable for generating patterns with correlated states. These rules extend the results of a recently proposed model for incorporating correlated states into associative networks.

For mathematical convenience we define the output of the neurons in terms of a variable that ranges between -1 (quiescent) and $+1$ (maximum firing rate), i.e.,

$$S_i = 2V_i - 1 \tag{7.33}$$

The embedded states are thus given by $S^1, S^2, \ldots, S^r$, $r \leq N$, where r is the length of the pattern and N is the number of neurons. For simplicity of notation we consider networks that generate a single pattern. We assume that each component of $S^\nu = \{S_i^\nu\}_{i=1}^N$ is either $+1$ or -1, and confine our results to the high-gain limit of the network (eq. 7.14).

The model makes use of the "pseudo-inverse" method (Kohonen and Ruohonen 1973; Personnaz, Guyon, and Dreyfus 1986; Kanter and Sompolinsky 1987). This method requires that the embedded states are linearly independent, but otherwise places no restrictions on the choice of states.

We define the correlation matrix, $\mathbf{C}$, between these states by

$$\mathbf{C}_{\mu\nu} = \frac{1}{N} \sum_{i=1}^{N} S_i^\mu S_i^\nu, \qquad \nu, \mu = 1, \cdots, r. \tag{7.34}$$

For orthogonal states, $\mathbf{C}$ reduces to $\mathbf{C}^{\mu\nu} = \delta^{\mu\nu}$. A set of r states, O^1, O^2, ..., O^r, that are orthogonal to the S^νs can be constructed from linear combinations of the S^νs, i.e.,

$$O_i^\mu = \sum_{\nu=1}^{r} \mathbf{C}_{\mu\nu}^{-1} S_i^\nu \tag{7.35}$$

It is straightforward to show that

$$\frac{1}{N} \sum_{i=1}^{N} O_i^\mu S_i^\nu = \delta^{\mu\nu} \tag{7.36}$$

Using this property, we define the synaptic strengths T_{ij}^S to be

$$T_{ij}^S = \frac{J_0}{N} \sum_{\mu=1}^{r} S_i^\mu O_j^\mu, \quad i \neq j \tag{7.37}$$

The synaptic connections T_{ij}^S (eq. 7.37) will map the state S^μ back onto S^μ regardless of the size of the correlations between the embedded states. Thus, these connections stabilize the network in each of the embedded states.

To generate a pattern of embedded states, we define the synaptic strengths T_{ij}^L to be

$$T_{ij}^L = \lambda \frac{J_0}{N} \sum_{\mu=1}^{r-1} S_i^{\mu+1} O_j^\mu, \quad i \neq j \tag{7.38}$$

This matrix maps the state S^μ onto the state $S^{\mu+1}$ (see also Guyon, Personnaz, Nadal, and Dreyfus, 1988).

A network using the above rules (eqs. 7.37 and 7.38) generates disjoint patterns with arbitrarily selected (linearly independent) states. The maximum number of states that can be embedded is $p = r \simeq N$ (cf. eq. 7.19). The lower bound on λ is now $\lambda > (1 - a) = (1 - p/N)$, which goes to zero as the number of embedded states approaches its maximum limit. Iterative algorithms for embedding additional (correlated) states into an existing network are discussed by Denker (1986a) and Diederich and Opper (1987).

Appendix 7.B: Calculation of t_0 for a Relatively Long Pattern

In this appendix we derive an expression for the steady-state value of t_0, the time between transitions, in terms of the transition strength λ and the slow synaptic response time τ_L. This expression is calculated for a network that produces a pattern that contains a relatively large number of embedded states ($1 \ll r \leq p \ll N$) (Sompolinsky and Kanter 1986). As in Appendix 7.A, we take $S_i = 2V_i - 1$.

Let $t = 0$ be the time at which the output state of the network has just changed to S^μ. The transition to the next state, at time $t = t_0$, is initiated by those neurons whose activity changes in going from the μth to the μ+1th state, but whose activity in the μ+1th state equals that in the first through μ–1th states. For this population of neurons, $S_i^\nu = -S_i^\mu$ for $\nu < \mu$ and for $\nu = \mu + 1$. The activity of the network during the interval $t < 2t_0$ is

$$S_i(t) = \begin{cases} -S_i^\mu & \text{for } t < 0 \\ +S_i^\mu & \text{for } 0 < t < t_0 \\ -S_i^\mu & \text{for } t_0 < t < 2t_0 \end{cases}$$

where we have assumed that $\tau_S \ll \tau_L$ and that the network is operating in the high-gain limit (eq. 7.14).

The transition time is found by comparing the time-averaged inputs $h_i^L(t)$ with the stabilizing inputs $h_i^S(t)$. The inputs t_0 the neurons discussed above, for time $0 < t \leq t_0$, are given by (eq. 7.4),

$$h_i^S(t) = \sum_{j=1}^{N} T_{ij}^S S_j(t) = +S_i^\mu$$

and (eqs. 7.6 and 7.7)

$$\begin{aligned} h_i^L(t) &= \lambda \sum_{j=1}^{N} T_{ij}^L \int_{-(\mu-1)t_0}^{t} S_j(t')\, w(t-t')\, dt' \\ &= \lambda \left[S_i^2 \int_{-(\mu-1)t_0}^{-(\mu-2)t_0} w(t-t')\, dt' + \cdots \right. \\ &\quad + S_i^{\mu-1} \int_{-2t_0}^{-t_0} w(t-t')\, dt' + S_i^\mu \int_{-t_0}^{0} w(t-t')\, dt' \\ &\quad \left. + S_i^{\mu+1} \int_{0}^{t} w(t-t')\, dt' \right] \\ &= \lambda S_i^\mu \left[-\int_0^{(\mu-1)t_0+t} w(t')\, dt' + 2\int_t^{t+t_0} w(t')\, dt' \right] \end{aligned}$$

where we took $\Delta\theta_i = 0$ (eq. 7.12). A transition will occur when the inputs $h_i^L(t_0)$ and $h_i^S(t_0)$ are equal in magnitude and opposite in sign. Confining ourselves to the limit $\mu t_0 \to \infty$ (i.e., $\mu t_0 \gg \tau_L$), so that the value of the first integral is unity (eq. 7.8), we find

$$\frac{1}{2}\left(1 - \frac{1}{\lambda}\right) = \int_{t_0}^{2t_0} w(t')\, dt' \tag{7.39}$$

The above equation has a solution only for $\lambda \geq 1$.

We used eq. 7.42 to calculate the dependence of t_0 on λ for four interesting response functions (see table 7.2). These functions, normalized to unity (eq. 7.7) with a mean response time of τ_L (eq. 7.9), are: (1) A delta function, corresponding to a sharp time delay, such as that caused

Response Function		Duration of Each State[a]	
Name	w(t)	$t_0(\lambda)$	Range
Delta function delay	$\delta(t - \tau_L)$	τ_L	$1 \leqslant \lambda < \infty$
Uniform averaging with delay	$\frac{1}{\tau_w}$; $(\tau_L - \tau_w/2) \leqslant t \leqslant (\tau_L + \tau_w/2)$ 0 ; otherwise	$\tau_w \left(\frac{\tau_L}{\tau_w} + \frac{1}{2\lambda} \right)$	$1 \leqslant \lambda < \infty$ $\tau_L < t_0 \leqslant 2\tau_L$ with $\tau_w \leqslant 2\tau_L$
Exponential averaging	$\frac{1}{\tau_L} e^{-t/\tau_L}$; $0 \leqslant t < \infty$ 0 ; otherwise	$\tau_L \ln \left(\frac{\lambda + \sqrt{\lambda(2-\lambda)}}{\lambda - 1} \right)$	$1 < \lambda < 2$[b] $0 < t_0 < \infty$
Linear averaging	$\frac{2}{3\tau_L} \left(1 - \frac{t}{3\tau_L} \right)$; $0 \leqslant t \leqslant 3\tau_L$ 0 ; otherwise	$3\tau_L \left(1 - \sqrt{\frac{\lambda - 1}{2\lambda}} \right)$	$1 \leqslant \lambda < \infty$ $3(1-\sqrt{1/2})\tau_L \leqslant t_0 \leqslant 3\tau_L$

(a) These results were derived for steady-state conditions, with $\tau_L >> \tau_S$ and with the network operating in the high-gain limit [Eq. (2.14)]; see text for details.

(b) The network will not produce stable oscillations for values of λ in the range $\lambda \geqslant 2$.

Table 7.2
Duration of the output states for a relatively long pattern.

by active propagation along an axon. For this case, $\overline{S(t)} = S(t - \tau_L)$. (2) Uniform averaging after a delay, used for the simulations shown in figs. 7.5 and 7.6. The width of the response is τ_W and the delay is given by $(\tau_L - \tau_W/2)$. (3) Exponential averaging, corresponding to the charging relation for a capacitor or to simple low-pass filtration. (4) Linear averaging, corresponding to a linearly decreasing ramp function.

An interesting result is that stable oscillations cannot be sustained with an exponential averaging function for values of λ greater than 2. Exponential averaging heavily contributes relatively recent values of $S_i(t)$ to the time-averaged outputs $\overline{S_i(t)}$. This leads to dephasing of the transition for large values of λ.

Appendix 7.C: Calculation of t_0 for Biphasic Oscillations

In this appendix we derive an expression for the steady-state value of t_0 for a network that produces biphasic oscillations. As in Appendixes 7.A and 7.B, we take $S_i = 2V_i - 1$. Let $t = 0$ be the time at which the output state of the network has just changed to S^μ. The state of the network at all previous times, assuming $\tau_S \ll \tau_L$ and that the network is operating in the high-gain limit (eq. 7.14), is

$$S(t<0) = \begin{cases} -S^\mu & \text{for } -(2n+1)t_0 < t < -2nt_0, \quad n = 0,1,2,\ldots \\ +S^\mu & \text{for } -2nt_0 < t < -(2n-1)t_0 \end{cases}$$

These states are used to determine the time-averaged output $\overline{S(t)}$. The inputs to each neuron at time t, $0 < t < t_0$, are thus (eq. 7.4)

$$h_i^S(t) = +S_i^\mu$$

and (eqs. 7.6 and 7.7)

$$h_i^L(t) = -\lambda S_i^\mu \left[\int_0^t w(t-t')\,dt' - \int_{-t_0}^0 w(t-t')\,dt' + \int_{-2t_0}^{-t_0} w(t-t')\,dt' - \cdots \right]$$

where we took $\Delta\theta_i = 0$ (eq. 7.12).

At time $t = t_0$ a transition to the state S^μ occurs, implying that $h_i^S(t_0) = -h_i^L(t_0)$. This leads to

$$\frac{1}{2}\left(1 - \frac{1}{\lambda}\right) = \sum_{n=1}^{\infty} \int_{(2n-1)t_0}^{2nt_0} w(t')\,dt' \tag{7.40}$$

where use has been made of eq. 7.8. The above equation for t_0 has a solution only for $\lambda \geq 1$.

We used eq. 7.40 to calculate the dependence of t_0 on λ for the four response functions discussed in Appendix 7.B. The linear averaging function, which approximates the slow synaptic response observed in *Tritonia*, was used for the simulations shown in figs. 7.10 and 7.11. The results are shown in table 7.3. A surprising result is that stable oscillations cannot be sustained with a linear averaging function (with no missing synaptic connections) for values of λ between $(2n)$ and $(2n+1)$,

Response Function		Duration of Each State[a]	
Name	w(t)	$t_0(\lambda)$	Range
Delta function delay	$\delta(t - \tau_L)$	τ_L	$1 \leqslant \lambda < \infty$
Uniform averaging with delay	$\frac{1}{\tau_w}$; $(\tau_L - \tau_w/2) \leqslant t \leqslant (\tau_L + \tau_w/2)$ 0 ; otherwise	$\tau_w \left(\frac{\tau_L}{\tau_w} + \frac{1}{2\lambda}\right)$	$1 \leqslant \lambda < \infty$ $\tau_L < t_0 \leqslant 2\tau_L$ with $\tau_w \leqslant 2\tau_L$
Exponential averaging	$\frac{1}{\tau_L} e^{-t/\tau_L}$; $0 \leqslant t < \infty$ 0 ; otherwise	$2\tau_L \tanh^{-1}\left(\frac{1}{\lambda}\right)$	$1 < \lambda < \infty$ $0 < t_0 < \infty$
Linear averaging	$\frac{2}{3\tau_L}\left(1 - \frac{t}{3\tau_L}\right)$; $0 \leqslant t \leqslant 3\tau_L$ 0 ; otherwise	$\frac{3\tau_L}{2n-1}\left(1 - \sqrt{\frac{\lambda - 2n + 1}{2n\lambda}}\right)$ with $n = 1, 2, 3, \cdots$	$(2n-1) \leqslant \lambda \leqslant 2n$[b] $\frac{3\tau_L}{2n} \leqslant t_0 \leqslant \frac{3\tau_L}{2n-1}$

(a) These results were derived for steady-state conditions, with $\tau_L >> \tau_S$ and with the network operating in the high-gain limit [Eq. (2.14)]; see text for details.

(b) The network will not produce stable oscillations for values of λ in the range $2n < \lambda < (2n+1)$, $n = 1, 2, 3, \ldots$.

Table 7.3
Duration of the output states for biphasic oscillations.

$n = 1, 2, 3, \ldots$. The network will initially oscillate for any value $\lambda \geq 1$, but if λ is in a forbidden range the oscillations will eventually decay. This phenomenon results in gaps in the allowed spectrum of $t_0(\lambda)$ (see table 7.3).

Appendix 7.D: Difference Equations for Numerical Simulations

The differential equations that describe sequence generation can be written as a set of finite difference equations. Time is quantized in terms of the discrete variable k, and the time constants τ_S and τ_L are given by

the integer variables κ_S and κ_L, respectively. These equations provide a suitable representation for numerical simulation of the sequence generator. As in Appendixes 7.A through 7.C, we take $S_i = 2V_i - 1$. The discrete versions of analog dynamic equations (eqs. 7.10 and 7.12) are

$$u_i(k+1) = \left(1 - \frac{1}{\kappa_S}\right) u_i(k) + \frac{1}{\kappa_S} \sum_{j=1}^{N} \left(T_{ij}^S S_j(k) + T_{ij}^L \overline{S_j(k)}\right) \quad (7.41)$$

where $S_i(k)$ and $u_i(k)$ are related by a nonlinear gain function, e.g., $S_i(k) = \tanh[2G(u_i(k) - \theta_i)]$, and (eq. 7.7)

$$\overline{S_i(k)} = \sum_{l=0}^{\infty} S_i(k-l)\, w(l) \quad (7.42)$$

The discrete convolution for $\overline{S_i(k)}$ can be turned into a recursion relation for broad classes of $w(k)$. We present four examples.

(1) Delta function time delay, i.e.,

$$w(k) = \delta(k - \kappa_L) \quad (7.43)$$

for which

$$\overline{S_i(k)} = S_i(k - \kappa_L) \quad (7.44)$$

(2) Uniform averaging after a delay, i.e.,

$$w(k) = \begin{cases} 1/\kappa_W & (\kappa_L - \kappa_W/2) \le k \le (\kappa_L + \kappa_W/2) \\ 0 & \text{otherwise} \end{cases} \quad (7.45)$$

for which

$$\begin{aligned} \overline{S_i(k)} \;=\; & \overline{S_i(k-1)} + (1/\kappa_W)\,[S_i(k - \kappa_L + \kappa_W/2) \\ & - S_i(k - 1 - \kappa_L - \kappa_W/2)] \end{aligned} \quad (7.46)$$

(3) Exponential averaging, i.e.,

$$w(k) = \begin{cases} (1/\kappa_L) e^{-k/\kappa_L} & 0 \le k \\ 0 & \text{otherwise} \end{cases} \quad (7.47)$$

for which

$$\overline{S_i(k)} = e^{-1/\kappa_L}\,\overline{S_i(k-1)} + (1/\kappa_L)S_i(k) \tag{7.48}$$

(4) Linear averaging, i.e.,

$$w(k) = \begin{cases} (3/2\kappa_L)(1 - k/3\kappa_L) & 0 \le k \le 3k_L \\ 0 & \text{otherwise} \end{cases} \tag{7.49}$$

for which

$$\begin{aligned} \overline{\overline{S_i(k)}} \;=\; & 2\overline{S_i(k-1)} - \overline{S_i(k-2)} + (3/2\kappa_L)\,[S_i(k) - S_i(k-1)] \\ & -(1/2\kappa_L^2)\,[S_i(k-1) - S_i(k - 3\kappa_L - 1)] \end{aligned} \tag{7.50}$$

Bibliography

Adams, P.R. and Brown, D.A. (1982) Pharmacological inhibition of the M-current. *J. Physiol. (London)* **332:** 263–272.

Adams, P.R., Brown, D.A., and Constanti, A. (1982a) M-currents and other potassium currents in bullfrog sympathetic neurones. *J. Physiol. (London)* **330:** 537–572.

Adams, P.R., Brown, D.A., and Constanti, A. (1982b) Voltage clamp analysis of membrane currents underlying repetitive firing of bullfrog sympathetic neurons. In: *Physiology and Pharmacology of Epileptogenic Phenomena*, Klee, M.R. *et al.* (eds.), Raven Press, New York, pp. 175–187.

Adams, D.J., Smith, S.J., and Thompson, S.H. (1980) Ionic currents in molluscan soma. *Ann. Rev. Neurosci.* **3:** 141–167.

Adams, P.R., Jones, S.W., Pennefather, P., Brown, D.A., Koch, C,. and Lancaster, B. (1986) Slow synaptic transmission in frog sympathetic ganglia. *J. Exp. Biol.* **124:** 259–285.

Adrian, E.D. (1950) The electrical activity of the mammalian olfactory bulb. *Electroenceph. clin. Neurophysiol.* **2:** 377–388.

Albus, A. (1975) Quantitative study of the projection area of the central and the paracentral visual field in Area 17 of the cat. I. The Precision of the Topography. *Exp. Brain Res.* **24:** 159–179.

Alkon, D.L. (1984) Calcium-mediated reduction of ionic currents – a biophysical memory trace. *Science* **226:** 1037–1045.

Amari, S.-I. (1972) Learning patterns and pattern sequences by self-organizing nets of threshold elements. *IEEE Trans. Comp.* **21:** 1197–1206.

Amit, D.J. (1988) Neural networks counting chimes. *Proc. Nat. Acad. Sci. USA* **85:** 2141–2145.

Amit, D.J., Gutfreund, H., and Sompolinsky, H. (1985a) Spin-glass models of neural networks. *Phys. Rev. A* **2:** 1007–1018.

Amit, D.J., Gutfreund, H., and Sompolinsky, H. (1985b) Storing infinite numbers of patterns in a spin-glass model of neural networks. *Phys. Rev. Lett.* **55:** 1530–1533.

Andrews, B.W. and Pollen, D.A. (1979) Relationship between spatial frequency selectivity and receptive field profile of simple cells. *J. Physiol. (London)* **287:** 163–167.

Atwater, I. and Rinzel, J. (1986) The β-cell bursting pattern and intracellular calcium. In: *Ionic Channels in Cells and Model Systems*, Latorre, R. (ed.), Plenum Press, New York.

Baer, S.M. and Tier, C. (1986) An analysis of a dendritic neuron model with an active membrane site. *J. Math. Biol.* **23:** 137–161.

Baird, B. (1986) Nonlinear dynamics of pattern formation and pattern recognition in the rabbit olfactory bulb. *Physica D* **22:** 150–175.

Barchi, R.L. (1987) Sodium channel diversity: subtle variations on a complex theme. *Trends Neurosci.* **10:** 221–223.

Barrett, J.N. and Crill, W.E. (1974) Influence of dendritic location and membrane properties on the effectiveness of synapses on cat motoneurones. *J. Physiol. (London)* **293:** 325–345.

Barron, I.M., Cavill, P., May, D. and Wilson, P. (1983) The transputer. *Electronics*, Nov. 17: 109.

Barto, A.G. and Sutton, R.S. (1982) Simulation of anticipatory responses in classical conditioning by a neuron-like adaptive element. *Behav. Brain. Sci.* **4:** 221–235.

Beaulieu, C. and Colonnier, M. (1983) The number of neurons in the different laminae of the binocular and monocular regions of Area 17 in the Cat. *J. Comp. Neurol.* **217:** 337–344.

Benevento, L.A., Creutzfeldt, O.D. and Kuhnt, U. (1972) Significance of intracortical inhibition in the visual cortex. *Nature New Biol.* **238:** 124–126.

Biedenbach, M.A. and Stevens, C.F. (1969a) Electrical activity in cat olfactory cortex produced by synchronous orthodromic volleys. *J. Neurophysiol.* **32:** 193–203.

Biedenbach, M.A. and Stevens, C.F. (1969b) Synaptic organization of the cat olfactory cortex as revealed by intracellular recording. *J. Neurophysiol.* **32:** 204–214.

Bishop, P.O., Coombs J.S., and Henry, G.H. (1971) Interaction effects of visual contours on the discharge frequency of simple striate neurones. *J. Physiol. (London)* **219:** 659–687.

Bishop, P.O., Kozak, W. and Vakkur, G.J. (1962) Some quantitative aspects of the cat's eye: axis and plane of reference, visual field coordinates and optics. *J. Physiol. (London)* **163:** 466–502.

Bloomfield, S.A., Hamos, J.E., and Sherman, S.M. (1987) Passive cable properties and morphological correlates of neurones in the lateral geniculate nucleus of the cat. *J. Physiol. (London)* **383:** 653–692.

Bolanowski, S.L. (1987) Contourless stimuli produce binocular brightness summation. *Vis. Res.* **27:** 1943–1951.

Boltz, J. and Gilbert, C. D. (1986). Generation of end-inhibiton in the visual cortex via interlaminar connections. *Nature* **320:** 362–365.

Borg-Graham, L.J. (1988) Simulations suggest information processing roles for the diverse currents in hippocampal neurons. In: *Neural*

Information Processsing Systems, Dana Z. Anderson (ed.), American Institute of Physics, New York, pp. 82–94.

Bower, J.M. and Rao, M. (1986) The modulation of synaptic facilitation in synapses associated with different fiber systems in piriform (olfactory) cortex of the rat. *Soc. Neurosci. Abst.* **12:** 27.

Bowler, K.C., Bruce, A.D., Kenway, R.D., Pawley, G.S., and Wallace, D.J. (1987) Exploiting highly concurrent computers for physics. *Physics Today*, October.

Boycott, B.B. and Wässle, H.(1974) The morphological types of ganglion cells of the domestic cat's retina. *J. Physiol. (London)* **240:** 307–410.

Braitenberg, V. and Braitenberg, C. (1979) Geometry of orientation columns in the visual cortex. *Biol. Cybern.* **33:** 179–186.

Brazier, M.A.B. (1959) The historical development of neurophysiology. In: *Handbook of Physiology, Neurophysiology, Sec. 1, Vol. 1*, Field, Magoun, and Hall (eds.), American Physiology Society, Washington, D.C., pp. 1–58.

Brown, T.H., Fricke, R.A., and Perkel, D.H. (1981) Passive electrical constants in three classes of hippocampal neurons. *J. Neurophysiol.* **46:** 812–827.

Bruce, A.D., Gardner, E.J., and Wallace, D.J. (1986) Static and dynamic properties of the Hopfield model. University of Edinburgh preprint 86/387.

Buhmann, J. and Schulten, K. (1987) Noise-driven temporal association in neural networks. *Europhys. Lett.* **4:** 1205–1209.

Bullier, J. and Norton, T.T. (1979) X and Y relay cells in cat lateral geniculate nucleus: quantitative analysis of receptive—field properties and classification. *J. Neurophysiol.* **42:** 244–291.

Bunow, B., Segev, I., and Fleshman, J.W. (1985) Modeling the electrical properties of anatomically complex neurons using a network analysis program: excitable membrane. *Biol. Cyber.* **53:** 41–56.

Burke, R.E. and ten Bruggencate, G. (1971) Electrotonic characteristics of α-motoneurones of varying size. *J. Physiol. (London)* **21:** 1–20.

Butz, E.G. and Cowan, J.D. (1974) Transient potentials in dendritic systems of arbitrary geometry. *Biophys. J.* **14:** 661–689.

Cannon, S., Robinson, D., and Shamma, S. (1983) A proposed neural network for the integrator of the oculomotor system. *Biol. Cybern.* **49:** 127.

Cannon, S.C. and Robinson, D.A. (1985) An improved neural-network model for the neural integrator of the oculomotor system: more realistic neuron behavior. *Biol. Cybern.* **53:** 53–108.

Carbone, E. and Lux, H.D. (1984) A low voltage activated fully inactivating Ca-channel in vertebrate sensory neurones. *Nature* **310:** 501–502.

Carnevale, N.T., and Lebeda, F.J. (1987) Numerical analysis of electrotonus in multicompartmental neuron models. *J. Neurosci. Meth.* **19:** 69–87.

Chay, T.R. and Keizer, J.E. (1983) Minimal model for membrane oscillations in the pancreatic β-cell. *Biophys. J.* **42:** 181–190.

Chomsky, N. (1965) *Aspects of the Theory of Syntax*, MIT Press, Cambridge.

Churchland, P.S., Koch. C., and Sejnowski, T.J. (1990) What is computational neuroscience? In: *Computational Neuroscience*, E. Schwartz (ed.), MIT Press, Cambridge, pp. 46–55.

Clay, J.R. and DeFelice, L.J. (1983) The relationship between membrane excitability and single channel open-close kinetics. *Biophys. J.* **42:** 151–157.

Cleland, B.G. and Levick, W.R. (1974) Properties of rarely encountered types of ganglion cells in the cat's retina and an overall classification. *J. Physiol. (London)* **240:** 457–492.

Cleland, B.G., Dubin, M.W., and Levick, W.R. (1971) Sustained and transient neurones in the cat's retina and lateral geniculate nucleus. *J. Physiol. (London)* **217:** 473–496.

Clements, J.D. and Redman, S.J. (1989) Cable properties of cat spinal motoneurones measured by combining voltage clamp, current clamp and intracellular staining. *J. Physiol. (London)* **409:** 63–87.

Coddington, E. and Levinson, N. (1955) *Theory of Ordinary Differential Equations*, McGraw-Hill Book Company, New York.

Cohen, M.A. and Grossberg, S. (1983) Absolute stability of global pattern formation and parallel memory storage by competitive networks. *IEEE Trans. Sys. Man Cybern.* **13:** 815–826.

Cohen, A.H., Rossignol, S., and Grillner, S., eds. (1986) *Neural Control of Rhythmic Movements*, John Wiley, New York.

Cole, K.S. (1968) *Membranes, Ions and Impulses: A Chapter of Classical Biophysics*, University of California Press, Berkeley.

Cole, K.S., Guttman, R., and Bezanilla, F. (1970) Nerve excitation without threshold. *Proc. Nat. Acad. Sci.* **65:** 884–891.

Cole, A.E. and Nicoll, R. (1984) Characterization of a slow cholinergic post-synaptic potential recorded in vitro from rat hippocampal pyramidal cells. *J. Physiol. (London)* **352:** 173–188.

Collatz, L. (1960) *The Numerical Treatment of Differential Equations*, Third Edition, Springer-Verlag, New York, Heidelberg, Berlin.

Connor, J.A. and Stevens, C.F. (1971a) Voltage clamp analysis of a transient outward membrane current in gastropod neural somata. *J. Physiol. (London)* **213:** 21–30.

Connor, J.A. and Stevens, C.F. (1971b) Inward and delayed outward membrane currents in isolated neural somata under voltage clamp. *J. Physiol. (London)* **213:** 31–53.

Connor, J.A., Walter, D., and McKown, R. (1977) Neural repetitive firing: modifications of the Hodgkin-Huxley axon suggested by experimental results from crustacean axons. *Biophys. J.* **18:** 81–102.

Connors, B.W. and Kriegstein, A.R. (1986) Cellular physiology of the turtle visual cortex: distinctive properties of pyramidal and stellate neurons. *J. Neurosci.* **6:** 164–177.

Conradi, S., Kellerth, J.-O., Berthold, C.-H. and Hammarberg, C. (1979) Electron microscopic studies of serially sectioned cat spinal α-motoneurons. IV. Motoneurons innervating slow-twitch (type S) units of the soleus muscle. *J. Comp. Neurol.* **184:** 769–782.

Conte, S.D. and de Boor, C. (1980), *Elementary Numerical Analysis: An Algorithmic Approach*, Third edition, McGraw-Hill Book Company, New York.

Cooley, J.W. and Dodge, F.A. (1966) Digital computer solutions for excitation and propagation of the nerve impulse. *Biophys. J.* **6:** 583–599.

Coombs, J.S., Eccles, J.C., and Fatt, P. (1955a) The electrical properties of the motoneurone membrane. *J. Physiol. (London)* **130:** 291–325.

Coombs, J.S., Eccles, J.C., and Fatt, P. (1955b) The specific ionic conductances and the ionic movements across the motoneurone membrane that produce the inhibitory post-sysnaptic potential. *J. Physiol. (London)* **130:** 326–373.

Crank, J. (1975) *The Mathematics of Diffusion*, Second edition, Clarendon Press, Oxford.

Crank, J. and Nicolson, P. (1947) A practical method for numerical evaluation of solutions of partial differential equations of the heat conduction type. *Proc. Camb. Phil. Soc.* **43:** 50–67.

Crick, F. (1984) The function of the thalamic reticular complex: the searchlight hypothesis. *Proc. Natl. Acad. Sci. USA* **81:** 4586–4590.

Crisanti, A., Amit, D.J., and Gutfreund, H. (1986) Saturation level of the Hopfield model for neural network. *Europhys. Lett.* **2:** 337–341.

Crunelli, V., Kelly, J.S., Leresheche N. and Pirchio, M. (1987) The ventral and dorsal lateral geniculate nucleus of the cat: intracellular recording in vitro. *J. Physiol. (London)* **384:** 587–601.

Cooley, J.W. and Dodge, F.A. (1966) Digital computer solution for excitation and propagation of the nerve impulse. *Biophys. J.* **6:** 583–599.

Courant, R. and Hilbert, D. (1962) *Methods of Mathematical Physics*, Vols. 1 and 2, Interscience Publishers, New York.

Cullheim, S., Fleshman, J.W., Glenn, L.L. and Burke, R.E. (1987) Membrane area and dendritic structure in type-identified triceps surae alpha-motoneurons. *J. Comp. Neurol.* **255:** 68–81.

Dahlquist, G. and Bjorck, A. (1974) *Numerical Methods*, Prentice-Hall, Englewood Cliffs, New Jersey.

Daugman, J.G. (1985) Uncertainty relation for resolution in space, spatial frequency, and orientation optimized by two-dimensional visual cortical filters. *J. Opt. Soc. Am.* **2:** 1160–1169.

Davis, L., Jr. and Lorente de Nó, R. (1947) Contribution to the mathematical theory of the electrotonus. *Studies from the Rockefeller Institute for Medical Research* **131:** 442–496.

Dawis, S., Shapley, R., Kaplan, E., and Tranchina, D. (1984) The receptive field organization of X-cells in the cat: spatiotemporal coupling and asymmetry. *Vision Res.* **24:** 549–564.

DeFelice, L.J. and Clay, J.R. (1983) Membrane current and membrane potential from single-channel kinetics. In: *Single-Channel Recording*, Sakmann, B. and Neher, E. (eds.), Plenum Press, New York, pp. 323–342.

DeFelipe, J., Hendry, S.H.C., and Jones, E.G. (1986) A correlative electron microscopic study of basket cells and large gabaergic neurons in the monkey sensory-motor cortex. *Neuroscience* **17:** 991–1009.

Dehaene, S., Changeux, J.-P., and Nadal, J.-P. (1987) Neural networks that learn temporal sequences by selection. *Proc. Natl. Acad. Sci. USA* **84:** 2727–2731.

Dekin, M.S., Getting, P.A., and Johnson, S.M. (1987) *In vitro* characterization of neurons in the ventral part of the nucleus tractus solitarius. I. Identification of neuronal types and repetitive firing properties. *J. Neurophysiol.* **58:** 195–214.

Delcomyn, F. (1980) Neural basis of rhythmic behavior in animals. *Science* **210:** 492–498.

Delgutte, B. (1984) Speech coding in the auditory nerve: II. Processing schemes for vowel-like sounds. *J. Acoust. Soc. Am.* **75:** 879–886.

Deng, L., Geisler. C.D., and Greenberg, S. (1987) A composite auditory model for processing speech sounds. *J. Acoust. Soc.* **82:** 2001-2012.

Denker, J.S. (1986a) Neural network models of learning and adaptation. *Physica D* **22:** 216–232.

Denker, J.S. (1986b) Neural network refinements and extensions. In: *Neural Networks for Computing*, Denker, J.S. (ed.), American Institute of Physics, New York.

De Schutter, E. (1986) Alternative equations for molluscan ion currents described by Connor and Stevens. *Brain Res.* **382:** 134–138.

De Schutter, E. (1989) Computer software for development and simulation of compartmental models of neurons. *Comput. Biol. Med.* **19:** 71–81.

DeValois, K.K, DeValois, R.K., and Yund, E.W. (1979) Responses of striate cortical cells to grating and checkerboard patterns. *J. Physiol. (London)* **291:** 483–505.

Devor, M. (1976) Fiber trajectories of olfactory bulb afferents in hamster. *J. Comp. Neurol.* **166:** 31–48.

Devor, M. (1977) Central processing of odor signals: lessons from adult and neonatal olfactory tract lesions. In: *Chemical Signals in Vertebrates*, Muller-Schwartz, D. and Mozell, M. (eds.), Plenum, New York.

Diederich, S. and Opper, M. (1987) Learning of correlated patterns in spin-glass networks by local learning rules. *Phys. Rev. Lett.* **58:** 949–952.

DiFrancesco, D. and Noble, D. (1985) A model of cardiac electrical activity incorporating ionic pumps and concentration changes. *Phil. Trans. R. Soc. Lond. B* **307:** 353–398.

Dionne, V.E. (1984) Synaptic noise. In: *Membranes, Channels, and Noise*, Eisenberg, R.S., Frank, M., and Stevens, C.F. (eds.), Plenum Press, New York.

DiPolo, R. and Beauge, L. (1983) The calcium pump and sodium-calcium exchange in squid axons. *Ann. Rev. Physiol.* **45:** 313.

Dodge, F.A. and Frankenhaeuser, B. (1958) Membrane currents in isolated frog nerve fibres under voltage clamp conditions. *J. Physiol. (London)* **143:** 76–90.

Doedel, E.J. (1981) AUTO: A program for the automatic bifurcation and analysis of autonomous systems. *Cong. Num.* **30:** 265–284.

Dongarra, J.J. (1987a) *Experimental Parallel Computing Architectures*, Dongarra, J.J. (ed.), North-Holland, Amsterdam.

Dongarra, J.J. (1987b) The LINPAK benchmark: an explanation. In: *Proceedings of ICS87, International Conference on Supercomputers*, published as *A Lecture Note in Computer Science*, Polychronoupolos, C. (ed.), Springer Verlag, New York, pp. 456–474.

Douglas, J., Jr. (1956) On the numerical integration of quasi-linear parabolic differential equations. *Pacific J. Math.* **6:** 35–42.

Douglas, J., Jr. (1958) The application of stability analysis in the numerical solution of quasi-linear parabolic differential equations. *Trans. Am. Math. Soc.* **89:** 484–518.

Durand, D. (1984) The somatic shunt cable model for neurons. *Biophys. J.* **46:** 645–653.

Durand, D., Carlen, P.L., Gurevich, N., Ho A. and Kunov, H. (1983) Measurements of the passive electrotonic parameters of granule cells in the rat hippocampus using HRP staining and short current pulse. *J. Neurophysiol.* **50:** 1080–1096.

Eckert, R. and Chad, J.E. (1984) Inactivation of calcium channels. *Prog. Biophys. Molec. Biol.* **44:** 215–267.

Edelstein-Keshet, L. (1988) *Mathematical Models in Biology*, Random House, New York.

Edwards, D.H. and Mulloney, B. (1984) Compartmental models of electrotonic structure and synaptic integration in an identified neurone. *J. Physiol. (London)* **348:** 89–113.

Eichenbaum, H., Shedlack, K.J., and Eckmann, K.W. (1980) Thalamocortical mechanisms in odor-guided behavior. I. Effects of lesions of the mediodorsal thalamic nucleus and frontal cortex on olfactory discrimination in the rat. *Brain Behav. Evol.* **17:** 255–275

Enroth-Cugell, C. and Robson, J.G. (1966) The contrast sensitivity of retinal ganglion cells of the cat. *J. Physiol. (London)* **187:** 517–552.

Enroth-Cugell, C., Robson, J.G., Schweizer-Tong, D.E., and Watson, A.B. (1983) Spatio-temporal interactions in cat retinal ganglion cells showing linear spatial summation. *J. Physiol. (London)* **341:** 279–307.

Ermentrout, G.B. (1981) n:m phase-locking of weakly coupled oscillators. *J. Math. Biol.* **12:** 327–342.

Ermentrout, G.B. and Cowan, J.D. (1980) Large scale spatially organized activity in neural nets. *SIAM J. Appl. Math.* **38:** 1–21.

Ermentrout, G.B. and Kopell, N. (1984) Frequency plateaus in a chain of weakly coupled oscillators, I. *SIAM J. Math. Analysis* **15:** 215–237.

Evans, J. and Shenk, N. (1970) Solutions to axon equations. *Biophys. J.* **6:** 583–599.

Fatt, P. and Katz, B. (1953) The effect of inhibitory nerve impulses on a crustacean muscle fibre. *J. Physiol. (London)* **121:** 374–389.

Fenwick, E.M., Marty, A., and Neher, E. (1982) Sodium and potassium channels in bovine chromaffin cells. *J. Physiol. (London)* **331:** 599–635.

Ferster, D. (1986) Orientation selectivity of the synaptic potentials in neurons of cat primary visual cortex. *J. Neurosci.* **6:** 1284–1301.

Ferster, D. (1988) Spatially opponent excitation and inhibition in simple cells of the cat visual cortex. *J. Neurosci.* **8:** 1172–1180.

Ferster, D. and Koch, C. (1987) Neuronal connections underlying orientation selectivity in cat visual cortex. *Trends Neurosci.* **10:** 487–492.

Fifkova, E., Markham, J.A., and Delay, R.J. (1983) Calcium in the spine apparatus of the dendritic spines in the dentate molecular layer *Brain Res. (London)* **266:** 163–168.

Finkel, A.S. and Redman, S.J. (1983) The synaptic current evoked in cat spinal motoneurons by impulse in single group Ia axons. *J. Physiol. (London)* **342:** 615–632.

Fischer, B. (1973) Overlap of receptive field centers and representation of the visual field in the opic tract, *Vision Res.* **13:** 2113–2120.

FitzHugh, R. (1960) Thresholds and plateaus in the Hodgkin-Huxley nerve equations. *J. Gen. Physiol.* **43:** 867–896.

FitzHugh, R. (1961) Impulses and physiological states in models of nerve membrane. *Biophys. J.* **1:** 445–466.

FitzHugh, R. (1969) Mathematical models for excitation and propagation in nerve. In: *Biological Engineering*, Schwan, H.P. (ed.), McGraw Hill, New York.

Fitzpatrick, D., Penny, G.R., and Schmechel, D.E. (1984) Glutamic acid decarboxylase immunoreactive neurons and terminals in the lateral geniculate nucleus of the cat. *J. Neurosci.* **4:** 1809–1829.

Flach, K., Carnevale, N.T. and Sussman-Fort, S.E. (1987) Neuron simulations using SABER. *Soc. Neurosci. Abst.* **13:** 45.19

Fleshman, J.W., Segev, I., and Burke, R.E. (1988) Electrotonic architecture of type- identified α-motoneurons in the cat spinal cord. *J. Neurophysiol.* **60:** 60–85.

Fox, G.C. (1987) A graphical approach to load balancing and sparse matrix vector multiplication on the hypercube. In: *Numerical Algorithms for Modern Parallel Computer Architectures*, Springer Verlag, New York.

Fox, S.E. and Chan, C.Y. (1985) Location of membrane conductance changes by analysis of the input impedance of neurons. II. Implementation. *J. Neurophysiol.* **54:** 1594–1606.

Fox, G.C. and Furmanski, W. (1987) Hypercube communication for neural network algorithms. Caltech report, $C^3P - 405$.

Fox, G.C. and Furmanski, W. (1988a) Load balancing loosely synchronous problems with a neural network. In: *Proceeding of the Third Conference on Hypercube Concurrent Computers and Applications*, Fox, G.C. (ed.), ACM, New York.

Fox, G.C. and Furmanski, W. (1988b) Optimal Communication Algorithms for Regular Decompositions on the Hypercube. In: *Proceeding of the Third Conference on Hypercube Concurrent Computers and Applications*, Fox, G.C. (ed.), ACM, New York.

Fox, G.C., Johnson, M.A., Lyzenga, G.A., Otto, S.W., Salmon, J.K. and Walker, D.W. (1988) *Solving Problems On Concurrent Processors*, Prentice Hall, New Jersey.

Fox, G.C. and Messina, P.C. (1987) Advanced Computer Architectures. *Sci. Am.* **256:** 66–77.

Fox, G.C. and Walker, D. (1988) Concurrent supercomputers in science. Proceedings of the conference on *Use of Computers in Physics*, North Carolina.

Frank, K. and Fuortes, M.G.F. (1956) Stimulation of spinal motoneurones with intracellular electrodes. *J. Physiol. (London)* **134:** 451–470.

Frankenhaeuser, B. (1963) A quantitative description of potassium currents in mylenated nerve fibres of *Xenopus laevin*. *J. Physiol. (London)* **169:** 424–430.

Frankenhaeuser, B. and Hodgkin, A.L. (1956) The after effects of impulses in the giant nerve fibres of *Loligo*. *J. Physiol. (London)* **131:** 341–376.

Frankenhaeuser, B. and Huxley, A.F. (1964) Action potential in mylenated nerve fibre of *Xenopus laevis* as computed on the basis of voltage clamp data. *J. Physiol. (London)* **171:** 302–315.

Freeman, W.J. (1959) Distribution in time and space of prepyriform electrical activity. *J. Neurophysiol.* **22:** 664–665.

Freeman, W.J. (1960) Correlation of electrical activity of prepyriform cortex and behavior in cat. *J. Neurophysiol.* **23:** 111–131.

Freeman, W.J. (1968) Relation between unit activity and evoked potentials in prepiriform cortex of cats. *J. Neurophysiol.* **31:** 337–348.

Freeman, W.J. (1975) *Mass Action in the Nervous System*, Academic Press, New York.

Freeman, W.J. (1979a) Nonlinear gain mediating cortical stimulus response relations. *Biol. Cybern.* **33:** 237–247.

Freeman, W.J. (1979b) Nonlinear dynamics of paleocortex manifested in the olfactory EEG. *Biol. Cybern.* **35:** 21–37.

Freeman, W.J. (1983) The physiological basis of mental images. *Biol. Psychol.* **18:** 1107–1125.

Freund, T.F., Martin, K.A.C., and Whitteridge, D. (1985a) Innervation of cat visual areas 17 and 18 by physiologically identified X- and Y-type thalamic afferents. I. Arborization patterns and quantitative

distribution of postsynaptic elements. *J. Comp. Neurol.* **242:** 263–274.

Freund, T.F., Martin, K.A.C., Somogyi, P., and Whitteridge, D. (1985b) Innervation of cat visual areas 17 and 18 by physiologically identified X- and Y-type thalamic afferents. II. Identification of postsynaptic targets by GABA immunocytochemistry and Golgi impregnation. *J. Comp. Neurol.* **242:** 275–291.

Fuortes, M.G.F. and Mantegazzini, F. (1962) Interpretation of the repetitive firing of nerve cells. *J. Gen. Physiol.* **45:** 1163–1179.

Fukushima, K. (1973) A model of associative memory in the brain. *Kybern.* **12:** 58–63.

Galvan, M., Grafe, P., and Bruggencate, G. (1982) Convulsant actions of 4-aminopyridine on the guinea-pig olfactory cortex slice. *Brain Res.* **241:** 75–86.

Gamble, E. and Koch, C. (1987) The dynamics of free calcium in dendritic spines in response to repetitive input. *Science* **236:** 1311–1315.

Gardner, E. (1988) The space of interactions in neural network models. *J. Phys. A* **21:** 257–270.

Gault, F.P. and Leaton, R.N. (1963) Nasal air flow and rhinencephalic activity. *Electroenceph. clin. Neurophysiol* **18:** 617–624.

Gault, F.P. and Coustan, D.R. (1965) Electrical activity of the olfactory system. *Electroenceph. clin. Neurophysiol.* **15:** 229–304.

Gear, C.W. (1971a) *Numerical Initial Value Problems in Ordinary Differential Equations*, Prentice-Hall, Englewood Cliffs, New Jersey.

Gear, C. W. (1971b) The automatic integration of ordinary differential equations. *Comm. ACM* **14**: 176–179.

Gelperin, A., Hopfield, J.J., and Tank, D.W. (1985) The logic of *Limax* learning. In: *Model Neural Networks and Behavior*, Selverston, A.I. (ed.), Plenum Press, New York, pp. 237–262.

Georgopoulos, A.P., Schwartz, A.B., and Kettner, R.E. (1986) Neuronal population coding of movement direction. *Science* **233:** 1416–1419.

Getting, P.A. (1977) Neuronal organization of escape swimming in *Tritonia*. *J. Comp. Physiol.* **121:** 325–342.

Getting, P.A. (1981) Mechanisms of pattern generation underlying swimming in *Tritonia*. I. Network formed by monosynaptic connections. *J. Neurophysiol.* **46:** 65–79.

Getting, P.A. (1983a) Mechanisms of pattern generation underlying swimming in *Tritonia*. II. Network recostruction. *J. Neurophysiol.* **49:** 1017–1035.

Getting, P.A. (1983b) Mechanisms of pattern generation underlying swimming in *Tritonia*. III. Intrinsic and cellular mechanisms of delayed excitation. *J. Neurophysiol.* **49:** 1036–1050.

Getting, P.A. (1983c) Neural control of swimming in *Tritonia*. In: *Neural Origin of Rhythmic Movements*, Roberts, A. and Roberts, B.L. (eds.), Cambridge University Press, London and New York, pp. 89-128.

Getting, P.A. (1988) Comparative analysis of invertebrate central pattern generators. In: *Neural Control of Rhythmic Movements in Vertebrates*, Cohen, A.H., Rossignol, S., and Grillner, S. (eds.), John Wiley and Sons, Inc., New York, pp. 101-128.

Getting, P.A. (1989) Emerging principles governing the operation of neural networks. *Ann. Rev. Neurosci.*, pp. 185–204.

Getting, P.A. and Dekin, M.S. (1985a) Mechanisms of pattern generation underlying swimming in *Tritonia*. IV. Gating of a central pattern generator. *J. Neurophysiol.* **53:** 466–480.

Getting, P.A. and Dekin, M.S. (1985b) *Tritonia* swimming: a model system for integration within rhythmic motor systems. In: *Model Neural Networks and Behavior*, Selverston, A.I. (ed.), Plenum Publishing, New York, pp. 3–20.

Getting, P.A., Lennard, P.R., and Hume, R.I. (1980) Central pattern generator mediating swimming in *Tritonia*. I. Identification and synaptic interactions. *J. Neurophysiol.* 44: 151–164.

Gilbert, C. (1977) Laminar differences in receptive field properties of cells in cat primary visual cortex. *J. Physiol. (London)* **268:** 391–421.

Gilbert, C.D. (1983) Microcircuitry of the visual cortex. *Ann. Rev. Neurosci.* **6:** 217–247.

Glass, L. and Mackey, M.C. (1988) *From Clocks to Chaos: The Rhythms of Life*, Princeton University Press, Princeton.

Glass, L. and Young, R.E. (1979) Structure and dynamics of neural network oscillators. *Brain. Res.* **179:** 208–218.

Glasser, S., Miller, J, Xuong, N.G. and Selverston, A. (1977) Computer reconstruction of invertebrate nerve cells. In: *Computer Analysis of Neuronal Structure*, Lindsay, R.D. (ed.), Plenum Publishing, New York, pp. 21–58.

Goldman, D.E. (1943) Potential, impedance, and rectification in membranes *J. Gen. Phys.* **27:**37–60.

Goldstein, S.S. and Rall, W. (1974) Changes in action potential shape and velocity for changing core conductor geometry. *Biophys. J.* **14:** 731–757.

Golub, G. H, and Van Loan, C. F. (1985) *Matrix Computations*, Johns Hopkins University Press, Baltimore.

Grasman, J. (1987) *Asymptotic Methods for Relaxation Oscillations and Applications*. Applied Mathematical Sciences **83**, Springer-Verlag, Heidelberg.

Gray, E.G. (1959) Axo-somatic and axo-dendritic synapses of the cerebral cortex: an electron microspcope study. *J. Anat.* **93:** 420–433.

Gregory. R.L. (1966) *Eye and Brain: The Psychology of Seeing*, McGraw-Hill, New York.

Gremillion, M., Mandell, A., and Travis, B. (1987) Neural nets with complex structure: a model of the visual system. In *IEEE 1st Intl. Conf. Neural Networks*, Vol. 4, Institute of Electrical and Electronics Engineers, San Diego, pp. 235–246.

Grillner, S. (1975) Locomotion in vertebrates. Central mechanisms and reflex interaction. *Physiol. Rev.* **55:** 247–304.

Grinvald, A. (1985) Real-time optical mapping of neural activity: from single growth cones to the mammalian brain. *Ann. Rev. Neurosci.* **8:** 263–305.

Grossberg, S. (1976) Adaptive pattern classification and universal recoding. I. Parallel development and coding of neural feature detectors. *Biol. Cybern.* **23:** 121–134.

Gurney, A.M., Tsien, R.Y., and Lester, H.A. (1987) Activation of a potassium current by rapid photochemically generated step increases of intracellular calcium in rat sympathetic neurons. *Proc. Natl. Acad. Sci. U.S.A.* **84(10):** 3496–3500.

Gutfreund, H. and Mézard, M. (1988) Processing temporal sequences in neural networks. *Phys. Rev. Lett.* **61:** 235–238.

Guthrie, P.B. and Westbrook, G.L. (1984) Non-uniform distribution of membrane resistivity in cultured mouse ventral horn neurons. *Soc. Neurosci. Abst.* **10:** 242.

Guttman, R., Lewis, S., and Rinzel, J. (1980) Control of repetitive firing in squid axon membrane as a model for a neuroneoscillator. *J. Physiol. (London)* **305:** 377–395.

Guyon, I., Personnaz, L., Nadal, J.P., and Dreyfus, G. (1988) Storage and retrieval of complex sequences in neural networks. *Phys. Rev. A* **38:** 6365–6372.

Haberly, L.B. (1973a) Unitary analysis of opossum prepyriform cortex. *J. Neurophysiol.* **36:** 762–774.

Haberly, L.B. (1973b) Summed potentials evoked in opossum prepyriform cortex. *J. Neurophysiol.* **36:** 775–788.

Haberly, L.B. (1978) Application of collision testing to investigate properties of multiple association axons originating from single cells in the piriform cortex of the rat. *Soc. Neurosci. Abst.* **4:** 75.

Haberly, L.B. (1983) Structure of the piriform cortex of the opossum. I. Description of neuron types with Golgi methods. *J. Comp. Neurol.* **213:** 163–187.

Haberly, L.B. (1985) Neuronal circuitry in olfactory cortex: anatomy and functional implications. *Chem. Senses* **10:** 219–238.

Haberly, L.B. and Behan, M. (1984) Structure of the piriform cortex of the opossum. III. Ultrastructural characterization of synaptic terminals of association and olfactory bulb afferent fibers. *J. Comp. Neurol.* **219:** 448–460.

Haberly, L.B. and Bower, J.M. (1984) Analysis of association fiber system in piriform cortex with intracellular recording and staining techniques. *J. Neurophys.* **51:** 90–112.

Haberly, L.B. and Presto, S. (1986) Ultrastructural analysis of synaptic relationships of intracellular stained pyramidal cell axons in piriform cortex. *J. Comp. Neurol.* **248:** 464–474.

Haberly, L.B. and Price, J.L. (1977) The axonal projection patterns of the mitral and tufted cells of the olfactory bulb in the rat. *Brain Res.* **129:** 152–157.

Haberly, L.B. and Price, J.L. (1978) Association and commissural fiber system of the olfactory cortex of the rat. I. System originating in the piriform cortex and adjacent areas. *J. Comp. Neurol.* **178:** 711–740.

Haberly, L.B. and Shepherd, G.M. (1973) Current density analysis of opossum prepyriform cortex. *J. Neurophysiol.* **36:** 789–802.

Hagiwara, S. and Ohmari, H. (1982) Studies of calcium channels in rat clonal pituitary cells with patch electrode voltage clamp. *J. Physiol. (London)* **331:** 231–252.

Halliwell, J. and Adams, P.R. (1982) Voltage clamp analysis of muscarinic excitation in hippocampal neurons. *Brain Res.* **250:** 71–92.

Harmon, L.D. (1964) Neuromimes: action of a reciprocally inhibitory pair. *Science* **146:** 1323–1325.

Harris-Warrick, R.M. (1988) Chemical modulation of central pattern generators. In: *Neural Control of Rhythmic Movements in Vertebrates*, Cohen, A.H., Rossignol, S., and Grillner, S. (eds.), John Wiley and Sons, Inc., New York, pp. 285–332.

Harth, E., Lewis, N.S., and Csermely, T.J. (1975) Escape of *Tritonia:* dynamics of neuromuscular control mechanisms. *J. Theor. Biol.* **55:** 210–228.

Hartline, H.K. (1974) *Studies on Excitation and Inhibition in the Retina*, Ratliff, E. (ed.), Rockefeller University Press, New York.

Hartline, D.K. and Gassie Jr., D.V. (1979) Pattern generation in the lobster (*Panulirus*) stomatogastric ganglion. I. Pyloric neuron kinetics and synaptic interactions. *Biol. Cyber.* **33:** 209–222.

Hartline, D.K. (1979) Pattern generation in the lobster (*Panulirus*) stomatogastric ganglion. II. Pyloric network simulation. *Biol. Cyber.* **33:** 223–236.

Hearon, J.Z. (1963) Theorems on linear systems. *Ann. N. Y. Acad. Sci.* **108:** 36–68.

Hebb, D.O. (1948) *The Organization of Behavior: A Neuropsychological Theory*, John Wiley, New York.

Heggelund, P. (1981) Receptive field organization of simple cells in cat striate cortex. *Exp. Brain Res.* **42:** 89–98.

Heggelund, P. (1986) Quantitative studies of the discharge fields of single cells in cat striate cortex. *J. Physiol. (London)* **373:** 272–292.

Heimer, L. (1968) Synaptic distribution of centripetal and centrifugal nerve fibers in the olfactory system of the rat: an experimental anatomical study. *J. Anat.* **102:** 413–432.

Hendry, S.H.C., Schwark, H.D., Jones, E.G., and Yan. J. (1987) Numbers and proportions of GABA- immunoreactive neurons in different areas of monkey cerebral cortex. *J. Neurosci.* **7:** 1503-1519.

Henrici, P. (1962) *Discrete Variable Methods in Ordinary Differential Equations*, John Wiley and Sons, Inc., New York.

Hille, B. (1984) *Ionic Channels of Excitable Membranes*, Sinauer, Sunderland, Massachusetts.

Hillis, W.D. (1985) *The Connection Machine*, MIT Press, Cambridge, Massachusetts.

Hillis, W.D. (1987) The Connection Machine. *Sci. Am.* **256:** 108–117.

Hinés, M. (1989) A program for simulation of nerve equations with branching geometries. *Int. J. Biomed. Comput.* **24:** 55–68.

Hines, M. (1984) Efficient computation of branched nerve equations. *Int. J. Bio-Med. Comp.* **15:** 69–76.

Hinton, G.E., McClelland, J.L., and Rumelhart, D.E. (1986) Distributed representations. In: *Parallel Distributed Processing: Explorations in the Microstructure of Cognition. Vol. 1: Foundations*, Rumelhart, D.E. and McClelland, J.L. (eds.), MIT Press, Cambridge.

Hodgkin, A.L. (1948) The local electric changes associated with repetitive action in a non-medullated axon. *J. Physiol. (London)* **107:** 165–181.

Hodgkin, A.L. and Huxley, A.F. (1952) A quantitative description of membrane current and its application to conduction and excitation in nerve. *J. Physiol. (London)* **117:** 500–544.

Hodgkin, A.L. and Katz, B. (1949) The effect of sodium ions on the electrical activity of the giant axon of the squid. *J. Physiol. (London)* **108:** 37–77.

Hodgkin, A.L. and Keynes, R.D. (1957) Movements of labelled calcium in squid giant axon. *J. Physiol. (London)* **138:** 253–281.

Hodgkin, A.L. and Rushton, W.A.H. (1946) The electrical constants of a crustacean nerve fibre. *Proc. Roy. Soc. London B* **133:** 444–479.

Hoffman, K.P., Stone, J., and Sherman, S.M. (1972) Relay of receptive-field properties in dorsal lateral geniculate nucleus of cat. *J. Neurophys.* **35:** 518–531.

Holmes, W.R. (1986) A continuous cable method for determining the transient potential in passive trees of known geometry. *Biol. Cyber.* **55:** 115–124.

Holmes, M.H. and Cole, J.D. (1984) Cochlear mechanics: analysis for a pure tone. *J. Acoust. Soc. Am.* **76:** 767–778.

Honma, S. (1984) Functional differentiation in SB and SC neurons of toad sympathetic ganglia. *Jap. J. Physiol.* **20:** 281.

Hopfield, J.J. (1982) Neural networks and physical systems with emergent collective computational abilities. *Proc. Nat. Acad. Sci. USA* **79:** 2554–2558.

Hopfield, J.J. (1984) Neurons with graded response have collective computational properties like those of two-state neurons. *Proc. Nat. Acad. Sci. USA* **81:** 3088–3092.

Hopfield, J.J. and Tank, D.W. (1985) "Neural" computation of decisions in optimization problems. *Biol. Cyber.* **52:** 141–152.

Hopfield, J.J. and Tank, D.W. (1986) Computing with neural circuits: a model. *Science* **233:** 625–632.

Horn, B.K.P. (1986) *Robot Vision*, MIT Press, Cambridge.

Horwitz, B. (1981) An analytical method for investigating transient potentials in neurons with branching dendritic trees. *Biophys. J.* **36:** 155–192.

Horwitz, B. (1983) Unequal diameters and their effect on time-varying voltages in branched neuron. *Biophys. J.* **41:** 51–66.

Hubel, D.H. and Wiesel, T.N. (1961) Integrative action in the cat's lateral geniculate body. *J. Physiol.(London)* **155:** 385–398.

Hubel, D.H. and Wiesel, T.N. (1962) Receptive fields, binocular interactions, and functional architecture in the cat's visual cortex. *J. Physiol. (London)* **160:** 106–154.

Hubel, D.H. and Wiesel, T.N. (1963) Shape and arrangement of columns in cat's striate cortex. *J. Physiol. (London)* **165:** 559–568.

Hubel, D.H. and Wiesel, T.N. (1965) Receptive fields and the functional architecture in two non-striate visual areas (18 and 19) of the cat. *J. Neurophysiol.* **28:** 229–289.

Hull, T. E., Enright, W. H., Fellen, B. M., and Sedgewick, A. E. (1971) Comparing numerical methods for ordinary differential equations. University of Toronto, Department of Computer Science Technical Report No. 29, Toronto, Canada.

Hume, R.I. and Getting, P.A. (1982) Motor organization of *Tritonia* swimming. II. Synaptic drive to flexion neurons from premotor interneurons. *J. Neurophysiol.* **47:** 75–90.

Humphrey, A.L., Sur, M., Uhlrich D.J., and Sherman, S.M. (1985) Projection patterns of individual X- and Y-cell axons from the lateral geniculate nucleus to cortical area 17 in the cat. *J. Comp. Neurol.* **233:** 159–189.

Ikeuchi, K. and Horn, B.K.P. (1981) Numerical shape from shading and occluding boundaries. *Artif. Intell.* **17:** 141–184.

Irvine, D. F. (1986) *The Auditory Brainstem: Sensory Physiology*, Springer Verlag, Berlin.

Isaacson, E. and Keller, H.B. (1966) *Analysis of Numerical Methods*, John Wiley and Sons, Inc., New York.

Jack, J.J.B., Noble, D., and Tsien, R.W. (1975) *Electrical Current Flow in Excitable Cells*, Second edition, Clarendon Press, Oxford.

Jack, J.J.B. and Redman, S.J. (1971) The propagation of transient potentials in some linear cable structures. *J. Physiol. (London)* **215:** 283–320.

Jack, J.J.B. and Redman, S.J. (1971b) An electrical description of the motonerone and its application to the analysis of synaptic potentials. *J. Physiol. (London)* **215:** 321–352.

Jahnsen, H. (1986) Responses of neurons in isolated preparations of the mammalian central nervous system. *Prog. Neurobiol.* **27:** 351–372.

Jahnsen, H. and Llinas, R. (1984) Electrophysiological properties of guinea pig thalamic neurones: an *in vitro* study. *J. Physiol. (London)* **349:** 205–226.

Jahr, C.E. and Stevens, C.F. (1987) Glutamate activates multiple single channel conductances in hippocampal neurons. *Nature* **325:** 522–525.

Jan, L.Y. and Jan, Y.N. (1982) Peptidergic transmission in sympathetic ganglion of the frog. *J. Physiol. (London)* **327:** 219–246.

Jeffrey, W. and Rosner, R. (1986) Optimization algorithms: simulated annealing and neural network processing. *Astrophys. J.* **310:** 473–481.

Jennings, D.M., Landweber, L.H., Fuchs, I.H., Farber, D.J., and Adrion, W.R. (1986) Computer networking for scientists. *Science* **231:** 943–950.

John, F. (1952) On integration of parabolic differential equations by difference methods. *Comm. Pure Appl. Math.* **5:** 155–211.

John, F. (1965) *Ordinary Differential Equations*, Courant Institute of Mathematical Sciences Lecture Notes, New York University, New York.

John, F. (1982) *Partial Differential Equations*, Fourth edition, Springer-Verlag, Heidelberg.

Jones, S.W. (1987) Sodium currents in dissociated bullfrog sympathetic neurons *J. Physiol. (London)* **389:**605–627.

Jones, J.P. and Palmer, L.A. (1987) An evaluation of the two-dimensional gabor filter model of simple receptive fields in cat striate cortex. *J. Neurophysiol.* **58:** 1233–1258.

Jones, E.G., Hendry, S.H.C., and DeFelipe, J. (1987) GABA-peptide neurons of the primate cerebral cortex: a limited cell class. In: *Cerebral Cortex*, Jones, E.G. and Peters, A. (eds.), Plenum Press, New York, pp. 237–266.

Jones, J.P., Stepnoski, A., and Palmer, L.A. (1987) The two-dimensional spectral structure of simple receptive fields in cat striate cortex, *J. Neurophys.* **58:** 1212–1232.

Joyner, R.W., Westerfield, M., and Moore, J.W. (1980) Effects of cellular geometry on current flow during a propagated action potential. *Biophys. J.* **31:** 183–194.

Julesz, B. (1971) *Foundations of Cyclopean Vision*, University of Chicago Press, Chicago.

Kaczmarek, L.K. and Levitan, I.B., eds. (1987) *Neuromodulation*, Oxford Univ. Press, New York.

Kandel, E.R. (1981) Calcium and the control of synaptic strength by learning. *Nature* **293:** 697–700.

Kaneko, C.R.S., Merickel, M., and Kater, S.B. (1978) Centrally programmed feeding in *Helisoma*: identification and characteristics of an electrically coupled premotor neuron network. *Brain Res.* **126:** 1–21.

Kanter, I. and Sompolinsky, H. (1987) Associative recall of memory without errors. *Phys. Rev. A* **35:** 380–392.

Kawato, M. (1984) Cable properties of a neuron model with non-uniform membrane resistivity. *J. Theoret. Biol.* **111:** 149–169.

Keeler, J.D. (1988) Comparison between Kanerva's SDM and Hopfield-type neural network models. *J. Cognitive Sci.* **12:** 299–329.

Kehoe, J. and Marty, A. (1980) Certain slow synaptic responses: their properties and possible underlying mechanisms. *Ann. Rev. Biophys. Bioeng.* **9:** 437–465.

Keller, H.B. (1976) *Numerical Solution of Two Point Boundary Problems*, CMBS-NSF Regional Conference Series in Applied Mathematics, number 24, SIAM, Philadelphia.

Kellerth, J.-O., Berthold, C.-H. and Conradi, S. (1979) Electron microscopic studies of serially sectioned cat spinal α-motoneurons. III. Motoneurons innervating fast-twitch (type FR) units of the gastrocnemius muscle. *J. Comp. Neurol.* **184:** 755–767.

Kennedy, D., Evoy, W.H., and Hanawaly, J.T. (1966) Release of coordinated behavior in crayfish by single central neurons. *Science* **154:** 917–919.

Kisvarday, Z.F., Martin, K.A.C., Whitteridge, D., and Somogyi, P. (1985) Synaptic connections of intracellularly filled clutch cells: a type of small basket cell in the visual cortex of the cat. *J. Comp. Neurol.* **241:** 111–137.

Klee, C.B. and Haiech, J. (1980) Concerted role of calmodulin and calcineurin in calcium regulation. *Ann. NY Acad. Sci.* **356:** 43–54.

Klee, M. and Rall, W. (1977) Computed potentials of cortically arranged populations of neurons. *J. Neurophysiol.* **40:** 647–666.

Kleinfeld, D. (1986) Sequential state generation by model neural networks. *Proc. Nat. Acad. Sci. USA* **83:** 9469–9473.

Kleinfeld, D. and Sompolinsky, H. (1988) Associative neural network model for the generation of temporal patterns: theory and application to central pattern generators. *Biophys. J.* **54:** 1039–1051.

Kling, U. and Szekély, G. (1968) Simulation of rhythmic activities. I. Function of networks with cyclic inhibitions. *Kybern.* **5:** 89–103.

Klopf, A.H. (1987) A drive-reinforcement model of single neuron function: an alternative to the Hebbian neuronal model. Air Force Wright Aeronautical Laboratories preprint.

Koch, C. (1987) The action of the corticofugal pathway on sensory thalamic nuclei: a hypothesis. *Neurosci.* **23:** 399–406.

Koch, C. (1987) A network model for cortical orientation selectivity in cat striate cortex. *Invest. Ophthalmol. Vis. Sci.* **28:** 126.

Koch, C. and Adams, P.R. (1984) Computer simulation of bullfrog sympathetic ganglion cell excitability. *Soc. Neurosci. Abst.* **11:** 48.7.

Koch, C. and Poggio, T. (1985) A simple algorithm for solving the cable equation in dendritic trees of arbitrary geometry. *J. Neurosci. Meth.* **12:** 303–315.

Koch, C. and Poggio, T. (1986) Computations in the vertebrate retina: motion discrimination, gain enhancement and differentiation. *Trends Neurosci.* **9:** 204–211.

Koch, C. and Poggio, T. (1987) Biophysics of computation: neurons, synapses, and membranes. In: *Synaptic Function*, Edelman, G.M., Gall, W.E., and Cowan, W.M. (eds.), Wiley, New York, pp. 637–698.

Koch, C., Marroquin, J., and Yuille, A. (1986) Analog "neuronal" networks in early vision. *Proc. Nat. Acad. Sci. USA 83:* 4263–4267.

Koch, C., Poggio, T., and Torre, V. (1982) Retinal ganglion cells: a functional interpretation of dendritic morphology. *Phil. Trans. R. Soc. Lond. (Biol.)* **298:** 227–264.

Koch, C., Poggio, T., and Torre, V. (1983) Nonlinear interactions in a dendritic tree: localization, timing, and role in information processing. *Proc. Natl. Avad. Sci. USA* **80:** 2799–2802.

Koenderink, J.J. and van Doorn, A.J. (1980) Photometric invariants related to solid shape. *Optica Acta* **27:** 981–996.

Kohonen, T. (1980) *Content-Addressable Memories*, Springer Verlag, New York.

Kohonen, T. and Ruohonen, M. (1973) Representation of associated data by matrix operators. *IEEE Trans. Comput.* **22:** 701–702.

Kopell, N. (1986) Coupled oscillators and locomotion by fish. In: Lect. Notes Biomath. 66, *Oscillations in Chemistry and Biology*, Othmer, H. (ed.), Springer Verlag, New York.

Kopell, N. 1988 Toward a theory of modelling central pattern generators. In: *Neural Control of Rhythmic Movements in Vertebrates*, Cohen, A.H., Rossignol, S., and Grillner, S. (eds.), John Wiley, New York, pp. 369–414.

Kristan Jr., W.B. (1980) Generation of rhythmic motor patterns. In: *Information Processing in the Nervous System*, Pinsker, H.M. and Willis Jr., W.D. (eds.), Raven Press, New York.

Krough, F. T. (1969) Variable order integrators for the numerical solution of ordinary differential equations. Jet Propulsion Laboratory Technical Memorandum, Pasadena, California.

Kuba, K. and Nishi, S. (1979) Characteristics of fast excitatory postsynaptic current in bullfrog sympathetic ganglion cells—effects of membrane potential, temperature and Ca ions. *Pflueger's Arch.* **378:** 205–212.

Kuffler, S.W. and Sejnowski, T.J. (1983) Peptidergic and muscarinic excitation at amphibian sympathetic synapses. *J. Physiol. (London)* **341:** 257–278.

Kulikowski, J.J. and Bishop, P.O. (1981) Linear analysis of the responses of simple cells in the cat visual cortex. *Exp. Brain Res.* **44:** 386–400.

Kupfermann, I. and Weiss, K.R. (1978) The command neuron concept. *Behav. Brain Sci.* **1:** 3–39.

Lambert, J.D. (1973) *Computational Methods in Ordinary Differential Equations*, John Wiley and Sons, Inc., New York.

Lancaster, B. and Adams, P.R. (1986) Calcium dependent current generating the afterhyperpolarization of hippocampal neurons. *J. Neurophysiol.* **55:** 1268–1282.

Lancaster, B. and Pennefather, P. (1987) Potassium currents evoked by brief depolarizations in bull-frog sympathetic gangliopn cells. *J. Physiol. (London)* **387:** 519–548.

Lax, P. D. and Richtmeyer, R. D. (1956) Survey of the stability of linear finite difference equations. *Comm. Pure Appl. Math.* **9**: 267–293.

Le Cun, Y. (1985) Une procedure d'apprentissage pour reseau a seuil assymetrique. In: *Proceedings of Cognitiva* June, 1985, Paris.

Lee, B.B., Cleland, B.G., and Creutzfeldt, O.D. (1977) The retinal input to cells in area 17 of the cat's cortex. *Exp. Brain Res.* **30:** 527–538.

Lees, M. (1959) Approximate solution of parabolic equations. *J. SIAM* **7:** 167–183.

Lehky, S.R. (1983) A model of binocular brightness and binaural loudness perception in humans with general applications to nonlinear summation of sensory inputs. *Biol. Cybern.* **49:** 89–97.

Lehky, S.R. (1988) An astable multivibrator model of binocular rivalry. *Perception* **17:** 215–228.

Lehky, S.R. and Sejnowski, T.J. (1988) Network model of shape from shading: neural function arises from both receptive and projective fields. *Nature* **333:** 452–454.

Lehky, S. and Sejnowski, T.J. (1990) Extracting surface curvature from shaded images using a neural network model. *Proc. Roy. Soc. Lond.*, in press.

Lennard, P.R., Getting, P.A., and Hume, R.I. (1980) Central pattern generator mediating swimming in *Tritonia*. II. Initiation, maintenance and termination. *J. Neurophysiol.* **44:** 165–173.

LeVay, S. (1986) Synaptic organization of claustral and geniculate afferents to the visual cortex of the cat. *J. Neurosci.* **6:** 3564–3575.

Linsenmeier, R.A., Frishman, L.J., Jakiela, H.G., and Enroth-Cugell, C. (1982) Receptive field properties of X and Y cells in the cat

retina derived from contrast sensitivity measurements. *Vision Res.* **22:** 1173–1183.

Little, W.A. (1974) The existence of persistent states in the brain. *Math. Biosci.* **19:** 101–120.

Lorenz, K. (1970) *Studies in Animal and Human Behavior*, Harvard University Press, Cambridge.

Luskin, M.B and Price, J.L. (1983a) The topographic organization of associational fibers of the olfactory system in the rat, including centrifugal fibers to the olfactory bulb. *J. Comp. Neurol.* **216:** 264–291.

Luskin, M.B and Price, J.L. (1983b) The laminar distribution of intracortical fibers originating in the olfactory cortex of the rat. *J. Comp. Neurol.* **216:** 292–302.

Lux, H.-D. (1967) Eigenschafen eines Neuron Modells mit Dendriten begrenzter Länge. *Pflueger's Arch. Ges. Physiol.* **297:** 238–255.

Lux, H.-D., Schubert, P., and Kreutzberg, G.W. (1970) Direct matching of morphological and electrophysiological data in cat spinal motoneurons. In: *Excitatory Synaptic Mechanisms*, Andersen, P. and Jansen, J.K.S. (eds.), Universitetsforlaget, Oslo, pp. 189–198.

MacGregor, R.J. (1987) *Neural and Brain Modeling*, Academic Press, New York.

Macrides, F. (1982) Temporal relationship between sniffing and the limbic theta rhythm during odor discrimination reversal learning. *J. Neurosci.* **2:** 1705–1717.

Madison, D.V. and Nicoll, R.A. (1984) Control of repetitive discharges of rat CA1 pyramidal neurons *in vitro*. *J. Physiol. (London)* **354:** 319–331.

Manor, Y., Gonczarowski, J., and Segev, I. (1990) Propagation of action potentials along axonal trees: model and implementation. *Biophys. J.*, submitted.

Marder, E. and Hooper, S.L. (1985) Neurotransmitter modulation of the stomatogastric ganglion of decapod crustaceans. In: *Model Neural Networks and Behavior*, Selverston, A.I. (ed.), Plenum, New York.

Marr, D. (1982) *Vision: A computational investigation into the human representation and processnig of visual information*, Freeman, San Francisco.

Marr, D. and Hildreth, E. (1980) Theory of edge detection. *Proc. R. Soc. Lond. B* **207:** 187–127.

Marr, D. and Poggio, T. (1976) Cooperative computation of stereo disparity. *Science* **194:** 283–287.

Martin, K.A., Somogyi, P., and Whitteridge, D. (1983) Physiological and morphological properties of identified basket cells in the cat's visual cortex. *Exp. Brain Res.* **50:** 193–200.

Mascagni, M. (1987a) *Negative Feedback in Neural Networks*, Doctoral Dissertation in Mathematics, Courant Institute of Mathematical Sciences, New York University.

Mascagni, M. (1987b) Computer simulation of negative feedback in neurons. *Soc. Neurosci. Abstr.* **13:** 375.4.

Mascagni, M. (1989a) An initial-boundary value problem of physiological significance for equations of nerve conduction. *Comm. Pure Appl. Math.* **42:** 213–227.

Mascagni, M. (1989b) Animation's role in modeling the nervous system. *Iris Universe* **Winter 1989:** 6–18.

Matsuoka, K. (1984) The dynamic model of binocular rivalry. *Biol. Cybern.* **49:** 201–208.

Matsuoka, K. (1985) Sustained oscillations generated by mutually inhibiting neurons with adaptation. *Biol. Cybern.* **52:** 367–376.

Matteson, D.R. and Armstrong, C.M. (1984) Na and Ca channels in a transformed line of anterior-pituitary cells. *J. Gen. Physiol.* **83:** 371–394.

Mayer, M.L., Westbrook, G.L. and Guthrie, P.B. (1984) Voltage dependent block by Mg^{2+} of NMDA response in spinal cord neurones. *Nature* **309:** 261–263.

McBurney, R.N. and Neering, I.R. (1987) Neuronal calcium homeostasis. *Trends Neurosci.* **10:** 164–169.

McClelland, J.L. and Rumelhart, D.E. (1986) *Parallel Distributed Processing: Explorations in the Microstructure of Cognition.* MIT Press, Cambridge, Massachusetts.

McClelland, J.L. and Rumelhart, D.E. (1988) *Explorations in Parallel Distributed Processing: a Handbook of Models, Programs, and Exercises.*, MIT Press, Cambridge, Massachusetts.

McCormick, D.A., Connors, B.W., Lighthall, J.W., and Prince, D.A. (1985) Comparative electrophysiology of pyramidal and sparsely spiny stellate neurons of the neocortex. *J. Neurophysiol.* **54:** 782–806.

McCulloch, W.S. and Pitts, W. (1943) A logical calculus of the ideas immanent in nervous activity. *Bull. Math. Biophys.* **5:** 115–133.

Mead, C. (1989) *Analog VLSI and Neural Systems*, Addison-Wesley, Reading, Massachusetts.

Meech, R.W. (1978) Calcium-dependent potassium activation in nervous tissues. *Ann. Rev. Biophys. and Bioeng.* **7:** 1–18.

Messina, P.C. (1987) Emerging Supercomputer Architectures. In: *A report to the Federal Coordinating Council on Science, Engineering and Technology on The U.S. Supercomputer Industry*, DOE/ER-0362, December 1987.

Miller, R.F. and Bloomfield, S.A. (1983) Electroanatomy of a unique amacrine cell in the rabbit retina. *Proc. Natl. Acad. Sci. A.* **80:** 3069–3073.

Miller, M.I. and Sachs, M.B. (1983) Representation of stop consonants in the discharge patterns of auditory-nerve fibers. *J. Acoust. Soc. Am.* **74:** 502–517.

Mingolla, E. and Todd, J.T. (1986) Perception of solid shape from shading. *Biol. Cybern.* **53:** 137–151.

Minsky, M. and Papert, S. (1969) *Perceptrons*, MIT Press, Cambridge.

Miranker, W.L. (1975) The computational theory of stiff differential equations, Istituto per le Applicazioni del Calcolo, Series 3, Number 102, Consiglio Nazionale delle Ricerche, Rome.

Moczydlowski, E. and Latorre, R. (1983) Gating kinetics of Ca^{2+} activated K^+ channels from rat muscle incorporated into planar lipid bilayers: evidence for two voltage-dependant Ca^{2+} binding reactions. *J. Gen. Physiol.* **82:** 511–542.

Moore, J.W. and Ramon, F. (1974) On numerical integration of the Hodgkin and Huxley equations for a membrane action potential. *J. theor. Biol.* **45:** 249–273.

Morishita, I. and Yajima, A. (1972) Analysis and simulation of networks of mutually inhibiting neurons. *Kybern.* **11:** 154–165.

Morris, C. and Lecar, H. (1981) Voltage oscillations in the barnacle giant muscle fiber. *Biophys. J.* **35:** 193–213.

Morrone, M.C., Burr, D.C., and Maffei, L. (1982) Functional implications of cross-orientation inhibition of cortical visual cells. I. Neurophysiological evidence. *Proc. R. Soc. Lond. B* **216:** 335–354.

Nagumo, J.S., Arimoto, S., and Yoshizawa, S. (1962) An active pulse transmission line simulating a nerve axon. *Proc. IRE* **50:** 2061–2070.

Neher, E. and Sakmann,B. (1983) *Single Channel Recording*, Plenum Press, New York.

Nelson, P.G. and and Lux, H.-D. (1970) Some electrical measurements of motoneuron parameters. *Biophys. J.* **10:** 55-73.

Nitzan, R., Segev, I., and Yarom, Y. (1990) Voltage behavior along the irregular dendritic structure of morphologically and physiologically characterized vagal motoneurons in the guinea pig. *J. Neurophysiol.* **63:** 333–346.

Nunez, P.L. (1981) *Electric Fields of the Brain*, Oxford University Press, New York.

Nowycky, M.C., Fox, A.P., and Tsien, R.W. (1983) Three types of neuronal calcium channels with different calcium agonist sensitivity. *Nature* **316:** 440–443.

O'Donnell, P., Koch, C., and Poggio, T. (1985) Demonstrating the nonlinear interaction between excitation and inhibition in dendritic trees using computer-generated color graphics: a film. *Soc. Neurosci. Abst.* **11:** 142.1.

Ogutzoreli, M.N. (1979) Activity analysis of neural networks. *Biol. Cybern.* **34:** 159–169.

O'Keefe, J. (1983) Spatial memory within and without the hippocampal system. In: *Neurobiology of the Hippocampus*, Seifert, W. (ed.), Academic Press, New York.

Oppenheim, A. and Schafer, R. (1976) *Digital Signal Processing*, Prentice-Hall, New Jersey.

Orban, G.A. (1984) *Neuronal Operations in the Visual Cortex*, Springer, Berlin.

Orban, G.A., Gulyas, B., and Vogels, R. (1987) Influence of moving textured background on direction selectivity of cat striate cortex. *J. Neurophysiol.* **57:** 1792–1812.

O'Shea, R. (1983) *Spatial and Temporal Aspects of Binocular Contour Rivalry*, Ph.D. dissertation, Department of Physiology, University of Queensland, Brisbane, Australia.

Palmer, J. (1986) The NCUBE: A VLSI parallel supercomputer. *Hypercube Multiprocessors*, Heath, M.T. (ed.), SIAM, Philadelphia.

Palmer, L.A. and Davis, T.L. (1981) Receptive-field structure in cat striate cortex. *J. Neurophysiol.* **46:** 260–276.

Parker, D.B. (1985) *Learning Logic*, MIT Center for Computational Research in Economics and Management Science Technical Report TR-47.

Parnas, I. and Segev, I. (1979) A mathematical model for the conduction of action potentials along bifurcating axons. *J. Physiol. (London)* **295:** 323–343.

Peichl, L. and Wässle, H. (1979) Size, scatter and coverage of ganglion cell receptive field centres in the cat retina. *J. Physiol. (London)* **291:** 117–141.

Pellionisz, A., Llinas, R., and Perkel, D.H. (1977) A computer model of the cerebellar cortex of the frog. *Neuroscience* **2:** 19–35.

Pennefather, P., Lancaster, B., Adams, P.R., and Nicoll, R.A. (1985a) Two distinct Ca-dependent K currents in bullfrog sympathetic ganglion cells. *Proc. Natl. Acad. Sci. USA* **82:** 3040–3044.

Pennefather, P., Jones, S.W., and Adams, P.R. (1985b) Modulation of repetitive firing in bullfrog sympathetic ganglion cells by two distinct K^+ currents, I_{AHP} and I_M. *Soc. Neurosci. Abst.* **11:** 48.6.

Pentland, A.P. (1984) Local shading analysis. *IEEE Trans. Patt. Anal. Mach. Intell.* **6:** 170–187.

Pentland, A.P. (1986) Perceptual organization and the representation of natural form. *Artif. Intell.* **28:** 293–331.

Pentland, A. (1989) A possible neural mechanism for computing shape from shading. *Neural Computation* **1:** 208–217.

Peretto, P. (1984) Collective properties of neural networks: a statistical physics approach. *Biol. Cyber.* **50:** 51–62.

Peretto, P. and Niez, J.J. (1986) Collective properties of neural networks. In: *Disordered Systems and Biological Organization*, Bienenstock, E., Fogelman, F., and Weisbuch, G. (eds.), Springer Verlag, Berlin.

Perkel, D.H. (1965) Applications of a digital computer simulation of a neural network. In: *Biophysics and Cybernetic Systems*, Maxfield, M., Callahan, A., and Fogel, L.J. (eds.), Spartan Books, Washington, D.C.

Perkel, D.H. and Mulloney, B. (1978a) Electrotonic properties of neurons: steady-state compartmental model. *J. Neurophysiol.* **41:** 627–639.

Perkel, D.H. and Mulloney, B. (1978b) Calibrating compartmental models of neurons. *Am. J. Physiol.* **235:** R93–R98.

Perkel, D.H., Mulloney, B., and Budelli, R.W. (1981) Quantitative methods for predicting neuronal behavior. *Neuroscience* **6:** 823–837.

Perkel, D.H., Schulman, J.H., Bullock, T.H., Moore, G.P., and Segundo, J.P. (1964) Pacemaker neurons: effects of regularly spaced synaptic input. *Science* **145:** 61–63.

Personnaz, L., Guyon, I., and Dreyfus, G. (1986) Information storage and retrieval in spin-glass like neural networks. *J. Phys. Lett.* **46:** 359–365.

Peskin, C. (1976) *Partial Differential Equations in Biology*, Courant Institute of Mathematical Sciences Lecture Notes, New York University, New York.

Peters, A. and Jones, E.G. (1984) *Cerebral Cortex*, Vols. 1 and 6, Plenum Press, New York.

Pineda, F.J. (1987) Generalization of back-propagation to recurrent neural networks. *Phys. Rev. Lett.* **59:** 2229–2232.

Pinsker, H.M. and Ayers, J. (1983) Neuronal oscillators. In: *The Clinical Neurosciences*, Eillis, W.D. (ed.), Churchill Livingston, New York.

Poggio, G.F. and Poggio, T. (1984) The analysis of stereopsis. *Ann. Rev. Neurosci.* **7:** 379–412.

Poggio, T. and Torre, V. (1977) A new approach to synaptic interactions. In: *Lecture Notes in Biomathematics. Theoretical Approaches to Computer Systems, Vol. 21*, Heim., H. and Palm, G. (eds.), pp. 89–115, Springer, Berlin, Heidelberg, New York.

Poggio, T., Torre, V., and Koch. C. (1985) Computational vision and regularization theory. *Nature* **317:** 314–317.

Poznanski, R.R. (1987) Techniques for obtaining analytical solutions for the somatic shunt cable model. *Math. Biosci.* **85:** 13–35.

Press, W.H., Flannery, B.P., Teukolsky, S.A., and Vetterling, W.T. (1986) *Numerical Recipes: The Art of Scientific Computing*, Cambridge University Press, Cambridge.

Price, J.L. (1973) An autoradiographic study of complementary laminar patterns of termination of afferent fibers to the olfactory cortex. *J. Comp. Neurol.* **150:** 87–108.

Qian, N., Sejnowski, T. (1986) Electro-diffusion model of electrical conduction in neuronal processes. *Proc. Intl. Un. Physiol. Sciences, Satellite Symposium on "Cellular Mechanisms of Conditioning and Behavioral Plasticity"* July 9-12, 1986, Seattle, Washington.

Rall, W. (1957) Membrane time constant of motoneurons. *Science* **126:** 454.

Rall, W. (1959) Branching dendritic trees and motoneuron membrane resistivity. *Exp. Neurol.* **2:** 503–532.

Rall, W. (1960) Membrane potential transients and membrane time constant of motoneurons. *Expt. Neurol.* **2:** 503–532.

Rall, W. (1962a) Theory of physiological properties of dendrites. *Ann. N.Y. Acad. Sci.* **96:** 1071–1092.

Rall, W. (1962b) Electrophysiology of a dendritic neuron model. *Biophys. J.* **2(2):** 145–167.

Rall, W. (1964) Theoretical significance of dendritic tree for input-output relation. In: *Neural Theory and Modeling*, Reiss, R.F. (ed.), Stanford University Press, Stanford, pp. 73–97.

Rall, W. (1967) Distinguishing theoretical synaptic potentials computed for different soma-dendritic distributions of synaptic inputs. *J. Neurophys.* **30:** 1138–1168.

Rall, W. (1969a) Time constant and electrotonic length of membrane cylinders and neurons. *Biophys. J.* **9:** 1483–1168.

Rall, W. (1969b) Distributions of potential in cylindrical coordinates and time constants for a membrane cylinder. *Biophys. J.* **9:** 1509–1541.

Rall, W. (1970) Dendritic neuron theory and dendrodendritic synapses in a simple cortical system. In: *The Neurosciences: Second Study Program*, Schmitt, F.O. (ed.), Rockefeller University Press, New York.

Rall, W. (1977) Core conductor theory and cable properties of neurons. In: *Handbook of Physiology: The Nervous System, Vol. 1*, Kandel, E.R., Brookhardt, J.M., and Mountcastle, V.B. (eds.), Williams and Wilkins, Co., Baltimore, Maryland, pp. 39-98.

Rall, W. (1980) Functional aspects of neuronal geometry. In: *Neurons Without Impulses*, Roberts, A., and Bush, B.M.H. (eds.), Cambridge University Press, Cambridge.

Rall, W. (1982) Theoretical models which increase R_m with dendritic distance help fit lower value for C_m. *Soc. Neurosci. Abst.* **8:** 414.

Rall, W. (1990) Perspectives on neuron modeling. In: *The Segmental Motor System*, Binder M.D. and Mendell, L.M. (eds.), Oxford Press, Oxford, in press.

Rall, W. and Rinzel J. (1973) Branch input resistance and steady attenuation for input to one branch of a dendritic neuron model. *Biophys. J.* **13:** 648-688.

Rall, W. and Segev, I. (1985) Space-clamp problems when voltage clamping branched neurons with intracellular microelectrodes. In: *Voltage and Patch Clamping With Microelectrodes*, Smith, T.G., Jr., Lecar, H., Redman, S.J., and Gage, P.W. (eds.), Am. Physiol. Soc., Bethesda, Maryland, pp. 191–215.

Rall, W. and Segev, I. (1987) Functional possibilities for synapses on dendrites and on dendritic spines. In: *Synaptic Function*, Edelman., G.M., Gall, E.E., and Cowan, W.M. (eds.), New York, Wiley, pp. 605–636.

Rall, W. and Shepherd, G.M. (1968) Theoretical reconstruction of field potentials and dendrodendritic synaptic interactions in olfactory bulb. *J. Neurophysiol.* **31:** 884–915.

Rall, W., Burke, R.E., Smith, T.G., Nelson, P.G., and Frank, K. (1967) Dendritic location of synapses and possible mechanism for the monosynaptic EPSP in motoneurons. *J. Neurophysiol.* **30:** 1169–1193.

Rall, W., Shepherd, G.M., Reese, T.S., and Brightman, M.W. (1966) Dendro-dendritic synaptic pathway for inhibition in the olfactory bulb. *Exptl. Neurol.* **14:** 44–56.

Ramachandran, V.S. (1988a) Perceiving shape from shading. *Scientific American* **259:** 76–83.

Ramachandran, V.S. (1988b) Perception of shape from shading. *Nature* **331:** 163–165.

Ramoa, A.S., Shadlen, M., Skottun, B.C., and Freeman, R.D. (1986) A comparison of inhibition in orientation and spatial frequency selectivity of cat visual cortex. *Nature* **321:** 237–239.

Rand, R.H. and Armbruster, D. (1987) *Perturbation Methods, Bifurcation Theory, and Computer Algebra*, Applied Mathematical Sciences **65**, Springer Verlag, Heidelberg.

Ratliff, F. (1974) *Studies on Excitation and Inhibition in the Retina*, Rockefeller University Press, New York.

Redman, S., and Walmsley, B. (1983) The time course of synaptic potentials evoked in cat spinal motoneurones at identified group Ia synapses. *J. Physiol. (London)* **343:** 117–133.

Reiss, R.F. (1964) A theory of resonant networks. In: *Neural Theory and Modeling*, Reiss, R.F. (ed.), Stanford University Press, California.

Richter, J. and Ullman, S. (1982) A model for the temporal organization of X- and Y-type receptive fields in the primate retina. *Biol. Cybern.* **43:** 127–145.

Richtmeyer, R. D. and Morton, K. W. (1967) *Difference Methods for Initial-Value Problems*, Second edition, Interscience Publishers, division of John Wiley and Sons, Inc., New York.

Rinzel, J. (1977) Repetitive nerve impulse propagation: numerical results and methods. In: *Research Notes in Mathematics—Nonlinear Diffusion*, Fitzgibbon, W.E. and Walker, H.F. (eds.), Pitman Publishing Ltd., London, pp. 186–212.

Rinzel, J. (1978) On repetitive activity in nerve. *Fed. Proc.* **37:** 2793–2802.

Rinzel, J. (1985) Excitation dynamics: insights from simplified membrane models. *Fed. Proc.* **44:** 2944–2946.

Rinzel, J. and Lee, Y.S. (1987) Dissection of a model for neuronal parabolic bursting. *J. Math. Biol.* **25:** 653–675.

Rinzel, J. and Rall, W. (1974) Transient response in a dendritic neuron model for current injected at one branch. *Biophys. J.* **14:** 759–790.

Roberts, A. and Roberts, B.L., eds. (1983) *Neural Origin of Rhythmic Movements*, Cambridge University Press, Cambridge.

Robertson, M. and Pearson, K.G. (1985) Neural circuits in the flight system of the locust. *J. Neurophysiol.* **53:** 110–128.

Rodieck, R. (1965) Quantitative analysis of cat retinal ganglion cell response to visual stimuli. *Vision Res.* **5:** 583–601.

Rodieck, R. (1979) Visual pathways. *Ann. Rev. Neurosci.* **2:** 193–225.

Rose, M.E. (1976) On the integration of nonlinear parabolic equations by implicit methods. *Quart. Appl. Math.* **15:** 237–248.

Ross, W.N. and Werman, R. (1987) Mapping calcium transients in the dendrites of Purkinje cells from the guinea-pig cerebellum in vitro. *J. Physiol. (London)* **389:** 319–336.

Rumelhart, D.E., Hinton, G.E., and Williams, R.J. (1986) Learning internal representations by error propagation. In: *Parallel Distributed Processing: Explorations in the Microstructure of Cognition, Vol. 1: Foundations*, Rumelhart, D.E. and McClelland, J.L. (eds.), MIT Press, Cambridge.

Sachs, M.B. and Young, E.D. (1979) Encoding of steady state vowels in the auditory-nerve: representation in terms of discharge rate. *J. Acoust. Soc. Am.* **66:** 470–479.

Sanderson, K.J. (1971) Visual field projection columns and magnification factors in the lateral geniculate nucleus of the cat. *Exp. Brain Res.* **13:** 159-177.

Sargent, P.B. (1983) The number of synaptic boutons terminating on *Xenopus* cardiac ganglion cells is directly correlated with cell size. *J. Physiol. (London)* **343:** 85–104.

Satou, M., Mori, K., Tazawa, Y., and Takagi, S.F. (1982) Long lasting disinhibition in pyriform cortex of the rabbit. *J. Neurophysiol.* **48:** 1157–1163.

Schierwagen, A. (1986) Segmental cable modelling of electrotonic transfer properties of deep superior culliculus neurons in the cat. *J. Hirnforsch* **27:** 679–690.

Schmid-Antomarchi, H., Hugues, M., and Lazdunski, M. (1986) Properties of the apamine sensitive Ca^{2+}-activated K^+ channels in PC12 pheochromocytoma cells which hyper-produce the apamin receptor. *J. Biol. Chem.* **261:** 8633–8637.

Schmidt, G.E. (1987) The Butterfly parallel processor. In: *Proceedings of the Second International Conference on Supercomputing*, St. Petersburg, Florida.

Scholfield, C.N. (1978) A depolarizing inhibitory potential in neurones of the olfactory cortex in vitro. *J. Physiol. (London)* **279:** 547–557.

Schwartz, E.L. (1980) Computational anatomy and functional architecture of striate cortex: a spatial mapping approach to perceptual coding. *Vision Res.* **20:** 645–669.

Schwob, J.E. and Price, J.L. (1978) The cortical projections of the olfactory bulb: development in fetal and neonatal rats correlated with quantitative variations in adult rats. *Brain Res.* **151:** 369–374.

Segev, I. and Parnas, I. (1977) Computer-model analysis of possible mechanisms underlying differetial channeling of information at bifurcating axons *Isr. J. Med. Sci.* **13:** 1145.

Segev, I. and Parnas, I. (1983) Synaptic integration mechanisms: a theoretical and experimental investigation of temporal postsynaptic interactions between excitatory and inhibitory inputs. *Biophys. J.* **41:** 41–50.

Segev, I. and Rall, W. (1983) Theoretical analysis of neuron models with dendrites of unequal electrical lengths. *Soc. Neurosci. Abst.* **9:** 102.20.

Segev, I., Fleshman, J.W., Miller, J.P., and Bunow, B. (1985) Modeling the electrical properties of anatomically complex neurons using a network analysis program: passive membrane. *Biol. Cyber.* **53:** 27–40.

Sejnowski, T. (1977) Storing Covariance with Nonlinearly Interacting Neurons. *J. Math. Biol.* **4:** 303–321.

Sejnowski, T.J. (1988) Neural populations revealed. *Nature* **332:** 308.

Sejnowski, T., Koch, C., and Churchland, P. (1988) Computational neuroscience. *Science*, **241:** 1299-1306.

Sellami, L. (1988) *Vowel Recognition in Adaptive Neural Networks*, Master's Thesis, Department of Electrical Engineering, University of Maryland, College Park.

Selverston, A.I. (1980) Are central pattern generators understandable? *Behav. Brain Sci.* **3:** 535–571.

Selverston, A.I., ed. (1985) *Model Neural Networks and Behavior*, Plenum Publishing, New York.

Selverston, A.I. and Moulins, M. (1986) *The Crustacean Stomatogastic System*, Springer Verlag, New York.

Seneff, S. (1984) Pitch and spectral estimation of speech based on auditory synchrony model. *Working Papers on Linguistics, MIT* **4:** 44.

Shamma, S. (1985a) Speech processing in the auditory system. I: Representation of speech sounds in the responses of the auditory-nerve. *J. Acoust. Soc. Am.* **78:** 1612–1621.

Shamma, S. (1985b) Speech processing in the auditory system. II: Lateral inhibition and the processing of speech evoked activity in the auditory-nerve. *J. Acoust. Soc. Am.* **78:** 1622–1632.

Shamma, S. (1986) Encoding the acoustic spectrum in the spatio-temporal responses of the auditory-nerve. In: *Auditory Frequency Selectivity*, Moore, B.C.J. and Patterson, R. (eds.), Plenum Press, Cambridge, pp. 289-298.

Shamma, S.A., Chadwick, R., Wilbur, J., Rinzel, J., and Moorish, K. (1986) A biophysical model of cochlear processing: intensity dependence of pure tone responses. *J. Acoust. Soc. Am.* **80(1):**133-145.

Shapley, R. and Enroth-Cugell, C. (1984) Visual adaptation and retinal gain control. *Prog. Retinal Res.* **3:** 263–346.

Shapley, R.M. and Lennie, P. (1985) Spatial frequency analysis in the visual system. *Ann. Rev. Neurosci.* **8:** 547–583.

Shapley, R.M. and Victor, J.D. (1978) The effect of contrast on the transfer properties of cat retinal ganglion cells. *J. Physiol. (London)* **285:** 275–298.

Shelton, D.P. (1985) Membrane resistivity estimated for the Purkinje neuron by means of a passive computer model. *Neuroscience* **14:** 41–50.

Shepherd, G.M. (1979) *The Synaptic Organization of the Brain*, second edition, Oxford University Press, New York.

Shepherd, G.M. (1990) *The Synaptic Organization of the Brain*, third edition, Oxford University Press, New York.

Shepherd, G.M. and Brayton, R.K. (1979) Computer simulation of a dendro-dendritic synaptic circuit for self- and lateral-inhibition in the olfactory bulb. *Brain Res.* **175:** 377–382.

Shepherd, G.M., Carnevale, N.T., and Woolf, T.B. (1988) Comparisons between computational operations generated by active responses in dendritic branches and spines, using SABER. *Soc. Neurosci. Abstr.* **14:** 252.6.

Sherman, M. (1985) Functional organization of the W-, X- and Y-cell pathways: a review and hypothesis. In: *Progress in Psychobiology and Physiological Psychology*, Vol. 11, Sprague. J.M. and Epstein, A.N. (eds.), Academic Press, New York, pp. 233-314.

Sherman, S.M. and Koch, C. (1986) The control of retinogeniculate transmission in the mammalian lateral geniculate nucleus. *Exp. Brain Res.* **63:** 1–20.

Siebert, W.M. (1970) Frequency discrimination in the auditory system: place or periodicity mechanisms? *Proc. IEEE* **58:** 723–730.

Siegelbaun, S.A. and Tsien, R.W. (1983) Modulation of gated ion channels as a mode of transmitter activity. *Trends Neurosci.* **6:** 307–313.

Sillito, A.M. (1975) The contribution of inhibitory mechanisms to the receptive field properties of neurons in the striate cortex of the cat. *J. Physiol. (London)* **250:** 305–322.

Sillito, A.M., Kemp, J.A., Milson, J.A., and Berardi, N. (1980) A re-evaluation of the mechanisms underlying simple cell orientation selectivity. *Brain Res.* **194:** 517–520.

Simon, S.M. and Llinas, R. (1985) Compartmentalization of the submembrane calcium activity during calcium influx and its significance in transmitter release. *Biophys. J.* **48:** 485–498.

Sinex, D.G. and Geisler, C.D. (1983) Responses of auditory-nerve fibers to consonent-vowel syllables. *J. Acoust. Soc. Am.* **73:** 602–615.

Singer, W. and Creutzfeldt, O.D. (1970) Reciprocal lateral inhibition of on- and off-center neurones in the lateral geniculate body of the cat. *Exp. Brain Res.* **10:** 311–330.

Skottun, B., Bradley, A., Sclar, G., Ohzawa, I., and Freeman, R. (1987) The effects on contrast on visual orientation and spatial frequency discrimination: a comparison of single cells and behaviour. *J. Neurophys.* **57:** 773–786.

Smith, G.D. (1985) *Numerical Solutions of Partial Differential Equations: Finite Difference Methods*, Third edition, Clarendon Press, Oxford.

Smith, S.J. (1987) Progress on LTP at hippocampal synapses: a postsynaptic Ca^{2+} trigger for memory storage? *Trends Neurosci.* **10:** 142–144.

Smith, T.G., Wuerker, R.B., and Frank, K. (1967) Membrane impedance changes during synaptic transmission in cat spinal motoneurons. *J. Neurophysiol.* **30:** 1072–1096.

Snyder, D.L. (1975) *Random Point Processes*, Wiley, New York.

Sod, G.A. (1985) *Numerical Methods in Fluid Dynamics: Initial and Initial Boundary-Value Problems*, Cambridge University Press, Cambridge.

Sompolinsky, H. and Kanter, I. (1986) Temporal association in asymmetric neural networks. *Phys. Rev. Lett.* **57:** 2861–2864.

Spray, D.C., Spira, M.E., and Bennett, M.V.L. (1980) Synaptic connections of buccal mechanosensory neurons in the opisthobranch mollusc, *Navanax inermis. Brain Res.* **182:** 271–286.

Stein, P.S.G., Camp, A.W., Robertson, G.A., and Mortin, L.I. (1986) Blends of rostral and caudal scratch reflex motor patters elicited by simultaneous stimulation of two sites in the spinal turtle. *J. Neurosci.* **6:** 2259–2266.

Stein, R.B., Leung, K.V., Oguztoreli, M.N., and Williams, D.W. (1974) Properties of small neural networks. *Kybern.* **14:** 223–230.

Stent, G.S., Kristan Jr., W.B., Friesen, W.O., Ort, C.A., Poon, M., and Calabrese, R.L. (1978) Neuronal generation of the leech swimming movement. *Science* **200:** 1348–1356.

Stoer, J. and Bulirsch, R. (1980) *Introduction to Numerical Analysis*, Springer Verlag, Heidelberg.

Stone, J. (1983) *Parallel Processing in the Visual System*, Plenum Press, New York.

Stone, J. and Dreher, B. (1973) Projection of X- and Y-cells of the cat's lateral geniculate nucleus to areas 17 and 18 of visual cortex. *J. Neurophysiol.* **36:** 551–567.

Tanabe, T., Iino, M. and Takagi, S.F. (1975) Discrimination of odors in olfactory bulb, amygdaloid areas, and orbitofrontal cortex of monkey. *J. Neurophysiol.* **38:** 1284–1296.

Tanaka, K. (1983) Cross-correlation analysis of geniculostriate neuronal relationships in cats. *J. Neurophysiol.* **49:** 1303–1318.

Tank, D.W. and Hopfield, J.J. (1987) Neural computation by time compression. *Proc. Nat. Acad. Sci. USA* **84:** 1896–1900.

Taxi, J. (1976) In: *Frog Neurobiology*, Llinas, R. and Precht, W. (eds.), Springer Verlag, Heidelberg, pp. 95–150.

Taylor, R.E. (1963) Cable theory. In: *Physical Techniques in Biological Research, Vol. 6*, Nastuk, W.L. (ed.), Academic Press, New York, pp. 219–262.

Tesauro, G.J. (1986) Simple neural models of classical conditioning. *Biol. Cybern.* **55:** 187–200.

Thompson, R.S. (1982) A model for basic pattern generating mechanisms in the lobster stomatogastric ganglion. *Biol. Cybern.* **43:** 71–78.

Tömböl, T. (1974) An electron microscopic study of the neurons of the visual cortex. *J. Neurocytol.* **3:** 525-531.

Tootel, R.B., Silverman, M.S., and DeValois, R.L. (1982) De-oxyglucose analysis of retinotopic organization in primate striate cortex. *Science* **218:** 902–904.

Traub, R.D. and Wong, R.K.S. (1983) Synchronized burst discharge in the disinhibited hippocampal slice. II. Model of the cellular mechanism. *J. Neurophysiol.* **49:** 459–471.

Tseng, G.F. and Haberly, L.B. (1986) A synaptically mediated K+ potential in olfactory cortex: characterization and evidence for interneuronal origin. *Soc. Neurosci. Abst.* **12:** 667.

Ts'o, D.Y., Gilbert, C.D., and Wiesel T.N. (1986) Relationships between horizontal interactions and functional architecture in cat striate cortex as revealed by cross-correlation analysis. *J. Neurosci.* **6:** 1160–1170.

Turner, D.A. and Schwartzkroin, P.A. (1984) Passive electrotonic structure and dendritic properties of hippocampal neurons. In: *Brain Slices*, Dingledine, G. (ed.), Plenum Press, New York.

Tusa, R.J., Palmer, L.A., and Rosenquist, A.C. (1978) The retinotopic organization of area 17 (striate cortex) in the cat. *J. Comp. Neur.* **177:** 213-236.

Ulfhake B. and Kellerth J.-O. (1981) A quantitative light microscopic study of the dendrites of cat spinal α-motoneurons after intracellular staining with horseradish peroxidase. *J. Comp. Neurol.* **202:** 571–583.

van Hateren, J.H. (1986) An efficient algorithm for cable theory, applied to blowfly photoreceptor cells and LMCs. *Biol. Cybern.* **54:** 301–311.

Varela, F. and Singer, W. (1987) Neuronal dynamics in the visual corticothalamic pathway revealed through binocular rivalry. *Exp. Brain Res.* **66:** 10–20.

Victor, J.D. (1987) The dynamics of the cat retinal X cell centre. *J. Physiol. (London)* **386:** 219–246.

Vidyasagar, T.R. and Heide, W. (1984) Geniculate orientation biases seen with moving sine wave gratings: implications for a model of simple cell afferent connectivity. *Exp. Brain Res.* **57:** 196–200.

Vladimirescu, A., Zhang, K., Newton, A.R., Pederson, D.O., and Sangiovani- Vincentelli, A. (1981) *SPICE Version 2G User's Guide*, EECS Dept., University of California, Berkeley.

Wässle, H., Boycott, B.B., and Illing, R.-B. (1981) Morphology and mosaic of on- and off-beta cells in the cat retina and some functional considerations. *Proc. R. Soc. Lond. B* **212:** 177–195.

Wässle, H., Peichl, L., and Boycott, B.B. (1983) A spatial analysis of on- and off- ganglion cells in the cat retina. *Vision Res.* **10:** 1151–1160.

Wallace, D.J. (1987) Scientific Computation on SIMD and MIMD Machines. Edinburgh preprint 87/429, Invited Talk at Royal Society Discussion Meeting, London, Dec. 9–10.

Waltman, P. (1986) *A Second Course in Elementary Differential Equations*, Academic Press, New York.

Wang, H.T., Mathur, B. and Koch, C. (1989) Computing optical flow in the primate visual system, *Neural Computation* **1:** 92–103.

Watkins, D.W. and Berkley, M.A. (1974) The orientation selectivity of single neurons in cat striate cortex. *Exp. Brain Res.* **19:** 433–446.

Waxman, S.G. and Ritchie, J.M. (1985) Organization of ion channels in the myelinated nerve fiber. *Science* **228:** 1502–1507.

Weeks, J.C. (1981) Neuronal basis of leech swimming: separation of swim initiation, pattern generation, and intersegmental coordination by selective lesions. *J. Neurophys.* **45:** 698–723.

Weight, F.F. and Votava, J. (1970) Inactivation of potassium conductance in slow postsynaptic excitation. *Science* **170:** 755–758.

Werbos, P.J. (1987) Building and understanding adaptive systems: a statistical-numerical approach to factory automation and brain research. *IEEE Trans. Systems, Man & Cybern.* **17:** 7–20.

Westerman, L.A. and Smith, R.L. (1984) Rapid and short term adaptation in auditory nerve responses. *Hear. Res.* **15:** 249–260.

White, E.L. and Rock, M.P. (1980) Three dimensional aspects and synaptic relationships of a Golgi impregnated spiny stellate cell reconstructed from serial thin sections. *J. Neurocytol.* **9:** 615–636.

Willows, A.D.O. (1967) Behavioral acts elicited by stimulation of single, identifiable brain cells. *Science* **157:** 570–574.

Willows, A.D.O. and Hoyle, G. (1969) Neuronal network triggering of fixed action pattern. *Science* **166:** 1549–1551.

Wilson, C.J. (1984) Passive cable properties of dendritic spines and spiny neurons. *J. Neurosci.* **4:** 281–297.

Wilson, D.M. (1961) The central nervous control of flight in a locust. *J. Exp. Biol.* **38:** 471–490.

Wilson, D.M. and Waldron, I. (1968) Models for the generation of the motor output pattern in flying locusts. *Proc. IEEE* **56:** 1058–1064.

Wilson, H.R. and Cowan, J.D. (1972) Excitatory and inhibitory interactions in localized populations of model neurons. *Biophys. J.* **12:** 1–24.

Wilson, J. and Sherman, S. (1976) Receptive field characteristics of neurones in cat striate cortex: changes with visual field eccentricity. *J. Neurophysiol.* **39:** 512–533.

Wilson, M.A. and Bower, J.M. (1987) A computer simulation of a three-dimensional model of piriform cortex with functional implications for storage and recognition of spatial and temporal olfactory patterns. *Soc. Neurosci. Abst.* **13:** 1401

Wilson, M.A. and Bower, J.M. (1988) A computer simulation of olfactory cortex with functional implications for storage and retrieval of olfactory information. *Proceedings of the Conference on Neural Information Processing Systems*, Anderson, D.(ed.), AIP Press, New York, pp. 114–126.

Wilson, M.A., Bower, J.M., Chover, J., and Haberly, L.B. (1986) A computer simulation of piriform cortex. *Soc. Neurosci. Abst.* **12:** 1358.

Winfield, D.A., Gatter, K.C., and Powell, T.P.S. (1980) An electron microscopic study of the types and proportions of neurons in the

cortex of the motor and visual areas of the cat and rat. *Brain* **103:** 245–258.

Winfree, A.T. (1980) The geometry of biological time. In: *Biomathematics* **8**, Springer Verlag, Heidelberg.

Wong, R.K.S. and Traub, R.D. (1983) Synchronized burst discharge in disinhibited hippocampal slice. I. Initiation in CA2-CA3 region. *J. Neurophys.* **49:** 442–458.

Yamada, W., Koch, C., and Adams, P.R. (1988) Modelling electrical excitability in the cell body and axon of type B bullfrog sympathetic ganglion cells. *Soc. Neurosci. Abst.* **14:** 118.11.

Young, E.D. and Sachs, M.B. (1979) Representation of steady state vowels in the temporal aspects of the discharge patterns of populations of auditory-nerve fibers. *J. Acoust. Soc. Am.* **66:** 1381–1403.

Zipser, D. and Andersen, R.A. (1988) A back-propagation programmed network that simulates response properties of a subset of posterior parietal neurons. *Nature* **331:** 679–684.